THESIS

LOW-COST DATA LOGGERS FOR USE WITH THE CONDUCTIVITY MASS BALANCE METHOD TO ESTIMATE BASEFLOW AT SNOWMELT-DOMINATED HEADWATER STREAMS IN NORTHWESTERN COLORADO

Submitted by

Amber Leigh Lidell

Department of Geosciences

In partial fulfillment of the requirements

For the Degree of Master of Science

Colorado State University

Fort Collins, Colorado

Summer 2021

Master's Committee:

Advisor: William E. Sanford

Daniel McGrath
Tim Covino

ABSTRACT

LOW-COST DATA LOGGERS FOR USE WITH THE CONDUCTIVITY MASS BALANCE METHOD TO ESTIMATE BASEFLOW AT SNOWMELT-DOMINATED HEADWATER STREAMS IN NORTHWESTERN COLORADO

Groundwater contribution to streamflow (baseflow) in snowmelt-dominated headwater streams, particularly following the snowmelt peak, is crucial for sustaining late season flow necessary for maintaining instream functions and fluvial ecosystems. Quantification of baseflow following snowmelt helps managers to determine the potential impacts of climate variability or management activities on streamflow, among others. One method of estimating baseflow is the conductivity mass balance (CMB), which requires continuous measurement of stream discharge and specific conductance (SC). Most headwater streams lack this information, as commonly used data loggers to measure SC are costly, and headwater streams have extreme variations in accessibility, temperature, discharge, and sediment. The purpose of this study is to investigate a new means to log continuous SC data in snowmelt-dominated headwater streams where data collection options are limited by costs. The primary objectives include deploying, calibrating, and testing a new low-cost data logger to continuously measure SC, gauging ungauged streams to determine continuous discharge, and estimating baseflow.

The low-cost Stream Temperature, Intermittency, and Conductivity (STIC) data loggers were developed by modifying Onset HOBO Pendant waterproof temperature and light data loggers. 17 of these loggers as well as three higher-cost SC loggers were deployed in 10 streams in the Medicine Bow-Routt National Forests in northwestern Colorado in 2017 and/or 2018.

Nine headwater streams were gauged, and rating curves developed to determine continuous discharge. 15 STIC loggers were then calibrated to known SC standards, and of those, in-stream data from 11 were used with discharge data to estimate baseflow at seven sites. Regression outputs for these 11 are available in the supplementary files. The conductivity-discharge relationships of two streams did not meet the requirements of the CMB method. Baseflow was also estimated at two streams with data from the higher-cost SC loggers.

During the 2018 post snowmelt-dominated period, the data from STIC and higher-cost loggers recorded data that were used to calculate a proportion of baseflow to total streamflow (baseflow index) within 0.7 percent of one another at North Fork of the Elk River. Data from two STIC loggers that were deployed at Roaring Fork of Slater Creek were used to estimate baseflow indexes within 0.2 percent of one another. The data recorded by STIC loggers worked well with discharge data to estimate baseflow at seven sites with the CMB method during the post snowmelt-dominated portion of each hydrograph, even after being subjected to extreme field conditions. Once calibration and data processing time were taken into account, seven STIC loggers can be used for approximately the same cost as one higher-cost SC logger.

For the best STIC logger data acquisition, it is recommended to deploy two low-cost loggers at each site as was done for this study, in a location that is not likely to experience heavy deposition, extremely turbulent flows, or long-term frozen water (e.g., in a glide or near a pool-tail crest). It is also recommended to calibrate the STIC loggers prior to field deployment, as was not done in this study. The findings of this study encourage the possibility of collecting more continuous data at more snowmelt-dominated headwater streams due to the low cost of these STIC loggers. This in turn increases potential for more baseflow data to be acquired at these streams, to inform and support public land and water management decisions and add to the active area of research surrounding baseflow estimation at headwater streams.

ACKNOWLEDGEMENTS

This project was funded by the U.S. Forest Service. Thank you to Tyler Carleton and Liz Schnackenberg, hydrologists on the Medicine Bow-Routt National Forests in Steamboat Springs, Colorado. Tyler worked with me, in the field to collect much of the data, and in the office to help analyze some of it. Liz discussed with me her knowledge about different watersheds' groundwater potential, history of disturbance, and rare and vulnerable species present to be a part of site selection and acquiring background information. Both Tyler and Liz shared what they knew about nearby stream gages and projects, as well as land and water management priorities.

Thank you to Joe Gurrieri, hydrogeologist and Tim Stroope, hydrologist of the Forest Service Washington Office Minerals and Geology Management program. Joe first piqued my interest in groundwater when I worked with him on a groundwater-dependent ecosystem study about 10 years ago on the Fremont-Winema National Forests in southern Oregon. When I began working for the Medicine Bow-Routt in 2017 he emphasized the importance of taking hold of this project. Joe and Tim worked in the field to deploy many low-cost data loggers and attended field visits to discuss site selection and field methods. Tim also attended my presentation on this research at the National Groundwater Association's Groundwater Week in 2019.

To my graduate advisor, Dr. Bill Sanford, thank you for believing in me enough to recommend me to the Forest Service for this work, and to hire me on to for this research. You showed me that streams can be a wonderous window into the mysterious groundwater world, combining my interests of surface and groundwater. I so appreciate you meeting with me countless times to be sure we were on the same page, and for your enduring patience and attention over the last several years.

To my committee members Dr. Dan McGrath and Dr. Tim Covino, thank you for your flexibility, interest, and time given to look at my thesis and provide feedback. I would also like to thank the Department of Geosciences for giving me a space to grow and interact, as well as the Colorado State University (CSU) Writes program and my fellow graduate students, for keeping me motivated and accountable during my final year.

TABLE OF CONTENTS

LIST OF TABLES

LIST OF FIGURES

LIST OF EQUATIONS

1. INTRODUCTION

This study investigates a low-cost means to log the data needed to estimate continuous groundwater contribution to streamflow at ten snowmelt-dominated headwater streams. Quantifying groundwater contribution to stream discharge in snowmelt-dominated headwater streams is of value to support public land and water management decisions and add to the active area of research surrounding baseflow estimation. This study defines baseflow as the groundwater contribution to stream discharge that sustains streamflow following snowmelt and is also a component of streamflow during high flow. Continuous baseflow discharge data are often summed and divided by the total discharge to find the baseflow index (BFI), the long-term proportion of baseflow to streamflow (Miller et al., 2014). Because baseflow sustains streamflow following snowmelt, it is crucial for maintaining instream functions and fluvial ecosystems which support species like native Colorado River cutthroat trout, boreal toads, mountain sucker, Greater sandhill cranes, brook trout, native riparian trees, and other aquatic and terrestrial biota (Schnackenberg, 2017).

Measuring headwater stream discharge and estimating baseflow helps managers to (1) develop more information about each watershed's water budget; (2) determine which headwater watersheds are more susceptible to being impacted by natural changes (climate, snowpack, etc.) or management activities (restoration, grazing, diversions, etc.); and (3) better understand what the water cycle response to changes may be in the short and long term, including using baseflow for baseline data and as a monitoring tool. Baseflow discharge estimates are desirable for multiple varying watershed types to establish how geology, land use (Miller et al., 2015), soil, climate, topography, and land cover characteristics affects baseflow discharge to headwater streams (Rumsey et al., 2015). Being able to log the data needed to estimate continuous groundwater contribution to streamflow at ten snowmelt-dominated headwater streams instead of one could increase the scientific and management community's knowledge about smaller watersheds where data collection options are limited by costs.

Nine of the ten streams in this study are headwaters of the Yampa River, in northwestern Colorado, which is a tributary of the Colorado River. About 3,000 acre-feet per year of groundwater is withdrawn from the Yampa River basin (YRB) and about one-third of this water is used for irrigation. Livestock and domestic uses are the main sinks for alluvial groundwater in this basin. Diversions for municipal use occur in Steamboat Springs, Craig, and many small towns in the YRB (Colorado Water Conservation Board, 2009). The Yampa River is unique as it is a largely unregulated and free-flowing river in the Colorado River Basin (Bauch et al., 2012). Headwater streams are hydrologically connected to downstream waters like the Yampa, maintaining the physical, chemical, and biological integrity of downstream waters and of the larger stream network (Nadeau, 2007). Despite the importance of headwater streams and the groundwater contributions to their discharge, research on baseflow estimation in headwater streams is lacking.

1.1. Baseflow Estimation

The approaches to quantify baseflow contributions to streamflow can be grouped into two categories: graphical methods, which rely exclusively on stream discharge data, and mass balance methods, which rely on stream discharge, chemical constituents in the stream, and streamflow end-member (runoff and baseflow) concentrations. Boussinesq (1877) was the first to develop an equation to separate baseflow using a graphical method with one-dimensional solutions . The Boussinesq equation uses the slope of the falling limb of a stream hydrograph (the baseflow recession curve) to determine a recession constant for the groundwater system that contributes baseflow to the stream. Recession curve methods, such as this, are often considered more objective than other graphical methods like digital or low-pass filter methods because they provide an assumed integrated signal of basin hydrologic and geologic characteristics (the linear recession constant) (Stewart et al., 2007; Miller et al., 2015). This hinges on many assumptions, however, that if violated, make the results inaccurate. The critical assumptions of this method include: (1) that the recession index, the hydraulic characteristics of the contributing aquifer, can be estimated from stream-discharge records; (2) that periods of solely ground water discharge can be consistently correctly identified; and (3) that stream-discharge peaks estimate the magnitude and timing of recharge events (Halford and Mayor, 2000). Some analytical automated tools based on digital filter graphical methods include the hydrograph separation program HYSEP (Sloto and Crouse 1996) and the hydrograph separation computer program called the BFI program (Wahl and Wahl 1995).

Mass balance methods use site-specific chemical concentrations and flows, making this method more objective than graphical methods. The unique, stable chemical concentrations are related to flow paths and physical processes in the watershed, which generate the distinct flow components of stream discharge. Therefore, the mass balance method is including watershed and site-specific hydrogeologic variables inherently as a lumped parameter (Stewart et al., 2007; Zhang et al., 2013). These methods require the simultaneous measurements of both the chemical constituent and stream discharge. The measurements of both components are not often recorded unless the watersheds are instrumented with stream gauges and a method for water sampling. Generally, it is relatively expensive for these data to be collected at headwater streams. Unless these data can be collected at a lower cost, the mass balance method may be difficult to use over long periods of time (Stewart et al., 2007).

Pinder and Jones (1969) and Dinçer et al. (1970) were some of the first to use (1) stable isotopes of water (deuterium and oxygen-18) as tracers, (2) major ions like calcium, silica, and sodium, and (3) specific conductance (SC), to quantify surface runoff and groundwater flow to streams. Later, hydrometric and natural tracer (oxygen 18, deuterium, electrical conductivity, chloride) observations were used in three lower order streams and in six throughflow pits to determine new and old water contributions to headwater catchments during three storm events (Sklash et al., 1986). Many consider stable isotopes to be the most accurate chemical tracers for hydrograph separation (Kendall and Caldwell, 1998), but the costs are prohibitive for frequent and long-term monitoring. Several types of geochemical tracers were later compared, finding that SC was the most effective single parameter for hydrograph separation (Cassie et al., 1996). SC is a measure of the ability of water to conduct electricity and is correlated to the sum of dissolved ions. SC is a parameter which can be easily and continuously measured on-site, allowing for high frequency baseflow estimation, at relatively inexpensive cost (Miller et al., 2014).

The conductivity mass balance (CMB) method uses SC as the chemical tracer. Continuous SC and discharge data have been used with the CMB method to successfully quantify two source water end-members (e.g., runoff and baseflow) contributions to stream flow across a variety of land use areas, as well as many different scales and types of watersheds. These scales include across a smaller mountain to alluvial valley transition in Montana (Covino and McGlynn, 2007), smaller rainfall-dominated streams in the southern United States (Stewart et al., 2007), streams with snowmelt and rainfall influence across the larger Upper Rio Grande

Basin (Rumsey et al., 2020), and across the larger Upper Colorado River Basin (UCRB) (Miller et al., 2014).

There are multiple flow paths which contribute to streamflow. These include direct precipitation, overland flow (as infiltration excess or saturation overland flow), and subsurface flow. Subsurface flow paths may be local shallow-flow paths or regional deep flow paths. The deeper regional flow paths respond more gradually to climate and anthropogenic activities than do local shallow paths, and usually have a greater SC because of longer contact times with subsurface materials. Stream peak flow and SC minimum values occur in the late spring or early summer in snowmelt-dominated watersheds. During this time, the stream is receiving more water from low SC sources (e.g., snowmelt) than groundwater sources (Figure 1.1). Low flow occurs from late summer through early spring, when SC values are higher in the stream, and groundwater flow is expected to be the dominant source-water component contributing to streamflow (Miller et al., 2014).

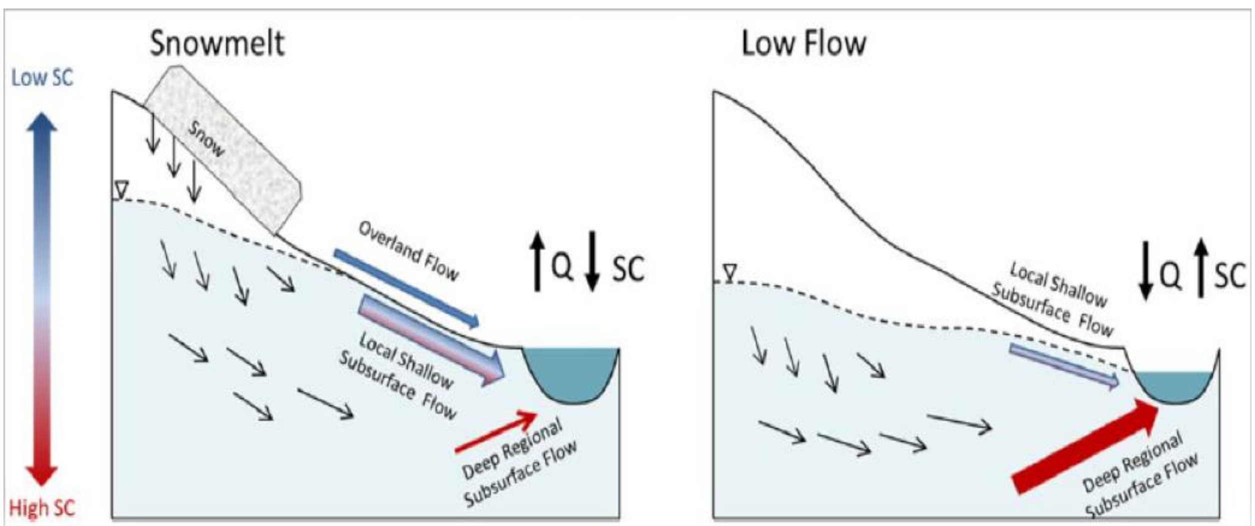

Figure 1.1. Streamflow source water components conceptual model (Miller et al., 2014).

The CMB equation to estimate baseflow discharge (Pinder and Jones, 1969) is:

$$Q_{BF} = Q \frac{(SC - SC_{RO})}{(SC_{BF} - SC_{RO})} \quad \text{[E1.1]}$$

where Q is the hourly discharge in cubic feet per second (cfs), SC is the in-stream hourly specific conductance (µS/cm), SC_{RO} is the specific conductance of the runoff end-member, or high-flow stable average SC minimum value for the entire time period of record, and SC_{BF} is the specific conductance of the baseflow end-member, or the low-flow stable average SC maximum for the time period or year of interest. The low-flow stable average is assumed to represent the integrated, weighted average conductivity of all subsurface water entering the stream above the site location's measurement point (Stewart et al., 2007). SC_{RO} is assumed to be constant throughout the period of record, and therefore the value selected for this end-member is held constant. SC_{BF} may change slightly from year to year, and therefore the value selected for this end-member should apply to the period or year of interest. More discussion about end-members can be found in Chapter 2.

In the past, the CMB method has been limited to locations that had continuous discharge and SC data readily available or to small watersheds that had been thoroughly sampled (Stewart et al., 2007; Rumsey et al., 2015). Miller et al. (2015) successfully estimated baseflow with the CMB method at 12 U.S. Geological Survey (USGS) sites using regression derived estimates of daily SC measurements from a median of 10 samples per year for a period of record of anywhere from 3 to 33 years. They demonstrated that for snowmelt dominated watersheds, baseflow can be estimated for the period of record using CMB with discrete SC data and daily stream discharge data. Rumsey et al. (2015) used similar methods at a larger scale. They used daily streamflow and discrete SC data collected at USGS stream gauges to estimate baseflow at 229 streams across the UCRB. Their data were compiled from the USGS National Water Information System (NWIS) database.

The approach used by these recent studies requires continuous discharge and discrete SC data, but such data may not be readily available, especially at smaller watersheds between 10 and 75 square miles. For the CMB method to be used at ungauged streams (such as smaller headwater streams), the streams must be instrumented to measure discharge and SC, on at least a daily basis. To make this method more accessible, the application of low-cost data loggers to measure SC would be advantageous.

1.2. Continuous Conductivity Data Loggers for use with the CMB Method

The methods outlined by Miller et al. (2015) and Rumsey et al. (2015) are not an option for streams that do not have discrete SC data available in NWIS, or streams where it would be difficult to return to 4 to 10 times to obtain discrete samples. In most cases, it is desired to collect continuous relative SC values, which is preferred to regression derived SC values. Onset HOBO fresh-water conductivity data loggers (hereafter referred to as U24 data loggers) are available for continuous SC data collection, however, these cost upwards of 750 US dollars. U24 loggers have a memory capacity of 18,500 temperature and conductivity measurements when using low conductivity range, a temperature measurement range of -2 degrees to 36 degrees Celsius (28° to 97°F), and a battery life of 3 years at a one-minute logging interval (Onset, 2021). The cost of a U24 logger may be prohibitive to collecting data at a larger number of headwater streams.

Recently a low-cost Stream Temperature, Intermittency, and Conductivity (STIC) data logger was designed (Chapin et al., 2014) to collect SC data in streams. Each STIC data logger was modified from an existing Onset HOBO Pendant waterproof temperature and light data logger (Model UA-002-64, $64 USD). HOBO Pendant loggers have sensors to measure water temperature and light intensity from 0 – 330,000 lux or can measure light intensity in lumens per square-foot. Each HOBO Pendant's temperature logging capabilities was retained. However, each HOBO Pendant's light sensor was removed, while existing light sensor circuitry was retained and connected to two external machine pin electrodes (Figure 1.2).

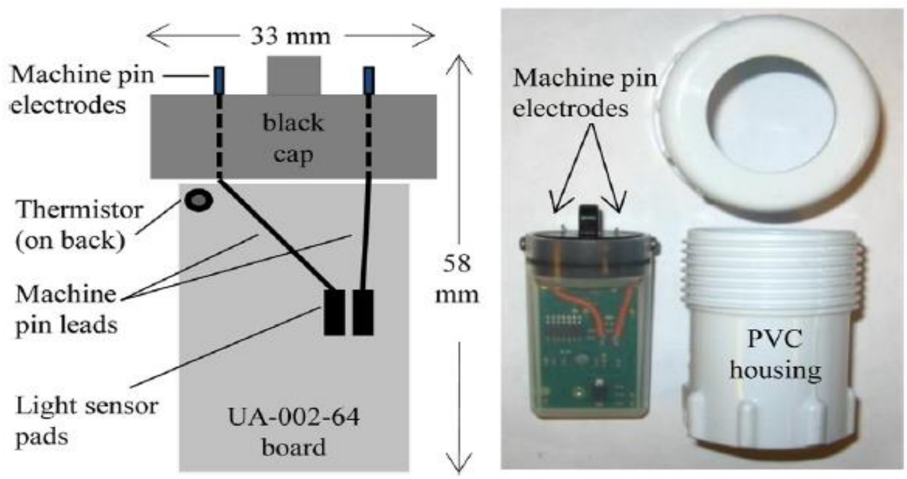

Figure 1.2. Two images showing the modifications made to HOBO Pendants to create new low-cost STIC data loggers (Chapin et al., 2014).

With the light sensor removed and the electrodes connected, "C" is now recorded on the light data channel (Chapin et al., 2014). The term C will be used to define the raw data collected by the STIC loggers prior to being calibrated to known SC standards (recorded as lumens/ft^2), as electrode response varies from one STIC logger to another. Once calibrated, STIC loggers measure and record electrical conductivity (EC), which can easily be converted to relative specific conductance (rSC) for use with hourly or daily discharge data to estimate continuous baseflow with the CMB method. Although STIC data loggers do not record absolute specific conductance (SC), they measure temporal variations in relative SC, which are equivalent to the absolute SC when used with the CMB method. STIC logger data storage holds over 28,000 measurements, which equates to 1200 days of data at hourly sampling.

1.3. Current Research

The purpose of this study is to investigate a new low-cost means to log continuous SC data in snowmelt-dominated headwater streams where data collection options are limited by budget, in order to quantify baseflow discharge using the conductivity mass balance (CMB) method at ten streams on the Medicine Bow-Routt National Forests in northwest Colorado and southern Wyoming. Gauging previously ungauged streams and measuring continuous SC will add to the active research surrounding baseflow estimation in headwater streams. To address the purpose of this study, STIC data loggers are examined as a low-cost means to collect continuous rSC data for the CMB method.

STIC data loggers have been used in previous studies for recording temperature and intermittency of streams (Wallin, 2019; Dorn et al., 2018), and for short-term (one month or less) testing of the data of no more than five loggers for the CMB method of baseflow estimation (Gillman et al., 2017). However, no published studies exist to our knowledge that have tested or confirmed the use of larger quantities of STIC loggers for acquiring continuous SC data for the CMB method over a complete water year in extreme field conditions at headwater streams with different watershed characteristics, nor compared STIC logger data and costs with conventional EC data loggers.

This study addresses these problematic gaps in knowledge by first consulting with the U.S. Forest Service to identify and select one gauged and nine ungauged snowmelt-dominated headwater streams where stage-discharge relationships and baseflow estimations are desired. Next, goals, objectives, and hypotheses were developed to address these gaps by acquiring new information about stream discharge, STIC loggers, the CMB method with data from different logger types, and baseflow. The goals and objectives of this study are presented in Table 1.1.

Table 1.1. Study Goals and Objectives

Goals	Objectives
(G1) Determine stage-discharge relationships for nine headwater streams over at least one annual hydrograph (a tenth site is already gauged).	(O1) Instrument nine ungauged snowmelt-dominated headwater streams in northwestern Colorado to generate continuous discharge data (a tenth stream is already gauged).
(G2) Determine if STIC loggers can be used in the field for extended periods of time (at least one year) and under extreme field conditions (e.g., temperature, freezing, sediment, flow).	(O2) Deploy low-cost STIC loggers in ten snowmelt-dominated headwater streams for at least one year under extreme field conditions.
(G3) Determine continuous in-stream relative specific conductance (SC) values with calibrated STIC loggers at ten snowmelt-dominated headwater streams.	(O3) Calibrate 17 STIC loggers in a lab using logger readings at different temperatures and known SC standards, and apply this to each STIC logger's continuous in-stream field data.
(G4) Determine if temporal STIC logger data trends are comparable to temporal data trends measured using a higher-cost HOBO U24 logger.	(O4a) Deploy both U24 and STIC loggers at 3 sites. (O4b) Quantitatively and qualitatively compare STIC and U24 logger temporal data trends, limitations, and advantages.
(G5) Determine if STIC logger data can be used from snowmelt-dominated headwater streams with different SC ranges (both wide and narrow differences between runoff and baseflow end-member values) (Rumsey et al., 2015) to estimate baseflow with the CMB method.	(O5) Deploy STIC loggers at watersheds that, based on geology, are likely to have different SC ranges (both wide and narrow differences between runoff and baseflow end-member values (Rumsey et al., 2015)).
(G6) Estimate baseflow in all streams suited for the CMB method.	(O6) Plot SC data with stream discharge data to determine which sites have data that are suited for the CMB method, then estimate baseflow at these sites.
(G7) Determine if BFI estimates calculated with STIC and U24 logger data are similar.	(O7) Compare BFI estimates calculated with STIC and U24 logger data.

Based on the demonstrated success of short-term STIC logger continuous SC studies for use with the CMB method to estimate baseflow (Gillman et al., 2017), this study hypothesizes that:

(1) Calibrated STIC loggers can be used to measure continuous relative SC in snowmelt-dominated headwater streams for at least one year in freezing temperatures, in both high and low stream flows, and while buried under sediment;

(2) Temporal STIC logger data trends are comparable to temporal SC data trends measured using a duplicate STIC logger or a higher-cost HOBO U24 logger;

(3) STIC logger data are more suitable for estimating baseflow with the CMB method at snowmelt-dominated headwater streams with a wide range of relative SC values (min and max SC values differ by greater than 100 µS/cm) than those with a narrow range (Rumsey, 2020);

(4) BFI estimates are similar (within 5%) at the same site location when calculated with STIC or U24 logger data; and

(5) Contribution of groundwater input to post snowmelt-dominated stream discharge in headwater streams can be estimated using the CMB method with STIC logger data.

The following chapter will describe the site locations and methods used to accomplish the goals and objectives of this project. Methods include field methods, laboratory calibrations, and statistical and data analysis. Results of this study are presented in Chapter 3,including stage-discharge rating curves, hourly discharge hydrographs, STIC logger calibration results, data logger field data comparisons, sites that are suited for the CMB method, and baseflow estimations. The discussion and interpretation of the data are in Chapter 4, including future rating curve development, how different data loggers performed in extreme field conditions and how their data compare, lab calibration successes, SC trends and end-member selection, estimating baseflow with different data loggers, and what implications BFI estimates have at different site locations. Hypotheses findings, recommendations, and a cost-benefit summary can be found in Chapter 5.

2. METHODS

This study aims to quantify baseflow discharge using the CMB method with data from low-cost STIC data loggers and compare these results with duplicate STIC and higher-cost U24 data loggers at ten snowmelt-dominated headwater streams. The CMB method uses equation E1.1. The CMB method is only applicable if these three assumptions are valid: (1) no other end-members contribute to streamflow or are considered negligible, (2) SC_{RO} is held constant during the period of record, and (3) SC_{RO} and SC_{BF} are significantly different from each other (Rumsey et al., 2015; Sklash and Farvolden, 1979).

2.1. Study Area and Site Descriptions

This study was completed in the Medicine Bow-Routt National Forests in northwest Colorado and southern Wyoming of the United States of America. Nine of the ten streams in this study are headwaters of the Upper Yampa River Watershed (Figure 2.1), in northwestern Colorado surrounding the town of Steamboat Springs. The Yampa River is unique as it is a largely unregulated and free-flowing river in the Colorado River Basin. The UYRW encompasses about 1,798 square miles (4656.8 km^2) and drains west of the Continental Divide in northwestern Colorado (Bauch et al., 2012). The tenth stream in this study, the Encampment River, is tributary to the North Platte River in southern Wyoming, which then flows east and into the Gulf of Mexico. Though the Encampment River is not a part of the UYRW or the Yampa River Basin, its headwaters are located on the Medicine-Bow Routt National Forest on the continental divide, within a few miles of a site that lies within the UYRW (Figure 2.2).

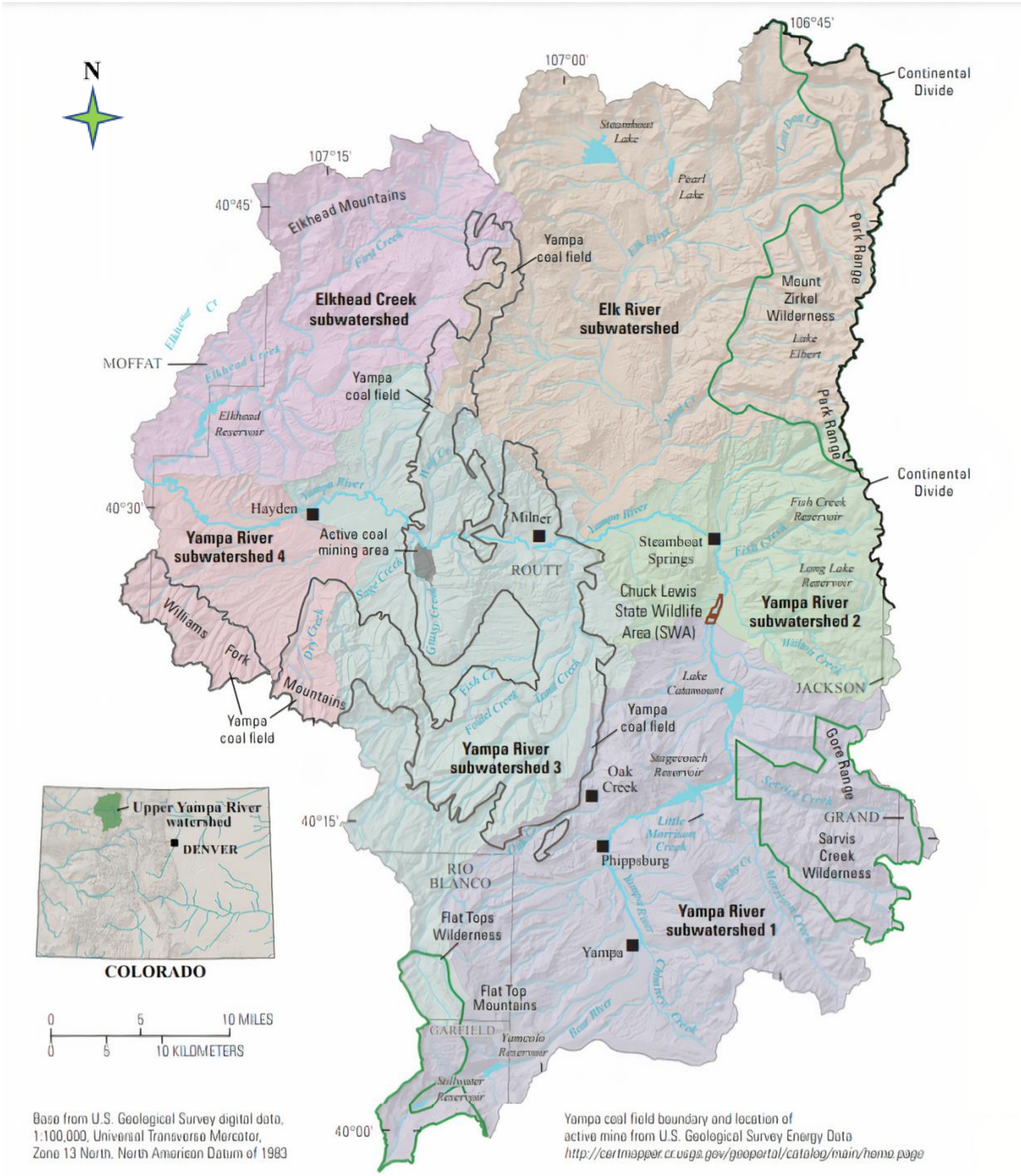

Figure 2.1. The Upper Yampa River Watershed (UYRW) (Bauch et al., 2012).

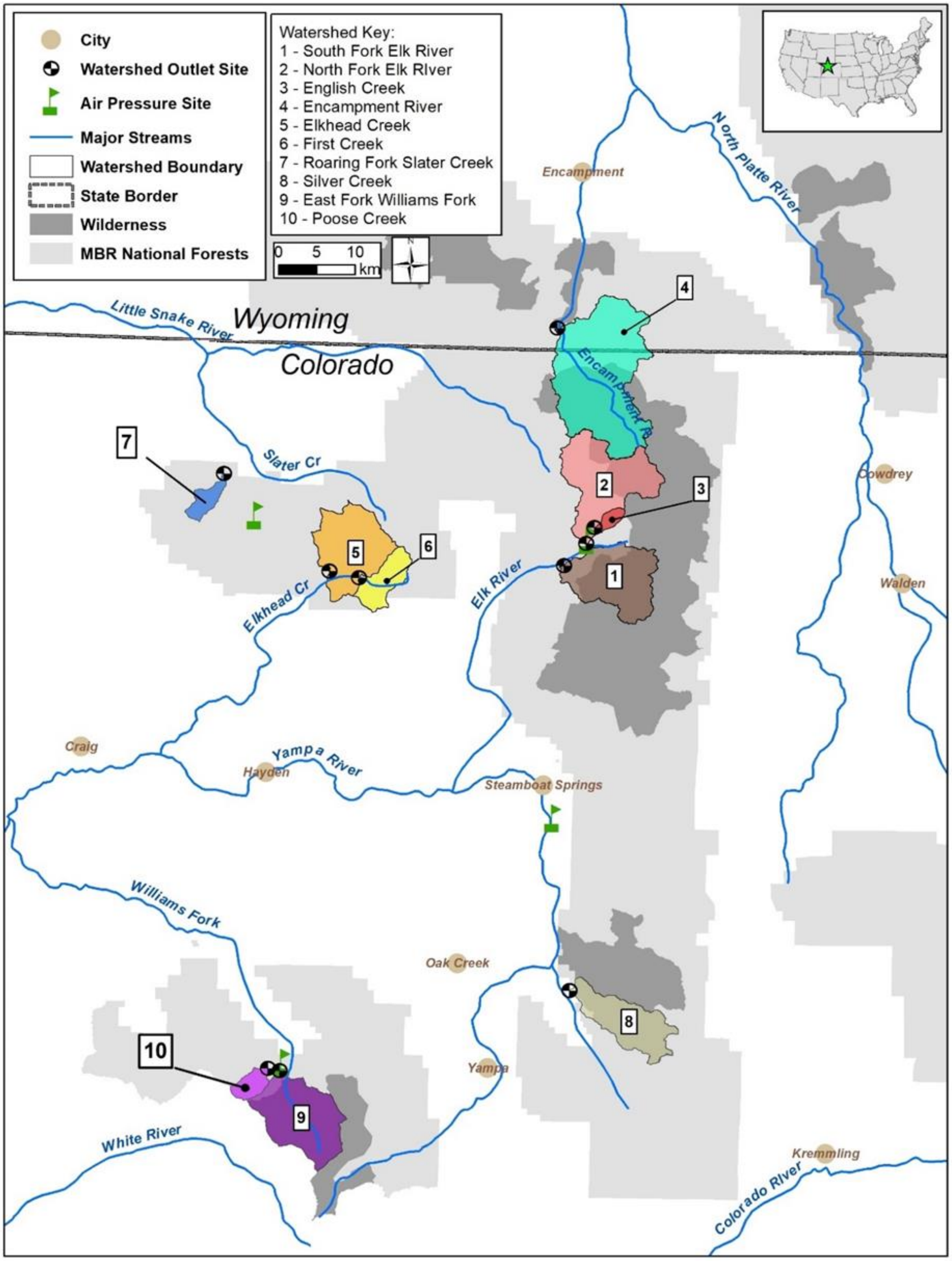

Figure 2.2. Baseflow estimation study area watersheds. Map includes watershed outlet sites which gives locations of STIC loggers, U24 loggers, water pressure transducers and stage-discharge sites. Air pressure transducer locations are also displayed (Carleton, 2020).

The streams in this study have minimal anthropogenic disturbances and can serve as good baselines sites for future work. All streams in this study are first, second, or third order streams, with an exception of the Encampment River, a fourth order stream (USDA FS, 2009). All streams in this study are snowmelt-dominated watersheds. Snowmelt-dominated watersheds are defined as sites where the peak stream discharge occurs during snowmelt in late spring or early summer and is about an order of magnitude greater than low-flow conditions, which persist from late summer until late spring. It is expected for there to be an inverse relationship between SC and stream discharge described by a power function at these locations (Miller et al., 2014).

This study includes streams from five different mountain ranges, with drainage areas ranging from 2.5 – 73 square miles (6.5 – 189.1 km^2). Watershed elevations range from 7,700 – 12,200 feet (2,347 – 3,718.5 m) with mean basin slopes of 21 – 31 percent (Clark, 2000; USGS, 2020). The streams in this study have flows as low as 0.2 cubic feet per second (cfs) after snowmelt and as high as 859 cfs during peak flow, with SC values between 4.5 µS/cm during high flow (crystalline bedrock) to 488 µS/cm during baseflow (sedimentary bedrock).

Each site was chosen for its minimal disturbance, rare and vulnerable species living in the watershed, proximity to a USGS site, and management priorities. More detail for each site is described in subsections *2.1.1 - 2.1.10* as well as in Table 2.1. In Table 2.1 general bedrock type was sorted into one of two categories: crystalline (igneous or metamorphic) or sedimentary. Each stream had one representative section chosen based on walking a few miles of the stream and finding a section that was not only representative of the greater stream, but also was accessible by both vehicle and foot, wadable during higher flows, and a relatively straight stretch where no changes in surface water inflow or outflow were occurring.

2.1.1. South Fork of the Elk River (Site 1)

Site 1, the South Fork of the Elk River lies in the Park Range of the Rocky Mountains, off Seedhouse Road near Clark, Colorado. Site 1 flows northwest to the Middle Fork of the Elk River, with headwaters in the Mt. Zirkel Wilderness. This watershed has mountainous, forested terrain as well as meandering wetlands just upstream of the site location. South Fork of the Elk River has Precambrian fractured crystalline bedrock underlain by metamorphic (gneiss) rock and overlain by eolian and glacial deposits (CSU CNHP, 2019). Site 1 was chosen in consultation with the US Forest Service due to its minimal anthropogenic and fire disturbance, the historic USGS stream discharge site adjacent to the site, and the presence of white flowered azalea (rare in Colorado) and brook trout here (CSU CNHP, 2019).

2.1.2. North Fork of the Elk River (Site 2)

Site 2, the North Fork of the Elk River is in the Park Range of the Rocky Mountains, off Seedhouse Road near Clark, Colorado. This site flows south to the Middle Fork of the Elk River, just upstream of the Middle Fork's confluence with the South Fork. Its headwaters originate in the Mount Zirkel Wilderness, and one of its tributaries is English Creek (Site 3). North Fork of the Elk River is mountainous and forested with mostly dead trees and there is at least one known spring upstream of Site 2. Precambrian fractured crystalline bedrock aquifers are overlain by glacial till and volcanic deposits here. Surficial geology is sedimentary (clastic) and metamorphic (gneiss) (CSU CNHP, 2019). North Fork of the Elk River was chosen in consultation with the US Forest Service due to its accessibility, minimal disturbance, and presence of boreal toad, white flowered azalea (rare in Colorado), Subalpine Riparian Willow Carr, Booth's Willow, and Montane Riparian Forests in the watershed (CSU CNHP, 2019).

2.1.3. English Creek (Site 3)

Site 3, English Creek lies in the Park Range of the Rocky Mountains, off Seedhouse Road below near Clark, Colorado. This site flows southwest to the North Fork of the Elk River (Site 2). Its headwaters originate in the Mount Zirkel Wilderness, near to a fen that is upstream of this site. The terrain is a moderately steep canyon into a small open valley. Precambrian fractured crystalline bedrock aquifers are overlain by glacial till at this site. Surficial geology is sedimentary (clastic) and metamorphic (gneiss) (CSU CNHP, 2019). English Creek was selected in consultation with the US Forest Service due to its accessibility, minimal disturbance, and presence of boreal toad, white flowered azalea (rare in Colorado), Subalpine Riparian Willow Carr, Booth's Willow, and Montane Riparian Forests in the watershed (CSU CNHP, 2019).

2.1.4. Encampment River (Site 4)

Site 4, Encampment River is in the Sierra Madre Range, an extension of the Park Range, above Hog Park Creek a few miles north of the Colorado-Wyoming border. Site 4 flows north to the North Platte River, and its headwaters are in the Mount Zirkel Wilderness. The terrain is mountainous and forested. Precambrian fractured crystalline bedrock is underlain by intrusive and metamorphic (gneiss) rock, which is overlain by glacial till (Clark et al., 2000). Encampment River was selected in consultation with the US Forest service due to its minimal disturbance, the active USGS stream gaging station at this site, and the historical USGS stream discharge and water quality data available here.

2.1.5. Elkhead Creek (Site 5)

Site 5, Elkhead Creek is in California Park in the Elkhead Mountains, below First Creek (Site 6). Elkhead creek flows southwest to Elkhead Reservoir and then to the Yampa River, with headwaters all over California Park. This area is considered a high meadow. The general bedrock of this watershed is Tertiary volcanic with Cretaceous sedimentary (clastic) units (Gurrieri, 2017). Elkhead Creek was selected in consultation with the US Forest Service due to being the Forest's number one priority watershed for restoration based on unique geological, zoological, historical, paleontological, and scenic values. Sensitive species in the watershed include Colorado River cutthroat trout, mountain sucker, boreal toad, Greater sandhill cranes, and Columbian sharp-tailed grouse (CSU CNHP, 2019). There is also an active USGS gage downstream.

2.1.6. First Creek (Site 6)

Site 6, First Creek is in California Park in the Elkhead Mountains and flows west to Elkhead Creek (Site 5). First Creek is also a high meadow and has general bedrock of Tertiary volcanic with Cretaceous sedimentary (clastic) units (Gurrieri, 2017). This site is within the same watershed at Elkhead Creek, so it was selected in consultation with the US Forest Service for the same reason of being the Forest's number one priority watershed for restoration, and for being headwaters of Elkhead Creek (CSU CNHP, 2019).

2.1.7. Roaring Fork of Slater Creek (Site 7)

Site 7, Roaring Fork of Slater Creek lies in the Elkhead Mountains off County Road 82, north of Lost Park Guard Station. The Roaring Fork flows northeast to the mainstem of Slater Creek with mossy groundwater-dependent ecosystems and springs all around the area and upstream (Schnackenberg, 2020). The terrain is mountainous and forested, and the general bedrock is Tertiary volcanic with Tertiary sedimentary units (Gurrieri, 2017). This site was selected in consultation with the US Forest Service due to the minimal disturbance and indicators of a strong groundwater component here, in the form of a rock glacier or other groundwater influence (Schnackenberg, 2020).

2.1.8. Silver Creek (Site 8)

Site 8, Silver Creek is in the Gore Range of the Rockies within Sarvis Creek Wilderness. This site is above Morrison Creek and flows northwest into Morrison Creek, with large sedge fens and wetlands upstream. The US Forest Service has proposed this area as a Research Natural Area, and the terrain is gentle mountains (montane wet meadow) dominated by willows (CSU CNHP, 2019). This area has Precambrian fractured crystalline bedrock (granitic) (Gurrieri, 2017), without Pleistocene glaciation influence (Routt National Forest, 1998). Silver Creek was chosen in consultation with the US Forest Service due the strong groundwater component of its headwaters (the South Fork of Sliver Creek and sedge fens) and the fact that it is largely undisturbed (the entire watershed is within wilderness) (Schnackenberg, 2020).

2.1.9. East Fork of the Williams Fork (Site 9)

Site 9, the East Fork of the Williams Fork lies in the Flat Tops of the Rocky Mountains in a canyon above Pyramid Guard Station. The East Fork flows northwest to the Williams Fork with headwaters is the Flat Tops Wilderness. The terrain is a forested narrow and steep mountain valley. The geology consists mainly of the Cretaceous Mancos Shale Formation, with western side slopes consisting of landslide deposits from the Holocene and Pleistocene. This watershed contains the best known montane deciduous riparian forest in the upper Colorado River Basin, including the globally vulnerable narrow-leaf cottonwood and thin-leaf alder (CSU CNHP, 2019). There is also Colorado River cutthroat trout present here (Schnackenberg, 2020). This site was selected in consultation with the US Forest Service due to being largely undisturbed and the presence of globally vulnerable species as well as species of special concern in Colorado (Schnackenberg, 2020).

2.1.10. Poose Creek (Site 10)

Site 10, Poose Creek is in the Flat Tops of the Rocky Mountains below County Road 8. Poose Creek has headwaters in the Flat Tops above Vaughan Lake, and flows north to the East Fork of Williams Fork, below Site 9. The terrain is montane riparian willow, and species present include Carr and Geyer's Willow-Rocky Mountain Willow, which are globally vulnerable. The geology consists mainly of the Cretaceous Mancos Shale Formation with inter-tongues of Frontier sandstone and Mowry Shale (CSU CNHP, 2019). This site was selected in consultation with the US Forest Service based on presence of the Colorado River cutthroat trout as well as available historic data, including stream temperatures and fish implanted Passive Integrated Transponder (PIT) detectors to assess movement behavior and habitat use (Schnackenberg, 2020).

Please see Table 2.1 for additional details about each site location.

2.2. Field Methods

The field research for this study took place between fall 2016 and fall 2018. When goals or objectives from Table 1.1 are described, each will be abbreviated with a G for a goal and an O for an objective, followed by the goal or objective's associated number. To determine stage-discharge relationships for nine headwater streams over at least one annual hydrograph, the first objective (O1) was to instrument the ungauged streams to generate continuous discharge data.

Table 2.1. Baseflow estimation study detailed descriptions of the ten study sites. Drainage area, elevation, mean basin slope, and annual precipitation data were obtained from StreamStats (USGS, 2020), except for Site 4 (Clark, 2000). Stream order was calculated using Strahler Stream Order (Strahler, A.N., 1952) and a US Forest Service visitor map (USDA FS, 2009). Note "General Bedrock Type" is sorted into one of two categories: Crystalline (Igneous or Metamorphic) or Sedimentary (Gurrieri, 2017; CSU CNHP, 2019).

Site Number: Stream Name	Location (UTM Zone 13N)	Drainage Area in mi^2 (km^2)	Elevation in feet (meters)	Stream Order	Terrain (CSU CNHP, 2019)	Mean Slope (%)	Annual Precipitation in inches (cm)	General Bedrock Type
1: South Fork of the Elk River	E 347409 N 4512038	34 mi^2 (88 km^2)	7,990 - 11,900 ft (2435 - 3627 m)	3rd order	Mountainous and forested	31% basin	45.6 in (115.8 cm)	Crystalline
2: North Fork of the Elk River	E 350303 N 4514943	41 mi^2 (106 km^2)	8,000 - 12,200 ft (2438 - 3719 m)	3rd order	Mountainous, forested, many dead trees	28% basin	45.5 in (115.6 cm)	Crystalline
3: English Creek	E 351400 N 4517015	2.5 mi^2 (6.5 km^2)	8,460 - 10,900 ft (2579 - 3322 m)	1st order	Moderately steep canyon into an open, small valley	21% basin	41.3 in (104.8 cm)	Crystalline
4: Encampment River	E 346551 N 4543090	73 mi^2 (189 km^2)	8,267 - 11,385 ft (2520 - 3470 m)	4th order	Mountainous and forested	1.9% mainstem	16.6 - 29.9 in (42.2-75.9 cm)	Crystalline
5: Elkhead Creek	E 316787 N 4511314	45 mi^2 (117 km^2)	7,730 - 10,900 ft (2356 - 3322 m)	3rd order	High meadow	24% basin	31.7 in (80.5 cm)	Sedimentary
6: First Creek	E 320623 N 4510462	12 mi^2 (31 km2)	7,960 - 10,900 ft (2426 - 3322 m)	1st order	High meadow	26% basin	33.6 in (85.3 cm)	Sedimentary
7: Roaring Fork of Slater Creek	E 303012 N 4524080	5.2 mi^2 (13 km^2)	8,490 - 10,800 ft (2588 - 3292 m)	1st order	Mountainous & forested	25% basin	46.3 in (117.6 cm)	Sedimentary
8: Silver Creek	E 348126 N 4456474	24.8 mi^2 (64 km^2)	7,890 - 10,800 ft (2405 - 3292 m)	3rd order	Gentle mountains, willow-dominated wet meadow	27.9% basin	35.8 in (90.9 cm)	Crystalline
9: East Fork of Williams Fork	E 310248 N 4446026	35 mi^2 (91 km^2)	8,510 - 12,000 ft (2594 - 3658 m)	3rd order	Forested narrow / steep mountain valley	23% basin	43.3 in (109.9 cm)	Sedimentary
10: Poose Creek	E 308754 N 4446325	5.2 mi^2 (13.5 km^2)	8,890 - 10,900 ft (2710 - 3322 m)	2nd order	Forested	22% basin	40.3 in (102.5 cm)	Sedimentary

2.2.1. Stage and Discharge Measurements

Once a representative section of stream was selected, a more specific cross-section, PVC pipe stilling well, and staff gauge locations were chosen. Each stilling well was installed in a perennially deep pool that was least likely to be downstream of moving boulders or dead wood. A staff gauge was mounted to the outside of each stilling well. UTM coordinates and elevation benchmarks were collected from the top of the stilling wells and at the cross-section locations. Once each stilling well and staff gauge were installed, an initial stage measurement was recorded by reading the water level on the staff gauge as close to the top of the hour as possible. Within this same timeframe, a discharge measurement was collected using the USGS velocity-area method (Turnipseed and Sauer, 2010).

Discharge was measured at one or two cross-section locations for each stream within 0 – 40 feet (0 – 12.2 m) of the stilling well, as close to the top of the hour as possible. Stream velocities were measured at 20 – 65 points with equal incremental widths between each measurement along the cross section, depending on the width of the stream at the cross-section. Current-velocity meter methods were used (Sanders, 1998).

The total discharge measurement represents one moment in time, although the measurements along the cross section took 20 – 60 minutes. For this reason, measurements were not taken during heavy rain or when discharge appeared to be rapidly changing. A stage reading was also taken after the discharge measurement, to track if and how much the water level, and therefore discharge, may have changed since the discharge measurement started. If the stage readings before and after the discharge measurement were different, the final stage value was interpolated based on the time of each stage reading and the time closest to the top of the hour.

2.2.2. Water and Barometric Pressure Measurements

Non-vented absolute water pressure transducers (HOBO U20 loggers) were installed in stilling wells in Fall 2016 or 2017. Metal wire fixed the pressure transducers to the removable cap at the top of each stilling well, so that the transducers were at a height which allowed for constant water submersion. Barometric pressure pushes down on the water, and non-vented pressure transducers do not self-compensate for barometric changes. Therefore, these must be compensated for using separate barometers. Barometric compensation or correction of non-vented water pressure transducers can be completed with the following equation:

$$h = \frac{Pw - Pa}{\rho * g} \qquad \text{[E2.1]}$$

where h is water level or stage height, Pw is the pressure of water, Pa is the barometric pressure, ρ is the density of fresh water at temperature, and g is the acceleration due to gravity. HOBOware Pro software also contains a barometric compensation tool, which is what was used for stage height computations.

Continuous water and barometric pressure data were obtained by deploying Onset HOBO U20 non-vented water and barometric pressure transducers. The same barometric pressure transducer was launched for both Elkhead and First Creek in November 2016. This transducer was installed inside PVC pipe near the ground within 10 miles of the pressure transducers at both creeks and within 200 feet of the elevations of the transducers. The same barometric pressure transducer was launched in November 2016 for the North Fork and the South Fork of the Elk River, as well as English Creek. This transducer was located inside the Seedhouse Guard Station within 3 miles of both rivers and at approximately the same elevation. Barometric pressure transducers were also launched at the Steamboat Springs Forest Service District office for the site at Silver Creek, and near the Pyramid Guard Station for the East Fork of Williams Fork and Poose Creek sites.

The Onset U20-001-01 HOBO Freshwater Water Level Data Logger (non-vented pressure transducer) measures water levels accurate within a typical error of ±0.05% FS, or 0.5 cm (0.015 ft) of water. The maximum error is ±0.1% FS, or 1.0 cm (0.03 ft) of water. Pressure response time (90% of the time) is less than one second. Temperature accuracy ±0.44°C from 0° to 50°C (±0.79°F from 32° to 122°F) with a response time (90% of the time) of five minutes in water. Battery life is five years for typical use with one minute or greater logging interval. Memory is 64K bytes memory (approximately 21,700 pressure and temperature samples). U20 loggers have a factory calibrated range of 69 to 207 kPa (10 to 30 psia), an operation range of 0 to 207 kPa (0 to 30 psia), an altitude range of approximately 0 to 9 m (0 to 30 ft) of water depth at sea level, or 0 to 12 m (0 to 40 ft) of water at 3,000 m (10,000 ft) of altitude (Onset, 2020).

2.2.3. STIC Logger Modifications and Conductivity Measurements

Objectives 2, 4a, and 5 were completed to address (G2) if STIC loggers can be used in the field for extended periods of time and under extreme field conditions, (G4) if temporal STIC logger data trends are comparable to temporal data trends measured using a higher-cost HOBO U24 logger, and (G5) if STIC logger data can be used from snowmelt-dominated headwater streams with different SC ranges (both wide and narrow differences between runoff and baseflow end-member values) (Rumsey et al., 2015) to estimate baseflow with the CMB method. (O2) STIC loggers were deployed in ten snowmelt-dominated streams for at least one year under extreme field conditions; (O4a) U24 loggers and STIC loggers were deployed at three site locations; and (O5) STIC loggers were deployed at watersheds that, based on geology, were likely to have different SC ranges.

STIC logger modifications for this study were completed by John Korfmacher of the U.S. Forest Service (USFS) Rocky Mountain Research Station and Timothy Stroope, a USFS Washington office hydrogeologist, but anyone with the required materials may make the modifications. Each HOBO Pendant's light sensor was removed, while existing light sensor circuitry was retained and connected to two external machine pin electrodes made from 24-gauge wire. The machine pin electrodes were inserted into drilled holes in the housing cap, soldered to the two light sensor contact pads on the inside of the HOBO Pendant, and attached to the external housing of each pendant with a two-part marine epoxy. The machine pin electrodes protrude at least 3 mm from the top of the housing cap and are approximately 1.6 cm apart from one another (Chapin et al., 2014). In fact, each STIC logger is unique, with slightly different spacing between electrodes, which is why calibration is required for one to accurately measure electrical conductivity (EC). The electrodes are bendable, so the entire STIC logger should be protected within PVC housing, as shown in Figure 1.2, for field deployment (Chapin et al., 2014).

Total STIC modification time for Chapin et al. (2014) was 15 minutes per unit (excluding epoxy drying) and 40 STIC loggers were built in 8 hours of work time. The cost for the electronic parts, epoxy, PVC housing, and other field deployment materials was under $10 USD per unit and the total cost for a field ready STIC logger was under $75 USD (Chapin et al., 2014). STIC logger launch setup, field checkups, and data download conveniently use the same Onset Base-U-4 USB Base Station or Onset U-DTW-1 waterproof shuttle as the HOBO Pendant. STIC loggers also use the same standard HOBOware Pro software that many other common

HOBO data loggers use, including the pressure transducers described in the previous section and the U24 low-range electrical conductivity (EC) data loggers that were used for comparison with the STIC loggers.

To regularly cross reference each stream's conductivity, a variety of methods were used to measure it, including a hand-held conductivity meter for discrete measurements and different types of continuous conductivity data loggers. Standard HOBOware Pro software, Onset Base-U-4 USB Base Station and Onset HOBO COUPLER-UA were used to pre-launch STIC loggers in the office with a delayed start to log on a continuous one-hour interval, at the top of the hour. STIC data loggers were deployed at ten sites in fall 2016 and/or 2017. The STIC loggers were protected by PVC housing and zip-tied to a one cubic foot (0.028 m^3) mesh bag filled with stones from the stream. Each bag was submerged within 40 feet (12.2 meters) of the site location where stage was measured, where no changes in surface water inflow or outflow were occurring, in a perennially deep pool downstream of a boulder or bend in the stream to protect the loggers from being washed downstream during high flows. The mesh bag was either flagged directly or marked by flagging a tree on the nearest bank. UTM coordinates were recorded of the STIC loggers' locations. STIC data loggers were downloaded while in the field one to two times per year, but never within five minutes of the top of the hour log time.

One Onset HOBO U24 low-range (0 - 1,000 µS/cm) conductivity logger was deployed at North Fork of the Elk River, Elkhead Creek, and Silver Creek in fall 2017. Each U24 logger was zip-tied to a two cubic foot (0.056 m^3) mesh bag filled with stones from the stream, adjacent to the STIC loggers. These U24 loggers were pre-launched in the office with standard HOBOware Pro software, Onset Base-U-4 USB Base Station and Onset HOBO COUPLER2-C with a delayed start to log on a continuous one-hour interval, at the top of the hour. U24 data loggers were downloaded in fall 2018. In addition, at each representative section of stream, when stage and discharge measurements were collected, hand-held conductivity, temperature, and pH measurements were also taken with an Oakton pH/CON10 meter, as close to on the top of the hour as possible.

2.3. STIC Logger Laboratory Calibration Materials and Methods

To address (G3) continuous in-stream relative specific conductance (SC) values with calibrated STIC loggers at ten snowmelt-dominated headwater streams, the first part of objective 3 was to calibrate 17 STIC loggers in a lab using logger readings at different temperatures and known SC standards. There were three STIC logger laboratory calibrations performed in 2019. All calibrations followed a similar procedure (Gillman et al., 2017) that is summarized here, and any differences between calibrations follow. The first STIC logger lab calibration placed 10 STIC loggers within the same 1000 mL beaker, the second placed all 17 STIC loggers in the same 1000 mL beaker, and the final STIC logger lab calibration placed 9 STIC loggers in the same 1000 mL beaker. Each calibration used different known conductivity standards.

2.3.1. STIC Logger Calibration Materials Used

- 5 dilutions or standards with known specific conductance (SC) (within SC range expected at streams of interest) at reference temperature (e.g., 10, 60, 125, 250, and 500 µS/cm at 25°C)
- Ice and ice bath container
- ~1000 mL glass beaker for every 10 STIC loggers
- Slightly smaller glass container to put on top
- 1–2 known conductivity standards (bracketed within expected SC range) for the conductivity meter calibration
- A calibrated conductivity meter (e.g., Oakton 600 series)
- DI water
- Onset HOBO UX120–006M logger with a TMC1-HD thermistor

- STIC loggers
- Standard HOBOware Pro software
- Onset Base-U-4 USB Base Station and Onset HOBO COUPLER-UA
- Clock or timer that displays seconds
- Camera (optional)

2.3.2. STIC Logger Calibration Methods

Five conductivity standards or volumetric dilutions at 25°C were prepared within a range of expected SC values for the streams of interest. As with any multi-point meter calibration, a 5-point calibration differs from a 1-point calibration in the amount of points checked for their accuracy. The 5-point calibration consists of a high, an approximate quartile 3, a middle, an approximate quartile 2, and a low check of SC value. Thus, 5-points give greater proof of accuracy over a larger range (Lui and Chow, 2018). Each dilution was left open to equilibrate with the atmosphere for at least four hours prior to use. The lowest conductivity standard or dilution was placed into a clean dry 1000 mL beaker and allowed to chill in a refrigerator for several hours.

Next, STIC logger(s) and the external thermistor were placed into the beaker filled with chilled standard, which was placed onto an ice bath in a freezer until the temperature approached 1–2°C. A smaller glass beaker was placed on top of the STIC loggers to keep them fully submerged. The conductivity was measured with a calibrated conductivity meter, the exact time was noted, the STIC logger(s) and external thermistor were launched (logging at a frequency of every 30 seconds), and the ice bath removed from the freezer (Figure 2.3). The data loggers and dilution were then allowed to sit undisturbed at room temperature over a 24 to 36-hour period, while the thermistor recorded continuous temperature data and the STIC loggers continuously recorded data to be used in EC-temperature calibration relationships. The conductivity standard

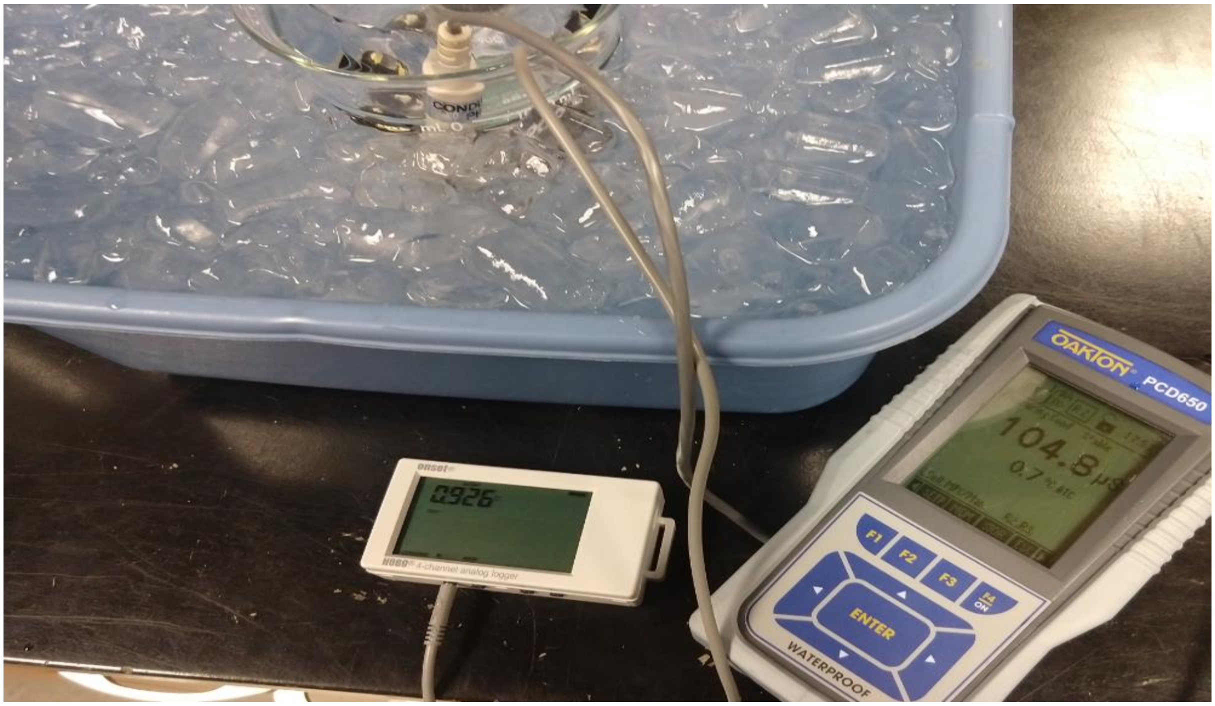

Figure 2.3. A photo of the start of the third point of the April STIC logger lab calibration.

was then measured at room temperature with the calibrated conductivity meter, the exact time noted, and then the data loggers were rinsed with DI water.

This procedure was then repeated with the other conductivity standards or known SC dilutions. The measurements made with the hand-held conductivity meter at the beginning and end of each calibration point were used to generate a continuous dataset of EC data that changed with temperature to be used in future EC-temperature calibration relationships (Gillman et al., 2017). In February 2019, the known SC standards were 15.6 µS/cm, 55.6 µS/cm, 125.0 µS/cm, 294.3 µS/cm, and 473.0 µS/cm. In April 2019, the known SC standards measured 11.3 µS/cm, 49.1 µS/cm, 99.3 µS/cm, 183.5 µS/cm, and 428.1 µS/cm. The final lab calibration in August 2019 had known SC standards of 15.2 µS/cm, 61.7 µS/cm, 148.5 µS/cm, 296.3 µS/cm, and 445.8 µS/cm.

2.4. Statistical and Data Analysis

2.4.1. Stage-Discharge Rating Curves and Hourly Discharge Data Developments

To address (G1) stage-discharge relationships for nine headwater streams over at least one annual hydrograph, the instrumentation described in sections 2.2.1 and 2.2.2 was used to satisfy the latter portion of objective 1, to generate continuous discharge data. All 2017–2018 (2015–2017 for Sites 9 and 10) interpolated stage (ft) and discrete total discharge (cfs) readings were plotted on a rating curve in Excel for each stream. It was assumed that no major changes in river channel morphology occurred at any cross-section. Discharge was plotted on the y axis and stage on the x axis. Outliers and inconsistent data points were removed such as those whose end stage value was quite different after the discharge measurement than the stage value at the start, those that had been collected with an Aquacalc rather than a Swoffer current velocity meter, those that had field complications with the current meter, or those that did not fall within a reasonable distance to the power function curve. For each stream, Excel's solver add-in was then used to minimize the sum of squared residuals for predicted vs measured stream discharge (Q) by changing the a and b parameters in the following power function:

$$Q = aX^{b} \qquad \text{[E2.2]}$$

where *X* is stage.

Once a power function was established for each stream, four to five of the most ideal stage readings were selected as potential reference points. These were selected based on best fit to the power function, least variability before and after the field discharge measurement, smallest squared residuals from predicted vs measured stream discharge, and preference was given to the lowest stage measurements, as higher flows were more difficult to accurately predict. Each of the potential reference dates, times, and stage levels (WL, ft) were then entered into HOBOware

Pro software one at a time with the water and local barometric pressure transducer datafiles. Each of the HOBOware potential stage reference output files containing continuous hourly predicted stream discharge data were then cross-referenced by checking the predicted stage and predicted stream discharge on days when these were also measured in the field. This information was organized into a table for stage and a table for stream discharge, where predicted vs measured values were compared. The final reference selected was that which had the lowest or second lowest sum of squared residuals for stream discharge and/or stage.

Tyler Carleton of the Medicine Bow-Routt National Forests completed the rating curves and hourly predicted discharges for Sites 8, 9, and 10. At Site 9, a 2018 stage height was selected as a reference point, although there were no discharge measurements associated with this stage height (Carleton, 2021). The HOBOware Pro software outputs (pressure, temperature, date-time, and the populated stage height series) for each selected reference stage were used with each power function to generate the final continuous hourly stream discharges for 2017 and/or 2018 for each stream. Field measured stream discharges (Q data) were then plotted alongside this data to confirm the accuracy of the final hourly Q data and reference stage chosen. R^2 values were calculated in excel by first finding the correlation coefficient (r) between measured Q data and the Q data predicted by the rating curve equation, and then squaring the coefficient.

2.4.2. Regression Analysis

To address (G3) continuous in-stream relative SC values with calibrated STIC loggers at ten snowmelt-dominated headwater streams, objective 3 was to calibrate 17 STIC loggers in a lab using logger readings at different temperatures and known specific conductance (SC) standards, and apply this to each STIC logger's continuous in-stream field data. Each STIC logger's raw 'C' (recorded as lumens/ft^2 or lux) 30-second interval calibration data were organized into their own CSV file with the associated external thermistor (°C) data and electrical conductivity (EC) value as it increased with temperature. STIC logger temperature data were not used for regressions because the logger's external housing slows its temperature logging response during the rapid temperature changes of the lab calibration. This is not an issue for STIC logger temperature data collection in the field, because temperature changes are not as rapid in the field. To predict electrical conductivity, a nonlinear regression was performed in SPSS version 26 for each CSV file of the form:

$$EC = a + bC + cT + dC^2 + eT^2 \tag{E2.3}$$

where *EC* is the electrical conductivity (µS/cm), *a*, *b*, *c*, *d*, and *e* are the model parameters, *C* is lumens/ft^2 or lux as recorded by the STIC logger, and *T* is the temperature (°C) as measured by the external thermistor. Both constraining and not constraining parameters c and e to positive values only were experimented with, as EC is positively correlated with temperature. Final regressions constrained parameters c and e to values greater than or equal to zero (Gillman et al., 2017). SPSS v26 output files with R^2 values and additional statistical summary information is available in Appendix 1. All regression equations, R^2 values, and duplicate STIC loggers (at the same location) comparisons are documented in chapter three.

2.4.3. Conductivity Comparisons

To address (G4) if temporal STIC logger data trends are comparable to temporal data trends measured using a higher-cost HOBO U24 logger, objective 4b was to quantitatively and qualitatively compare STIC and U24 logger temporal data trends, limitations, and advantages. In addition, at sites where two STIC loggers were launched in the same water year, their temporal data trends were compared. Hourly EC data from the U24 data loggers launched at North Fork of the Elk River, Elkhead Creek, and Silver Creek were converted to SC data with HOBOware

Pro's conductivity assistant software because as temperature changes so does EC, whereas SC compensates for changing temperatures (measurements are reported as if at 25°C). Therefore, converting to SC allows one to compare SC values across different sites (Gillman et al., 2017):

$$SC = \frac{EC}{(1+a(T-25))} \quad \text{[E2.4]}$$

where a is the linear temperature compensation factor of 2.1% per degree Celsius, T is the temperature (°C) from the U24 logger, and 25 is present because SC is reported as if it was measured at 25°C.

When STIC logger predicted EC regression equations from lab calibrations are applied to field data, STIC logger predicted EC and SC values follow the same relative trends as U24 logger values, and therefore, when discussing STIC logger predicted field EC or SC trends, they will be referred to as relative EC (rEC) or relative SC (rSC). The regression equation for each STIC logger was applied to its hourly raw 'C' and temperature (°C) field data to determine hourly relative electrical conductivity (rEC) at each of the ten sites. Because rEC changes with temperature, rEC was converted to relative specific conductance (rSC) to compare rSC across different sites (Gillman et al., 2017):

$$rSC = \frac{rEC}{(1+a(T-25))} \quad \text{[E2.5]}$$

where a is the linear temperature compensation factor of 2.1% and T is the temperature from the STIC logger. STIC logger hourly rSC temporal data trends were compared to U24 logger hourly SC temporal data trends, STIC logger temporal data trends were compared to other STIC logger trends from the same site, and hourly baseflow was calculated with both STIC logger rSC data as well as U24 SC data.

2.4.4. Baseflow Estimation Methods

Hourly discharge calculations were described in section 2.4.1, and hourly SC and/or rSC data were described in sections 2.4.2 and 2.4.3. Together, these are the components needed for the conductivity mass balance equation to estimate baseflow. To (G5) determine if STIC logger data can be used from snowmelt-dominated headwater streams with both wide and narrow (differences between end-member) SC values to estimate baseflow with the CMB method, (G6) estimate baseflow in all streams suited for the CMB method, and (G7) determine if BFI estimates calculated with STIC and U24 logger data are similar, the following objectives took place. (O5) STIC loggers were deployed at watersheds that, based on geology, are likely to have different SC ranges (both wide and narrow differences between runoff and baseflow end-member values); (O6) Continuous SC data were plotted with continuous discharge data to determine which sites have data that are suited for the CMB method, then baseflow was estimated at these sites; and (O7) BFI estimates calculated with STIC and U24 logger data were compared.

First, continuous SC data from STIC or U24 loggers was plotted with continuous discharge data to display each dataset's inverse or other type of relationship. Many studies have demonstrated that SC can be used as an environmental indicator of flow component separation for a streamflow hydrograph. These studies show that streamflow SC values vary inversely with streamflow discharge (Stewart et al., 2007). Alterations to natural hydrologic processes, such as direct impacts from anthropogenic activities, can result in a non-consistent inverse relationship between discharge and SC. Therefore, the CMB method and other SC-based hydrograph separation approaches are usually not appropriate for these systems (Miller et al., 2014). Streams in this study with discharge data that were inversely related to SC were suited for the CMB method of hydrograph separation. Figures 3.20 – 3.29 display this.

Next, at the streams suited for this method of baseflow estimation, the following equations were used (Pinder and Jones, 1969):

$$Q_{BF} = Q\ \frac{(SC - SC_{RO})}{(SC_{BF} - SC_{RO})} \qquad \text{[E1.1]}$$

or,

$$Q_{BF} = Q\ \frac{(rSC - rSC_{RO})}{(rSC_{BF} - rSC_{RO})} \qquad \text{[E2.6]}$$

Equation 2.5 is a variation of Equation 1.1 where *Q* is the hourly discharge (cfs), *rSC* is the in-stream hourly relative specific conductance (µS/cm) of the STIC logger, rSC_{RO} is the relative specific conductance of the runoff end-member, or high-flow stable average rSC minimum value for the entire time period of record, rSC_{BF} is the relative specific conductance of the baseflow end-member, or the low-flow stable average rSC maximum for the year or time period of interest. rSC_{RO} and SC_{RO} are assumed to be constant throughout the period of record, and therefore these values are held constant. rSC_{BF} and SC_{BF} change slightly from year to year. To represent temporal variability in the integrated subsurface SC during low-flow and high conductivity conditions, a SC_{BF} value can be calculated for each year during the period of record as the SC of the 99th percentile of the daily SC values for the year in question (Miller et al, 2014). This study followed these methods for streams that demonstrated expected temporal SC variability, and used the low-flow stable average SC maximum as the baseflow end-member for all other streams (Stewart et al., 2007).

For the CMB method to work with STIC logger data, it's necessary for the rSC_{RO} and rSC_{BF} end-members to be recorded with the same STIC logger that has or will be recording the continuous stream rSC data, so as to remain consistent with the relativity requirement. For comparability between U24 loggers and STIC loggers, the STIC logger methods for end-member value selection were also followed for U24 loggers, except that the second mass balance equation was used rather than the first, and U24 logger data were used.

Continuous annual baseflow discharge data are often summed and divided by the total annual discharge to find the annual baseflow index (BFI), the long-term proportion of baseflow to streamflow. It is also common to sum BFI for the snowmelt period of the hydrograph and for the post snowmelt-dominated period, as the proportion of baseflow to streamflow varies temporally (Miller et al., 2014). BFI represents the slow or delayed contribution to river flow and may be influenced to a significant extent by catchment geology (Bloomfield et al., 2009). Calculating BFI for the post snowmelt-dominated time period of a stream hydrograph is of importance for snowmelt-dominated streams, as this is the time when water in the stream is limited, and quantification of BFI can aid in management decisions to maintain instream flows (Sanford and Hack, 2013).

The hydrograph for each site was assigned three different parts: rising limb, falling limb, and 'post snowmelt-dominated.' The snow is still melting at the beginning of the post snowmelt-dominated time frame, but snowmelt contributions to streamflow are beginning to decrease and baseflow contributions are beginning to become more significant, relative to snowmelt. The start of the post snowmelt-dominated date for each site was selected based on two factors: (1) the daily change in slope of the hydrograph starting to noticeably lessen and (2) the daily BFI increasing to above 20 percent. The first factor uses equation 2.6:

$$\frac{d^2Q}{dt^2} \rightarrow \varepsilon \qquad \text{[E2.7]}$$

where Q is the daily discharge (cfs), t is time in days, and ε is a noticeably smaller value than previous days.

To (G7) determine if BFI estimates calculated with STIC and U24 logger data are similar, objective 7 was to compare BFI estimates calculated with STIC and U24 logger data. The ratio of cumulative baseflow to cumulative streamflow (BFI) for the annual hydrograph and for the post snowmelt-dominated portion of the hydrograph was calculated at all sites where baseflow was calculated. The BFI estimates produced with U24 logger data and STIC logger data were then compared (Miller et al., 2015).

3. RESULTS

This chapter first describes the stage-discharge rating curves created and hourly discharge data computed from these rating curves for the nine sites that did not already have staff gauges and hourly discharge data. Next, results from STIC logger lab calibrations and regressions are presented, allowing for comparison between STIC logger and U24 logger hourly relative specific conductance data. After this, stream discharge (Q) is plotted with specific conductance (SC) on the secondary axis to demonstrate that any sites which have an inverse relation of these parameters are suitable for the conductivity mass balance method (CMB) of baseflow estimation. At the end of this chapter, baseflow estimations are calculated for all sites suited for the CMB method, using both U24 and STIC logger hourly data.

3.1. Rating Curves

Nine of the ten streams in this study had stage-discharge rating curve equations established based on the field-collected stage and discharge measurements described in the previous chapter. Site 4, Encampment River, already had a staff gauge and hourly flow data available through the USGS National Water Information System (Wyoming Water Data Support Team, 2020). The stage-discharge graphs are presented in Figure 3.1 with the best-fit curve used to develop the rating curve. Note the different scales for both the x and y-axes at different sites. R^2 correlations ranged from 0.963 (Site 10, Poose Creek) to 0.999 (Site 6, First Creek) using a power function. Table 3.1 summarizes these correlations and the final rating curve equation for each site.

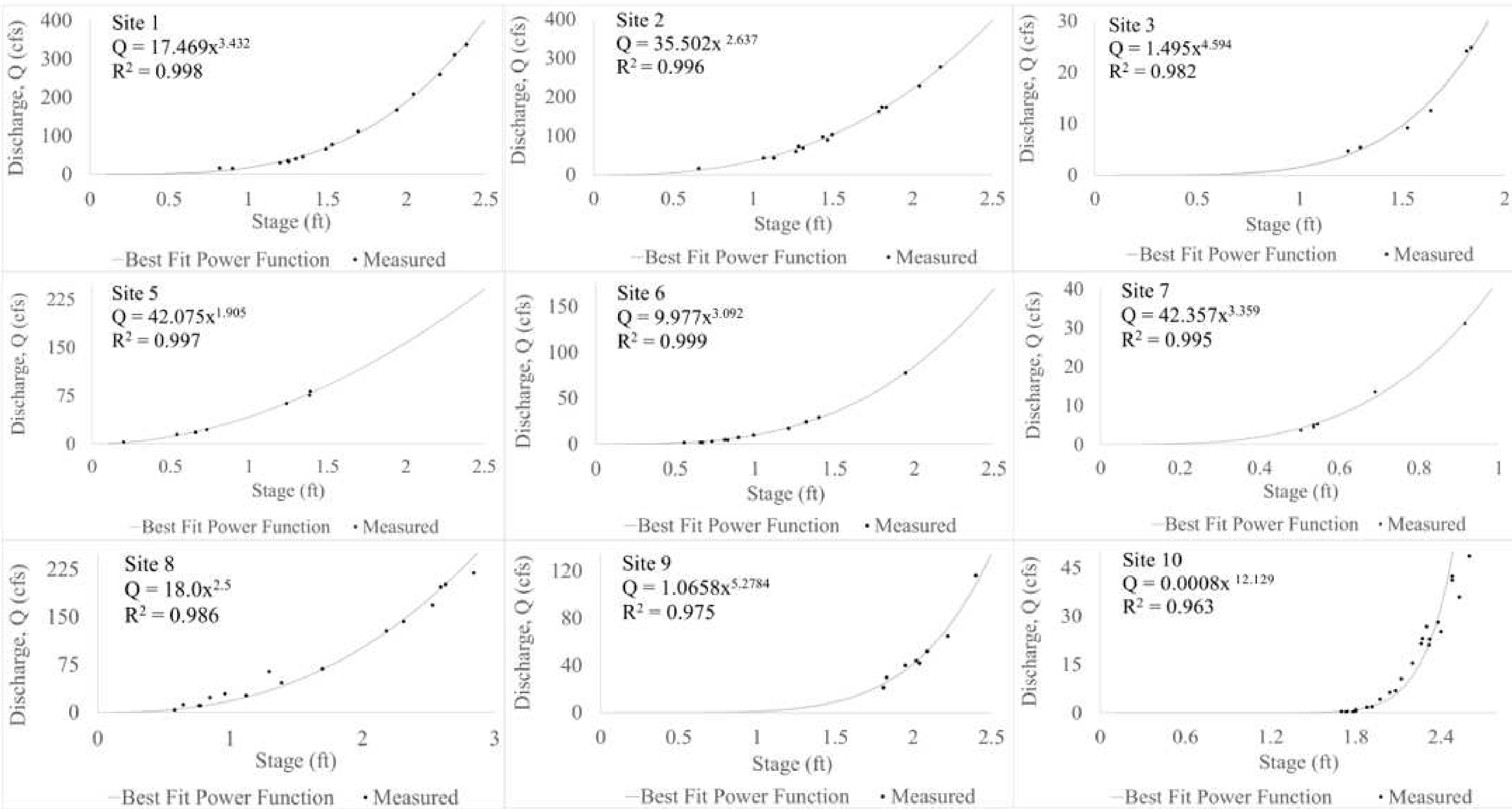

Figure 3.1. Rating Curves for Sites 1-3 and 5-10, where manual field discharge (Q) and stage (x) measurements, denoted with black points, were collected during water year(s) 2017 and/or 2018. The grey solid curve is the best fit power function. Tyler Carleton, a hydrologist for the Medicine Bow-Routt National Forests, completed the rating curves for Sites 8, 9, and 10. Please note the different scales for the x and y axes at different sites.

Table 3.1. Summary of rating curve equations and R^2 correlations. Site 4, Encampment River above Hog Park Creek, already had a staff gage and rating curve established by the U.S. Geological Survey (Wyoming Water Data Support Team, 2020). Tyler Carleton, a hydrologist for the Medicine Bow-Routt National Forests, completed the rating curves for Sites 8, 9, and 10.

Site No. and Stream Name	Rating Curve Equation	R^2
1 – South Fork of the Elk River	$Q = 17.469 x^{3.432}$	0.998
2 – North Fork of the Elk River	$Q = 35.502 x^{2.637}$	0.996
3 – English Creek	$Q = 1.495 x^{4.594}$	0.982
4 – Encampment River	USGS 06623800	N/A
5 – Elkhead Creek	$Q = 42.075 x^{1.905}$	0.997
6 – First Creek	$Q = 9.977 x^{3.092}$	0.999
7 – Roaring Fork of Slater Creek	$Q = 42.357 x^{3.359}$	0.995
8 – Silver Creek	$Q = 18.0 x^{2.50}$	0.986
9 – East Fork Williams Fork	$Q = 1.0658 x^{5.2784}$	0.975
10 – Poose Creek	$Q = 0.0008 x^{12.129}$	0.963

3.2. Hourly Discharge

Hourly discharge for 2017 and/or 2018 at all sites are displayed in Figures 3.2 to 3.11.

3.2.1. Site 1: South Fork of the Elk River

Figure 3.2 shows computed hourly discharge data for Site 1, which fits measured points well. The South Fork of the Elk River hydrograph spans from June 26, 2017 – October 03, 2018. The August 10, 2018 11:00 am measured stage height was used as the reference point in HOBOware Pro for Site 1 discharge (Q) computations.

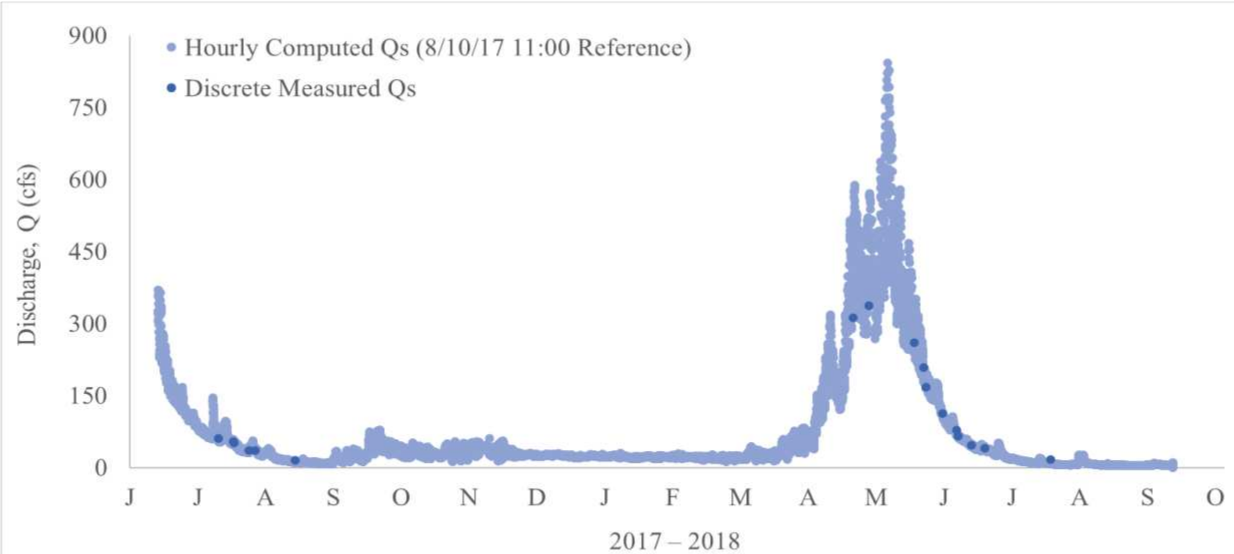

Figure 3.2. Site 1: South Fork of the Elk River falling limb of 2017 and 2018 hydrograph hourly computed discharge (light blue) with discrete measured discharge points (dark blue).

3.2.2. Site 2: North Fork of the Elk River

Figure 3.3 shows computed hourly discharge data for Site 2, which fits measured points well. This North Fork of the Elk River hydrograph spans from November 08, 2017 to October 03, 2018. The July 3, 2018 9:00 am measured stage height was used as the reference point for Site 2 discharge (Q) computations.

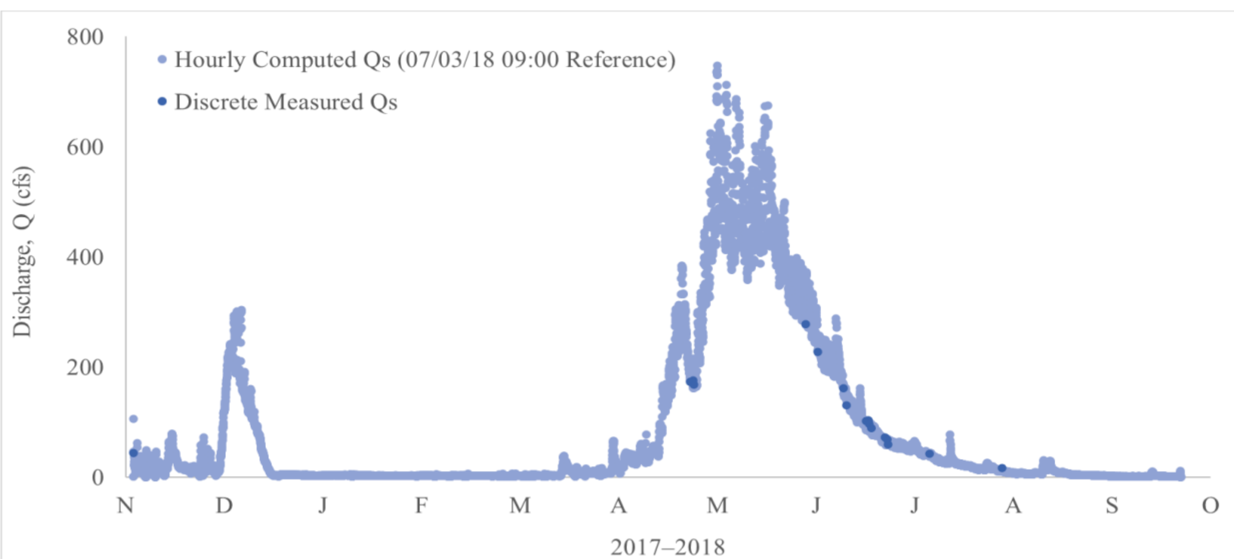

Figure 3.3. Site 2: North Fork of the Elk River 2017–2018 hourly computed discharge (light blue) with discrete field-measured discharge points (dark blue).

3.2.3. Site 3: English Creek

Figure 3.4 shows computed hourly discharge and discrete measured discharge data for Site 3, English Creek for October 05, 2017 to October 03, 2018. The May 31, 2018 3:00 pm measured stage height was used as the reference point for Site 3 discharge (Q) computations.

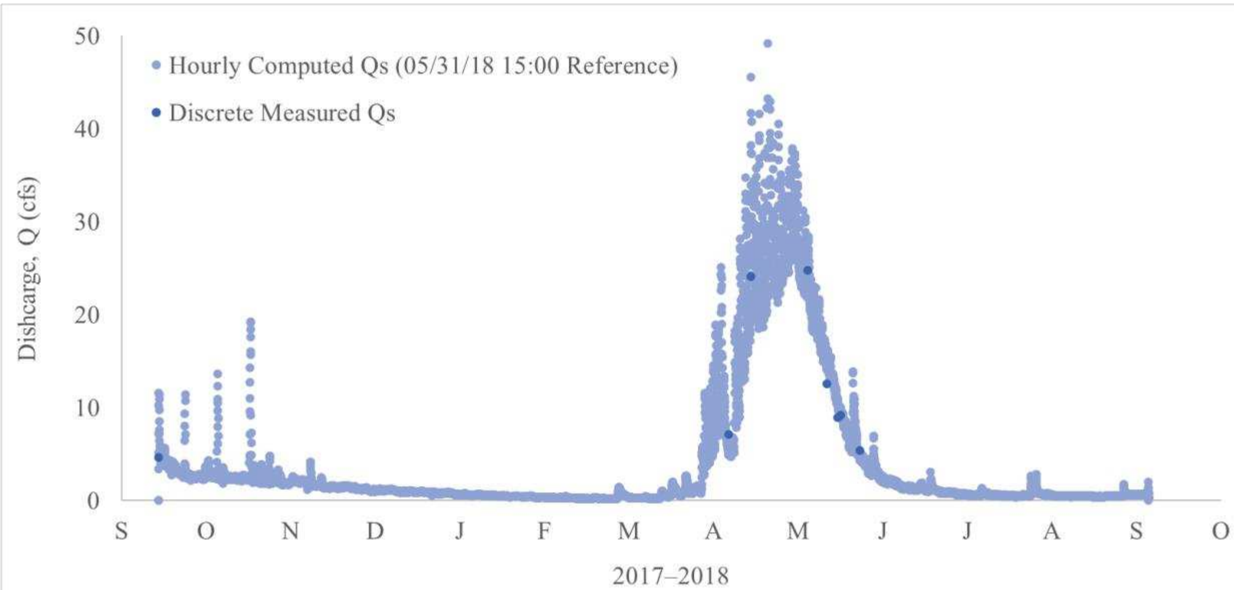

Figure 3.4. Site 3: English Creek 2017–2018 hourly computed discharge (light blue) with discrete field-measured discharge points (dark blue).

3.2.4. Site 4: Encampment River

Figure 3.5 displays USGS gaging station hourly discharge data for Site 4, Encampment River for October 12, 2017 until September 30, 2018 (Wyoming Water Data Support Team, 2020). Discrete stream discharge was not measured at this site.

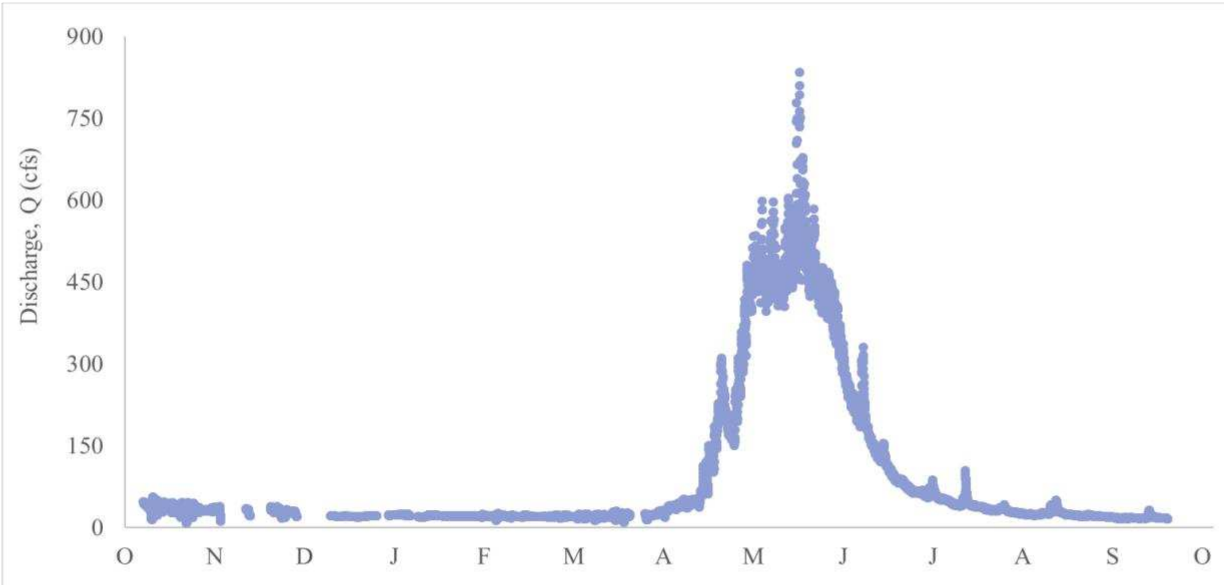

Figure 3.5. Site 4: Encampment River 2017–2018 hourly discharge in light blue (USGS, 2019).

3.2.5. Site 5: Elkhead Creek

Figure 3.6 shows computed hourly discharge and discrete measured discharge data for Site 5, Elkhead Creek for June 28, 2017 to October 02, 2018. The May 25, 2018 11:00 am measured stage height was used as the reference point for Site 5 discharge (Q) computations.

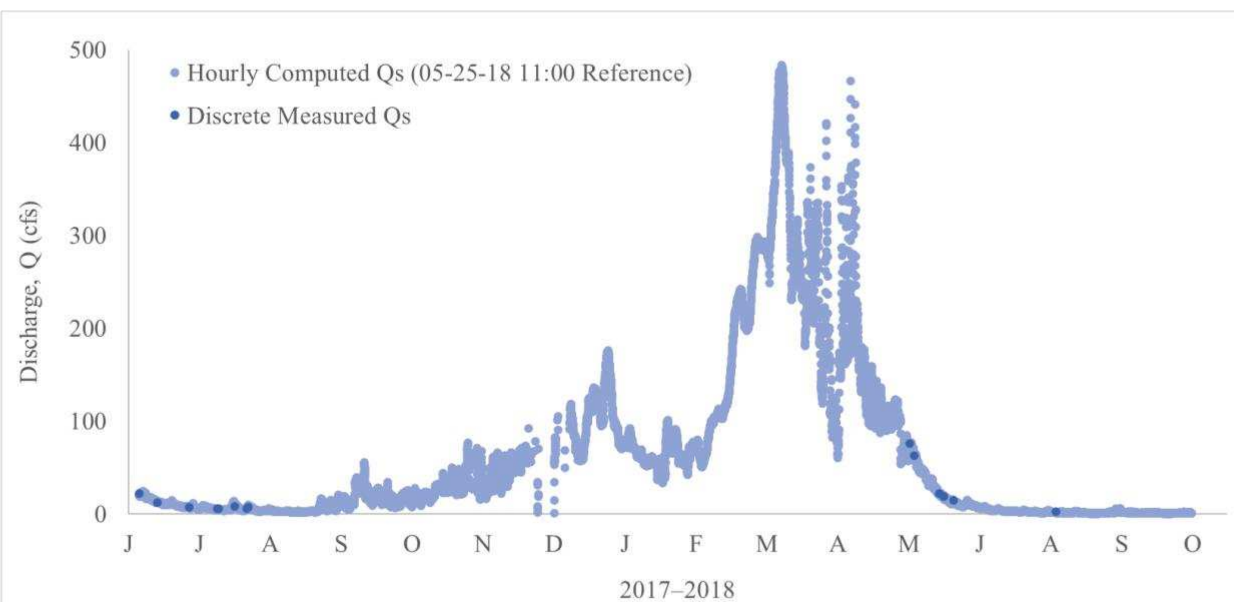

Figure 3.6. Site 5: Elkhead Creek end of 2017 falling limb as well as the 2018 hydrograph for hourly computed discharge (light blue), with discrete measured discharge points (dark blue).

3.2.6. Site 6: First Creek

Figure 3.7 displays computed hourly discharge and discrete measured discharge data for Site 6, First Creek for November 09, 2016 to October 02, 2018. The June 5, 2018 10:00 am measured stage height was used as the reference point for Site 6 discharge (Q) computations. Site 6, First Creek, reaches and remains at a temperature of 0.01°C on November 26, 2016 until March 24, 2017. Due to no temperature fluctuations at all in this timeframe, the water within the stilling well that housed the pressure transducer was assumed to be frozen. This occurs again between December 6, 2017 and April 5, 2018. Water levels are unreasonably high and inconsistent during this timeframe; winter data are considered inaccurate and will not be used.

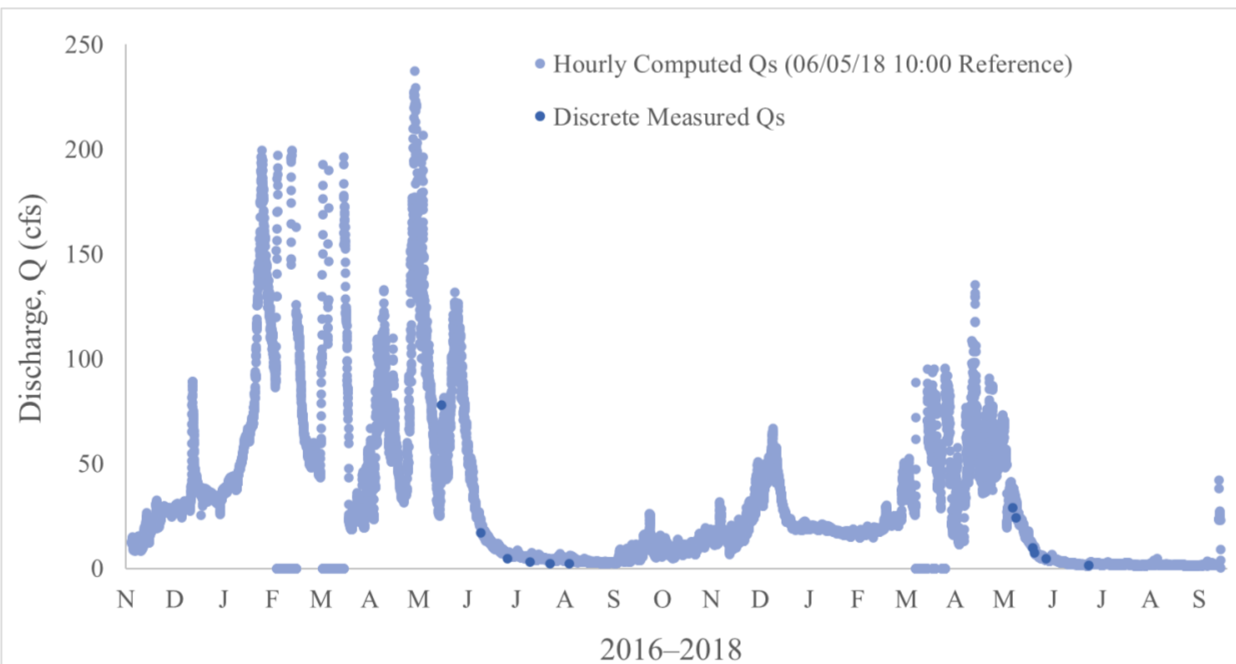

Figure 3.7. Site 6: First Creek 2016–2018 discharge data. Hourly computed discharge is depicted in light blue, with discrete measured discharge points in dark blue.

3.2.7. Site 7: Roaring Fork of Slater Creek

Figure 3.8 depicts computed hourly discharge and discrete measured discharge data for Site 7, Roaring Fork of Slater Creek for November 8, 2016 to October 2, 2018. The August 2, 2017 12:00 pm measured stage height was used as the reference point for Site 7 discharge (Q) computations.

Roaring Fork of Slater Creek frozen water affected wintertime data. Initial freezing temperatures recorded were on November 17, 2016. After the freeze on November 17, pressure and water level data increased higher than summer peak water levels. By March 18, 2017 the pressure, water level, and discharge data had returned to expected levels (under 10 cfs). On October 10 and 15 of the following season flows become more unreasonable (more than 50 cfs). After November 8, most likely frozen water made most data inconsistent and/or unreasonable (higher than summer peak flows). After April 8, 2018, stream discharge data returned to expected levels (less than 10 cfs).

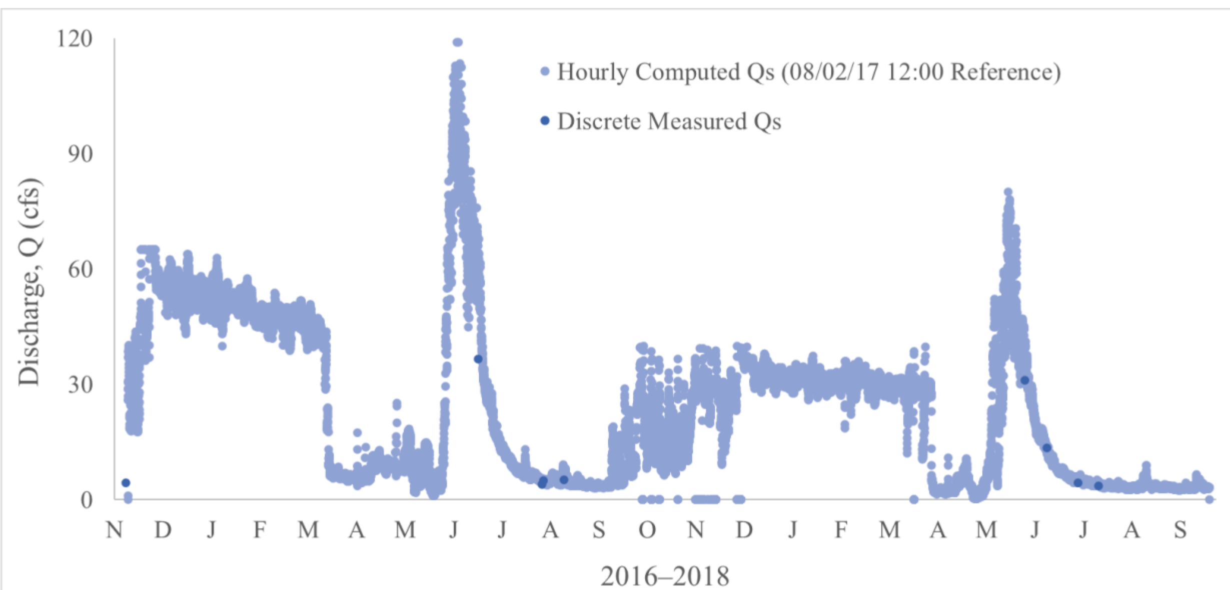

Figure 3.8. Site 7: Roaring Fork of Slater Creek 2016–2018 discharge data. Hourly computed discharge is depicted in light blue, with discrete measured discharge points in dark blue.

3.2.8. Site 8: Silver Creek

Figure 3.9 depicts computed hourly discharge and discrete measured discharge data for Site 8, Silver Creek for September 25, 2017 to September 30, 2018. Tyler Carleton of the

Medicine Bow-Routt National Forests (MBR NF) computed the final hourly computed discharges at Site 8. The June 25, 2018 11:00 am measured stage height was used as the reference point for Site 8 discharge (Q) computations.

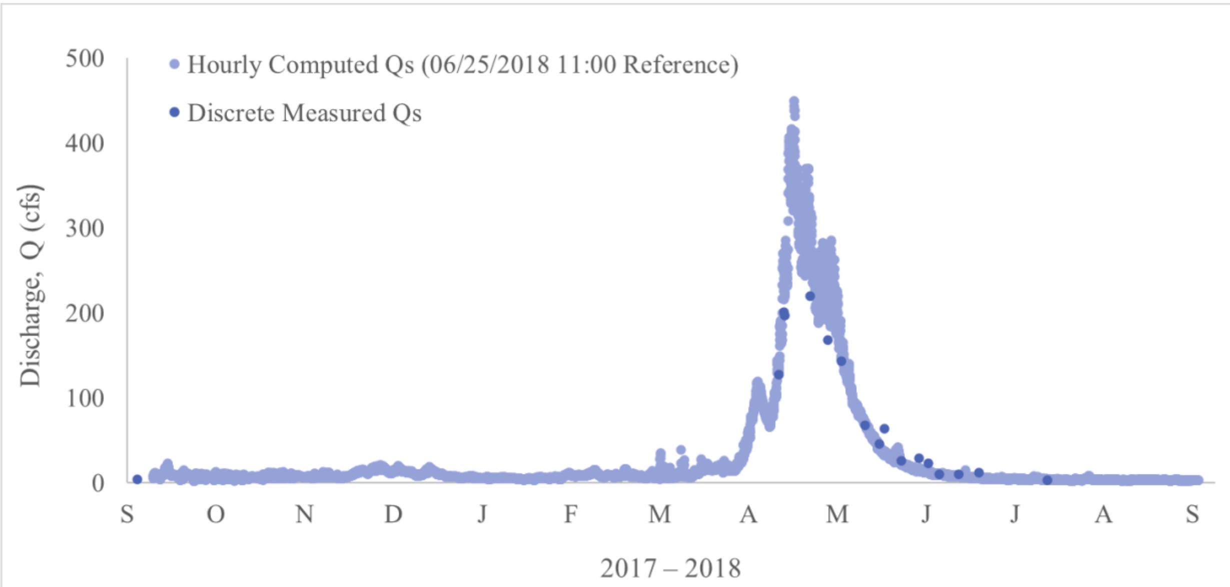

Figure 3.9. Site 8: Silver Creek 2018 hydrograph. Hourly computed discharge is depicted in light blue, with discrete measured discharge points in dark blue. Final hourly Q data were computed by Tyler Carleton of the Medicine Bow-Routt National Forests (MBR NF).

3.2.9. Site 9: East Fork of the Williams Fork

Figure 3.10 shows computed hourly discharge and discrete measured discharge data for Site 9, East Fork of the Williams Fork for September 16, 2017 to October 4, 2018. Tyler Carleton of the MBR NF computed the final hourly computed stream discharges at Site 9. The 10/04/2018 12:00 measured stage height was used as the reference point for Site 9 discharge (Q) computations. December computed Q data were corrected to not exceed 300 cfs to remain no higher than the highest discharges in November, and no higher than May peak flows. There were no measured Q data during the same period as the computed Q data (measured Q data occurred prior to November 2017).

The East Fork of the Williams Fork had notes documenting a potential ice jam in December 2017. There is an unreasonably high peak in recorded pressures and calculated water levels in December 2017, which were corrected to resemble a horizontal line at about 300 cfs. December 4 – 20, 2017 shows higher pressures and water levels (stream discharges as high as 1299 cfs) when temperatures were at lows of (and usually no higher than) 0.01°C. In addition, a seasonal low occurred just one day prior, on December 3 (– 0.102°C), which it is assumed froze the water within the stilling well that housed the U20 pressure transducer until temperatures rose enough to thaw it after December 20. Such extreme stream flows of as much as 1299 cfs are not possible on a river with peak flows of about 712 cfs. Therefore, this wintertime water level data will not be included in any further calculations.

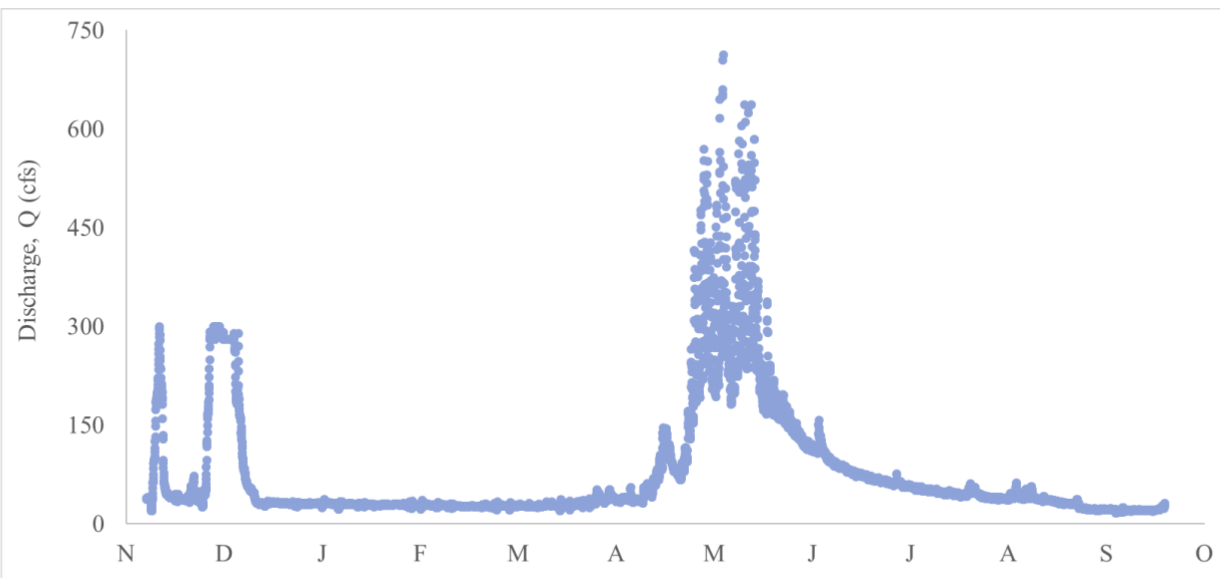

Figure 3.10. Site 9: East Fork of the Williams Fork 2018 hydrograph. Hourly discharge was computed by Tyler Carleton of the MBR NF. There were no discrete measured Q data during the same time frame as computed hourly Q data (measured Q occurred prior to November 2017).

3.2.10. Site 10: Poose Creek

Figure 3.11 displays hourly computed discharge and discrete measured discharge data for Site 10, Poose Creek for November 07, 2016 to October 04, 2017. Tyler Carleton of the MBR

NF computed the final hourly computed stream discharges for Site 10 based on 24 discrete flow measurements from 2015 to 2017. The 06/20/2017 10:00 measured stage height was used as the reference point for Site 10 discharge (Q) computations.

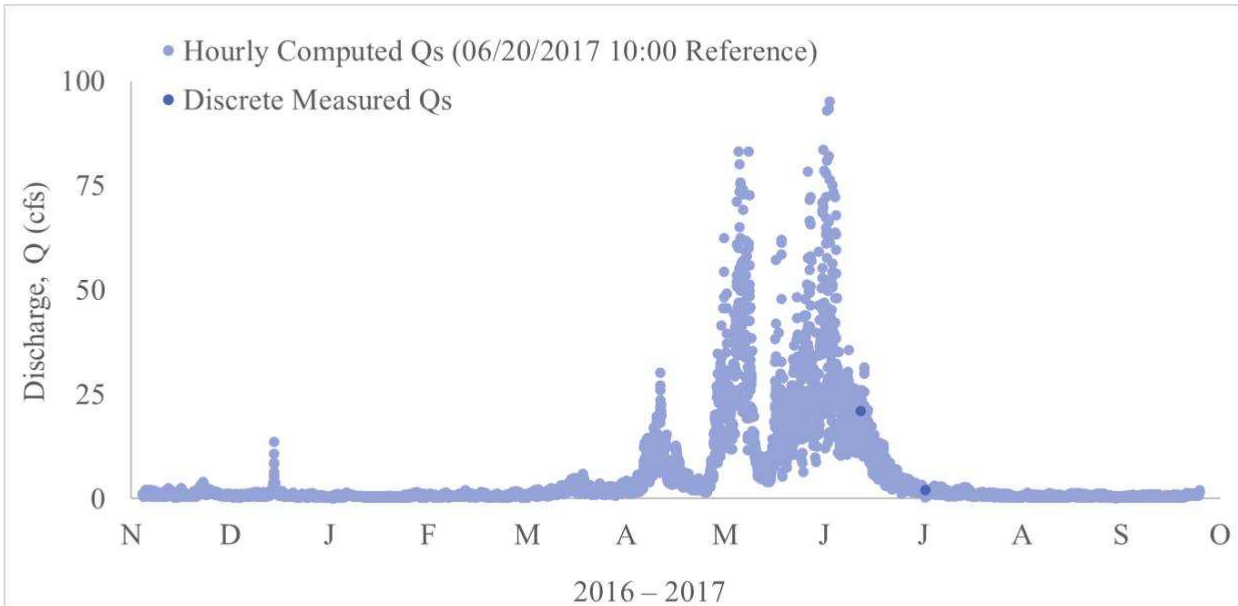

Figure 3.11. Site 10: Poose Creek 2017 hydrograph. Computed hourly stream discharge (light blue) (Carleton, 2020), with discrete measured Q points (dark blue, two during 2017).

3.2.11. Summary of Stream Discharge Results

Table 3.2 summarizes the peak and lowest stream discharge values in cubic feet per second (cfs) at each site location. Total stream discharge ranges between less than one cfs and 859 cfs.

3.3. STIC Loggers and Calibration Results

STIC logger data before and after calibration will be shown in this section. The raw, uncalibrated hourly STIC logger number 2 field data collected at North Fork of the Elk River (Site 2) from April 2018 to July 2018 is displayed in Figure 3.12. The uncalibrated hourly STIC logger data depicted in red were recorded on the HOBO pendant's re-used light intensity channel

Table 3.2. Minimum and maximum stream discharge ranges at each study site location.

Site Number: Stream Name	Stream Discharge Range (cfs)
1: South Fork of the Elk River	4.4 - 859
2: North Fork of the Elk River	1.4 - 747
3: English Creek	0.009 – 49.2
4: Encampment River	9 – 834
5: Elkhead Creek	0.32-484
6: First Creek	0.33-135
7: Roaring Fork of Slater Creek	0.23 – 127.4
8: Silver Creek	2.6 – 449
9: East Fork Williams Fork	16.2 - 712
10: Poose Creek	0.2 - 95

as lumens/ft^2, but until calibrated, the STIC logger's raw data remains unitless. Hourly temperature data are depicted in purple.

The data recorded by STIC logger 2 on a 30-second frequency during the five-point lab

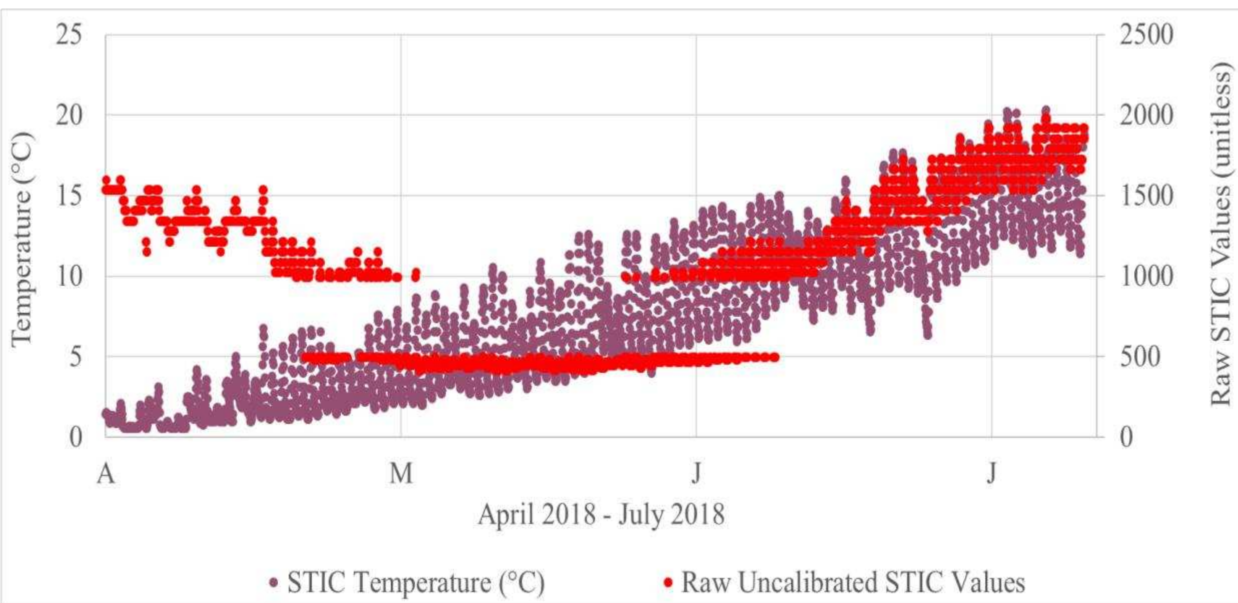

Figure 3.12. Uncalibrated STIC logger 2 data collected at North Fork of the Elk River (Site 2).

calibration in August 2019 are shown in Figure 3.13. Temperatures (°C) recorded on a 30-second frequency are shown in purple with uncalibrated STIC data shown in red. Each of the fives curves represent a new calibration standard and ice bath.

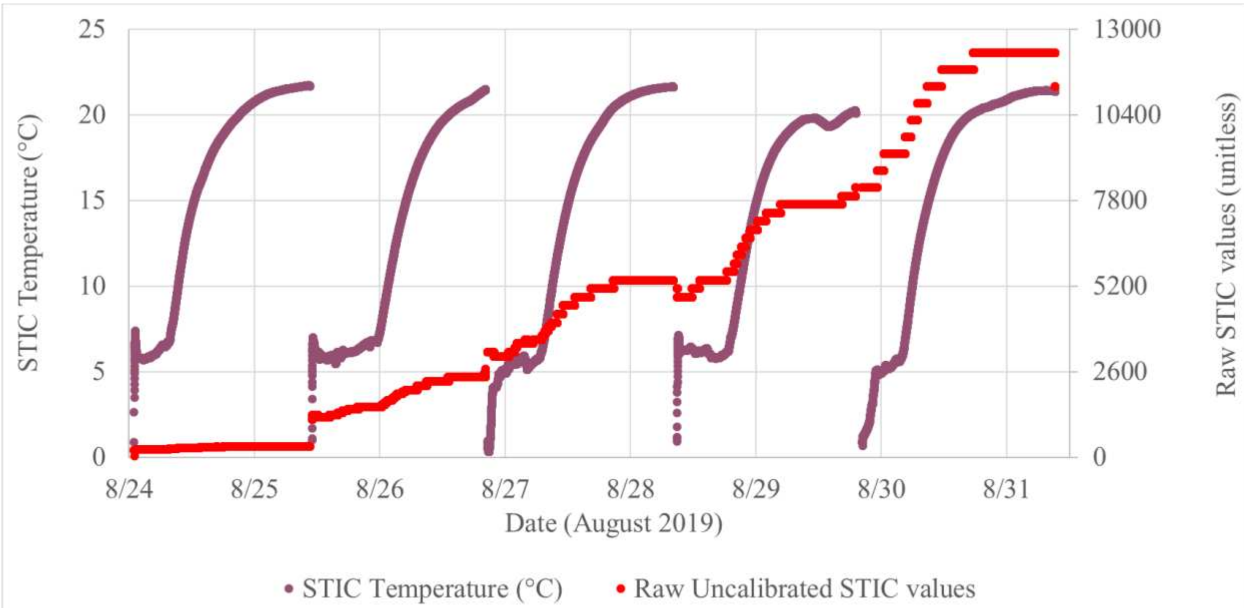

Figure 3.13. STIC logger 2 August 2019 five-point lab calibration data (30-second frequency).

The regression equations and calibration results for all 17 STIC loggers are displayed in Table 3.3. Regressions with R^2 values of 0.986 or greater produce successful predicted electrical conductivity (EC) values that when converted to SC, if the stream is suitable for the CMB method, can be used in this method to estimate baseflow. For example, STIC logger 1b logged inconsistent, overlapping data during the third point of August's five-point calibration (largely differing data recorded for the same standard), leading to regression results with a lower R^2 than most other STIC loggers, of 0.948. When rSC data based on this regression were plotted over time, the rSC variations of this logger were not as reasonable as expected. Relative SC values did not decrease during 2017 peak flows as much or as smoothly as expected; instead they waivered up and down in a way that did not demonstrate an inverse relationship with discharge

Table 3.3. STIC logger regression equations based on February, April, and August 2019 lab calibrations. The dependent variable is measured Electrical Conductivity (EC).

STIC Site No.	Equation	R^2 Value	Cal Mo.	STIC S/N
1a	$EC = 0.99 + 0.021C + 0.047T + 0.000001C^2 + 0.015T^2$	0.991	Aug	4971
1b	$EC = 2.03E\text{-}7 + 0.171C + 7.781E\text{-}10T - 7.437E\text{-}6C^2 + 1.186E\text{-}8T^2$	0.948	Aug	4989
2	$EC = -1.157 + 0.027C + 0.048T + 5.494E\text{-}7T^2$	0.987	Aug	4992
3a	$EC = 5.948 - 0.003C + 0.254T + 0.0000003918C^2$	0.996	Apr	4984
3b	STIC logger header/offload errors; calibrations unsuccessful	--	--	4977
4a	$EC = 0.043 + 0.002C^{*} + 0.045T + 0.00000001416C^{2*} + 0.007T^2$	0.997	Feb	4995
4b	$EC = 0.394 + 0.028C + 6.204E\text{-}6T + 8.832E\text{-}7C^2 + 3.083E\text{-}10T^2$	0.986	Aug	4982
5a	$EC = 3.432 + 0.024C + 0.000001916C^2$	0.997	Aug	4990
5b	STIC logger repeated battery failure; calibrations unsuccessful	--	--	4983
6a	$EC = -3.640 + 0.028C + 0.036T + 8.608E\text{-}7C^2 + 0.016T^2$	0.991	Aug	4991
6b	$EC = 6.068 – 0.004C + 0.260T + 5.478E\text{-}7C^2$	0.982	Apr	4973
7a	$EC = 1.548 + 0.018C + 0.301T + 0.000001315C^2 + 0.003T^2$	0.998	Apr	4972
7b	$EC = 0.074 + 0.002C + 0.093T + 0.00000001288C^2 + 0.026T^2$	0.992	Feb	4968
8	$EC = 18.206 + 0.043C + 0.00001911C^2$	0.993	Feb	4988
9	$EC = 0.074 + 0.002C + 0.084T + 0.00000001459C^2 + 0.017T^2$	0.996	Feb	4993
10a	$EC = 2.741 + 0.02C + 0.179T + 0.00000138C^2 + 0.002T^2$	0.990	Aug	4970
10b	$EC = -1.919 + 0.03C + 0.149T + 1.227E\text{-}6C^2 + 7.995E\text{-}6T^2$	0.989	Aug	4997

*lux calibration data were used for C rather than lumens/ft^2 data

during higher flows. Relative SC values also began to decrease sooner than expected in November 2017, when they should have begun to fall closer to the onset of spring runoff. Finally, rSC values did not follow the same relative trends as STIC logger 1a, which was deployed at the same site location, but had a higher R^2 of 0.991.

As another example, the regression equation for STIC logger 6b was applied to its raw unitless field data to predict rSC, and when rSC results were plotted over time, the results did not predict realistic temporal rSC data trends (rSC rose during peak flows and fell post-snowmelt, the opposite of what was expected). STIC 6b had a calibration equation R^2 of 0.982, and no STIC loggers had R^2 values between 0.982 and 0.986. Therefore, any calibration results with R^2 values at or below 0.982 should not be used for rSC predictions, or in the CMB method equation. STIC loggers with R^2 values of 0.986 or greater did not experience any issues during calibration, and when plotted over time, either demonstrated expected temporal variations, expected inverse relations, or did not stand out as having unreasonable data. For example, with an R2 of 0.986, STIC 4b predicted rSC well and was comparable to STIC 4a that was deployed at the same site location. Therefore, STIC loggers with R^2 values at or above 0.986 should produce reasonable rSC data that can be used in the CMB method equation. SPSS Statistics v26 regression output files for 11 of these STIC loggers (Sites 1, 2, 4, 6, 7, 8, 9, and 10) are available in the supplementary files. These supplementary files regarding duplicate STIC loggers are available to provide more detail on the calibration results and reasoning for which STIC loggers were deemed to have a successful calibration vs an unsuccessful calibration.

STIC logger calibration predicted EC at temperature (T) vs measured EC at T are shown for STIC loggers 2, 5a, and 8 (Sites 2, 5, and 8) in Figures 3.14 and 3.15, which display STIC logger calibration results at sites where U24 loggers were also launched. The same graphs for STICs 3a, 4a, and 7a (Sites 3, 4, and 7) are shown in Figures 3.15 and 3.16 to further demonstrate visual examples of calibration results and why certain R^2 values were considered successful. Figure 3.14 shows two examples of predicted EC at T vs measured EC at T out of the 8 total STIC loggers that used the August 2019 calibration data for their regressions. STIC logger 2 predicted EC at T has a 0.987 R^2 fit with measured EC at T. STIC 5a has a 0.997 R^2. Both STIC loggers were at sites where U24 loggers were also launched (North Fork of the Elk

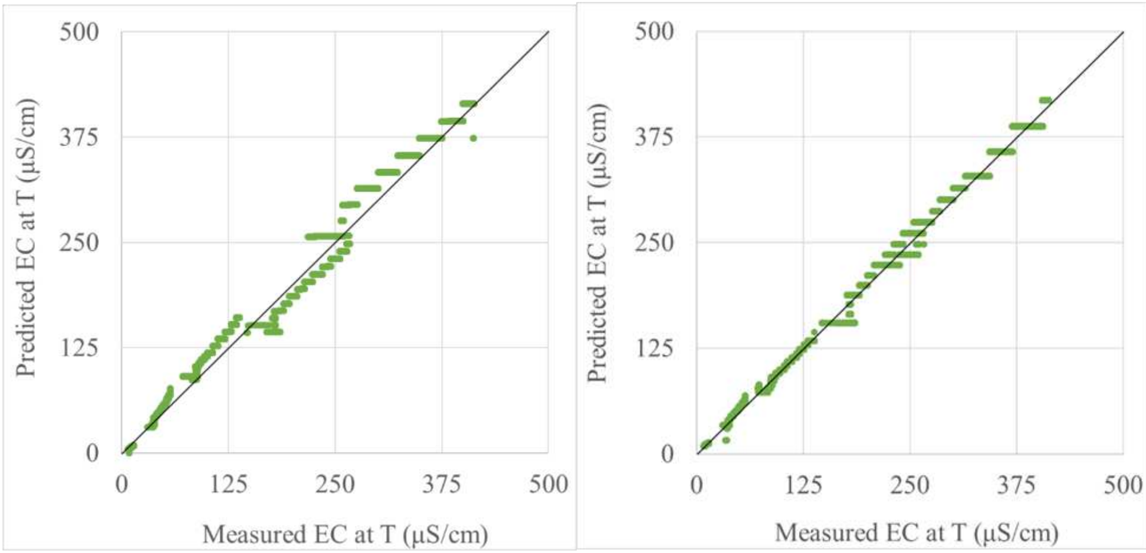

Figure 3.14. August 2019 STIC logger calibration results. A perfect 1:1 fit would lie on the black line. STIC logger 2 is shown on the left, STIC logger 5a on the right.

River and Elkhead Creek, respectively).

Figure 3.15 shows two examples of 4 total STIC loggers that used the February 2019 calibration data for their regressions. STIC 8 predicted EC at T has a 0.993 R^2 fit with measured EC at T. This STIC logger was at Site 8 (Silver Creek) where a U24 logger was also launched. STIC 4a (Site 4, Encampment River) has a 0.997 R^2.

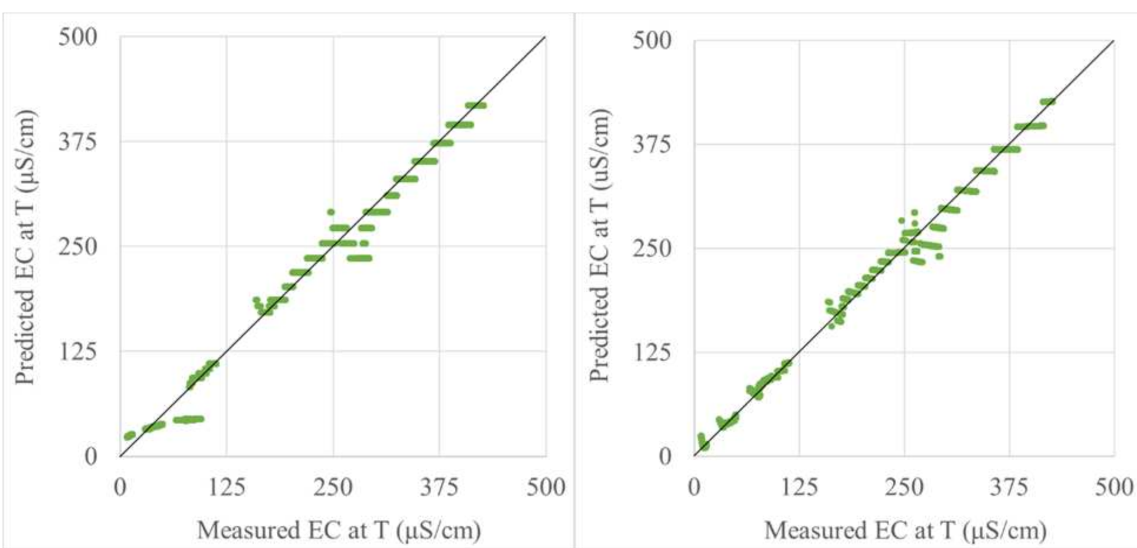

Figure 3.15. February 2019 STIC logger calibration results. A perfect 1:1 fit would lie on the black line. STIC logger 8 results are shown on the left, STIC logger 4a on the right.

Figure 3.16 shows two examples of 3 total STIC loggers that used the April 2019 calibration data for their regressions. These results represent the best predicted EC at T vs measured EC at T R^2 values obtained with the April calibration data. STIC logger 7a (Roaring Fork of Slater Creek) has a 0.998 R^2 and STIC logger 3a (English Creek) has a 0.996 R^2.

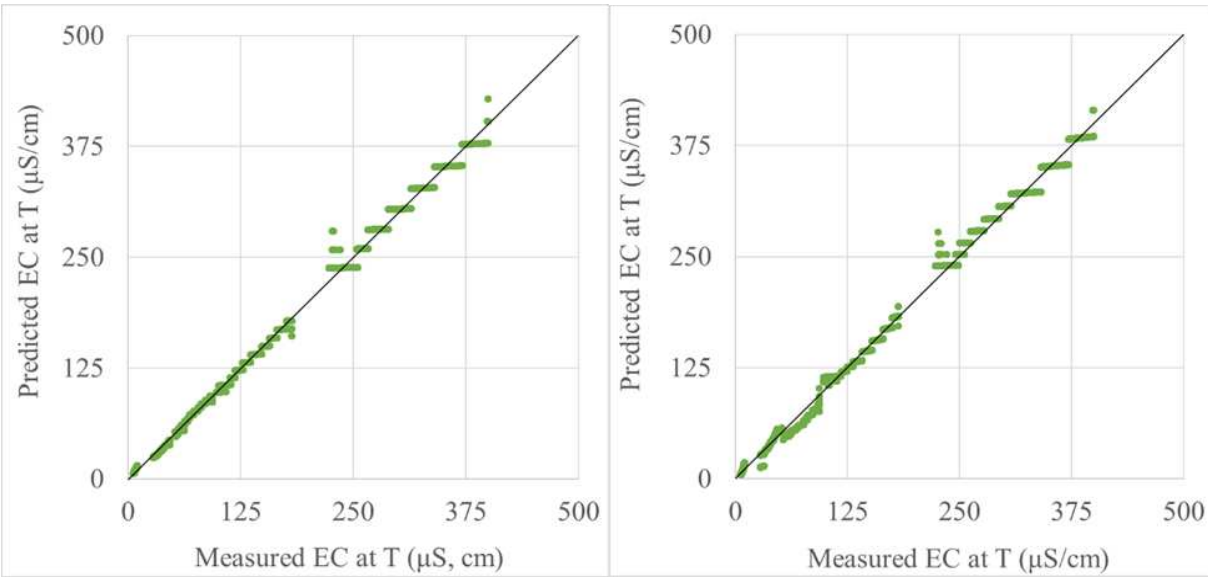

Figure 3.16. April 2019 STIC logger calibration results. A perfect 1:1 fit would lie on the black line shown. STIC logger 7a is shown on the left, STIC logger 3a on the right.

3.4 Specific Conductance Data

Table 3.4 shows the range of 2016 to 2018 specific conductance (SC) data that were collected at each site location. Lower SC values generally occurred during higher flows and higher SC values during lower flows. Due to the relativity of STIC logger SC data, these data were not used to summarize SC values. Instead, continuous hourly data from U24 loggers and discrete data from a hand-held conductivity meter were used. Site 4 data comes from the USGS (Clark, 2000).

Table 3.4. The range of specific conductance (SC) values measured at each site.

Site Number: Stream Name	SC Range (µS/cm)
1: South Fork of the Elk River	19.4-60 (discrete)
2: North Fork of the Elk River	4.5-91.5
3: English Creek	21.6-37.9 (discrete)
4: Encampment River	17-140
5: Elkhead Creek	101-488
6: First Creek	65-194 (discrete)
7: Roaring Fork of Slater Creek	28.5 – 83.7 (discrete)
8: Silver Creek	19.1 – 51.3
9: East Fork Williams Fork	109.8 (07/17 discrete)
10: Poose Creek	131-194 (2017 discrete)

3.4.1. U24 and STIC Field Data

When STIC logger predicted EC regression equations are applied to field data, these values may remain as is or be converted to specific conductance (SC). In the field, STIC logger recorded EC and SC values follow the same relative trends as U24 logger values, and therefore, as mentioned in chapter 1.2, 2.4.3 and 2.4.4, STIC logger recorded field EC or SC trends will be referred to as relative EC (rEC) or relative SC (rSC). Because rEC and EC change with temperature, STIC field rEC was converted to rSC to compare rSC across different sites (Gillman et al., 2017):

$$rSC = \frac{rEC}{(1+a(T-25))} \quad \text{[E2.4]}$$

where *a* is the linear temperature compensation factor (2.1% per °C) and *T* is temperature. Figures of 3.17 to 3.19 display hourly U24 SC and STIC rSC over time.

Figure 3.17 shows hourly and discrete data from Site 2, North Fork of the Elk River. Hourly STIC logger rSC values follow the same relative trends as U24 logger hourly SC values for most of 2018, but not during freezing winter months. Oakton discrete SC data points fall in line with hourly U24 logger data, expect on June 19 and 20 when they fall between U24 and STIC logger values.

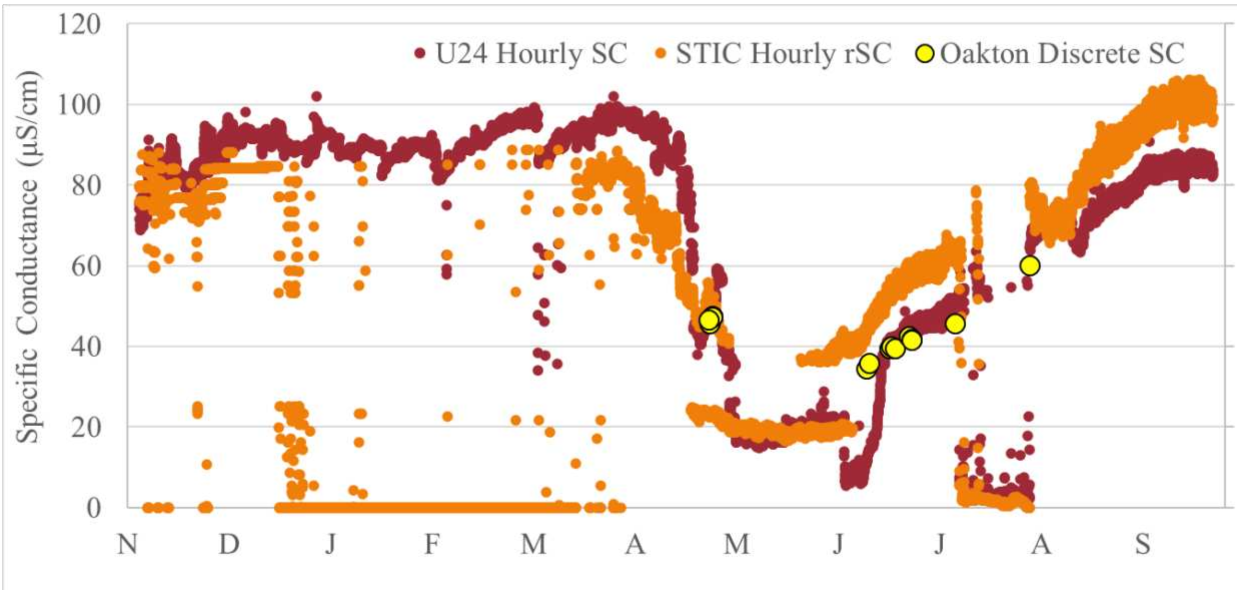

Figure 3.17. Site 2: North Fork of the Elk River 2017 – 2018 U24 and STIC logger hourly SC and rSC data (maroon and orange, respectively), with Oakton meter discrete SC data points (yellow).

Figure 3.18 displays hourly data from Site 5, Elkhead Creek. The U24 logger (maroon) produced unreasonable SC data when temperatures dropped between –0.25 and –1.16°C for the period of 12/12/2017 – 02/09/2018. During this same period, STIC rSC data remained reasonable. All SC and rSC data for this period were removed for baseflow index comparisons between data loggers (section 3.5). The STIC logger produced unreasonable rSC predictions for the high flow period of April 22 – June 5, 2018. Field notes indicate the STIC logger was buried under sediment during this time.

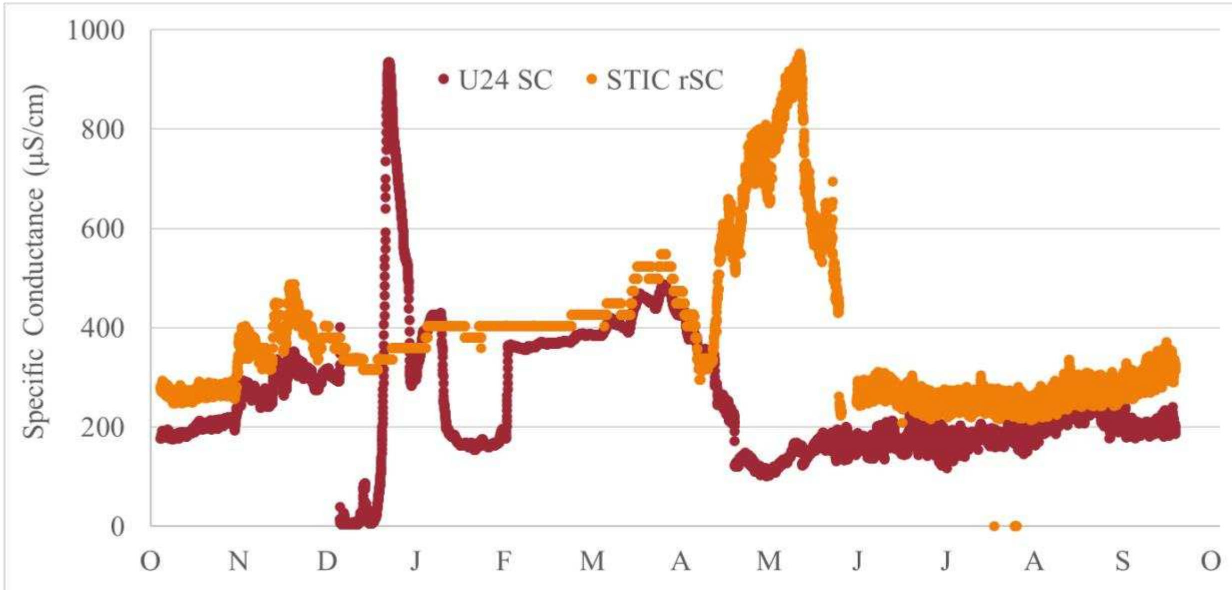

Figure 3.18. Site 5: STIC 5a and U24 hourly data from loggers launched at Elkhead Creek 2017–2018.

Figure 3.19 shows Site 8, Silver Creek hourly data. This figure displays minimal variations in U24 and STIC logger SC and rSC. STIC logger 8 stopped logging on April 4, 2018.

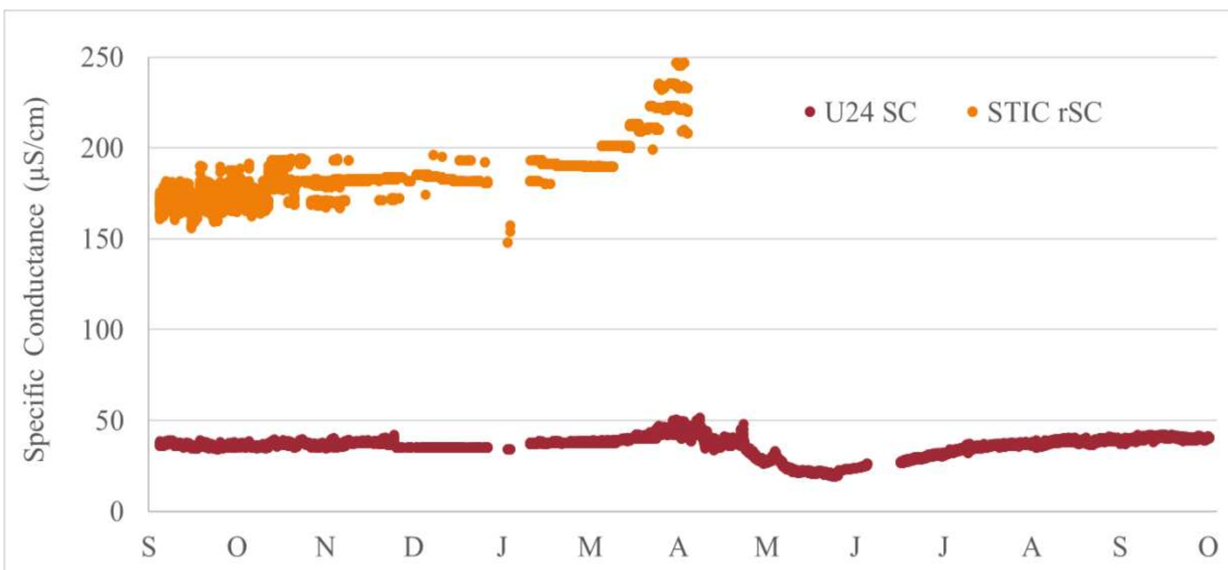

Figure 3.19. Site 8: STIC 8 and U24 hourly data from loggers launched at Silver Creek 2017–2018.

3.4.2. Duplicate STIC Loggers

Duplicate STIC loggers were deployed at seven site locations. Of these, two could not be calibrated, two had R^2 values of 0.982 or lower (STIC 1b and 6b, see supplementary files), and the other three sets of duplicate STIC loggers had calibrations with R^2 of 0.986 or greater. These three sets of duplicate STIC loggers were deployed at Site 4, Encampment River; Site 7, Roaring Fork of Slater Creek; and Site 10, Poose Creek. The Duplicate STIC loggers 10a and 10b were deployed in different water years. Hourly field data comparisons of duplicate STIC loggers are possible at Site 4, Encampment River, and Site 7, Roaring Fork of Slater Creek, if the relativity requirement is taken into account by using CMB equation 2.5. But first this study will determine if these sites are suited for this method of baseflow estimation.

3.5. Specific Conductance and Stream Discharge Relationships

As described in Chapter 1, streamflow conductivity values are often inversely related to streamflow discharge. This relationship may not be exact, but the general trend is what will be considered here. Most of the following sites show hourly rSC or SC values dropping quickly with increasing discharge, arriving at a minimum during peak discharge, rising slowly with decreasing discharge, and arriving at a high value or maximum once runoff ends. Any sites where these trends do not occur do not meet the requirements of the CMB method. Figure 3.20 displays South Fork of the Elk River (Site 1) hourly discharge data and hourly STIC rSC data for October 1, 2017 – September 10, 2018. Stream rSC is inversely related to stream discharge at this site. Therefore, this stream is suited for the CMB method.

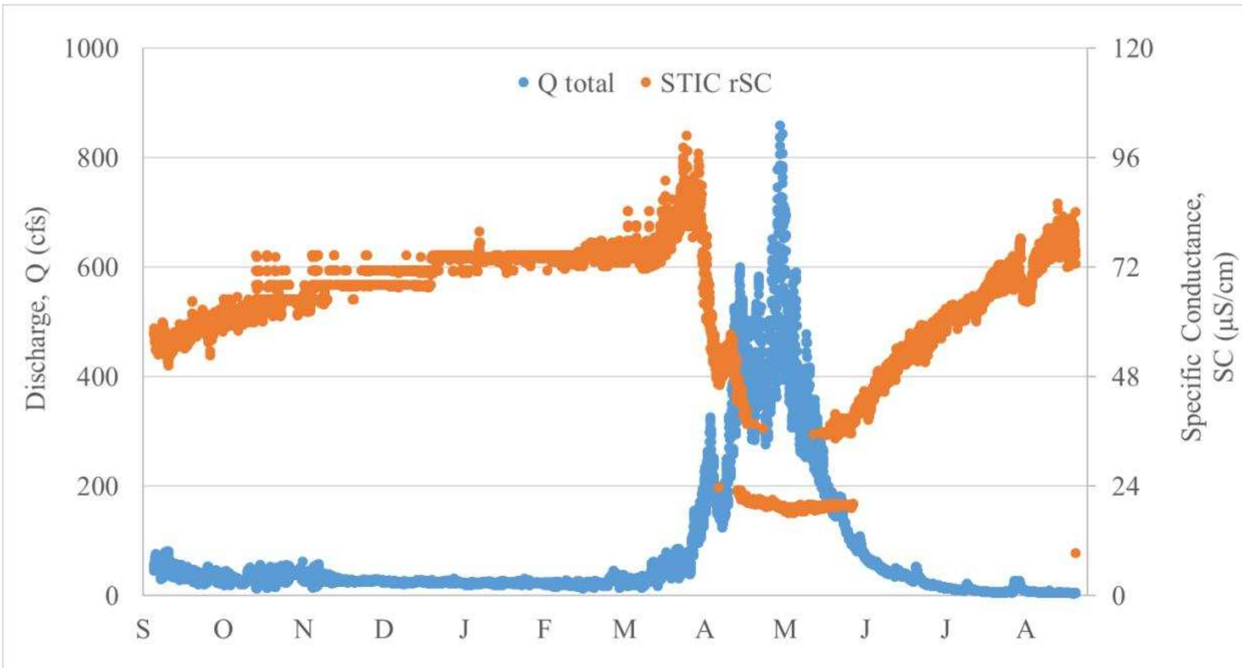

Figure 3.20. Stream discharge (blue) and STIC logger rSC (orange) data for October 2017 – September 2018 at Site 1, South Fork of the Elk River.

Figure 3.21 uses hourly U24 SC data and hourly STIC rSC data to demonstrate its inverse relation with total discharge (Q) at Site 2, North Fork of the Elk River for April 5, 2018 – October 3, 2018. This river is also suited for the CMB method of baseflow estimation. As can be seen in Figure 3.17 (section 3.4.1), both U24 and STIC loggers recorded values close to zero for the 13-day period between July 26 – August 7, 2018. These values were omitted in Figure 3.21.

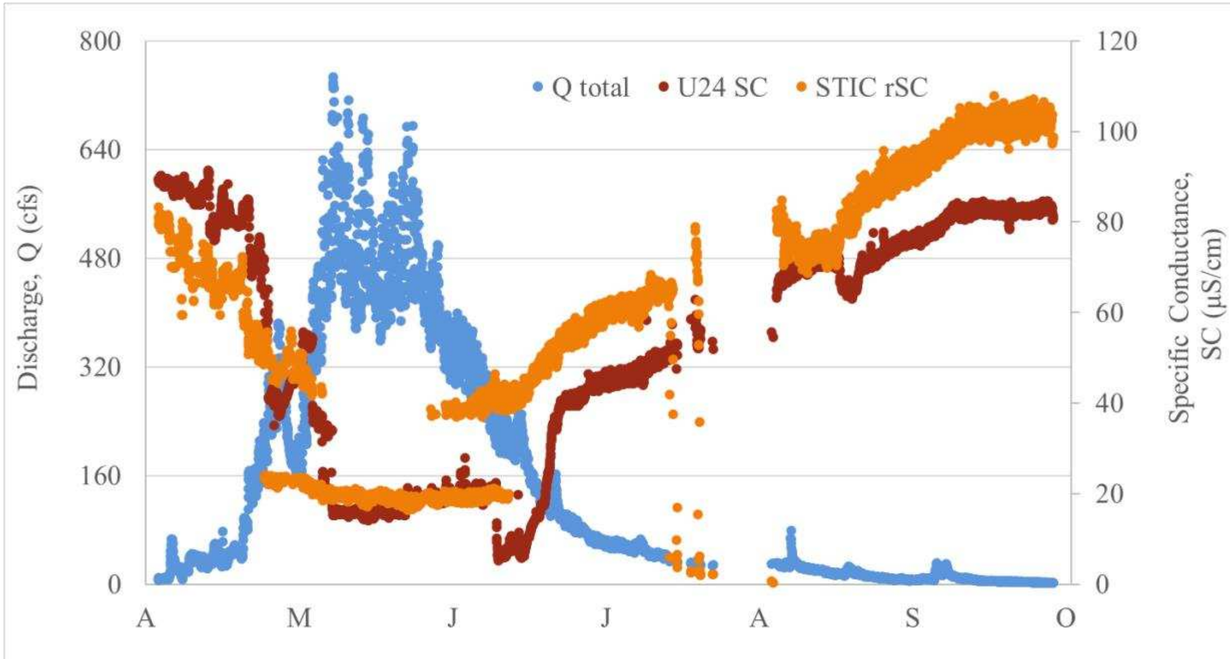

Figure 3.21. Hourly stream discharge (blue), hourly U24 SC (maroon), and hourly STIC rSC (orange) data for April – October 2018 at Site 2, North Fork of the Elk River.

Figure 3.22 displays Site 3, English Creek hourly STIC rSC (10/05/17 – 06/12/18) and hourly stream discharge (10/05/17 – 10/03/18). This site is not suited for the CMB method. English Creek's rSC data are not inversely related to its stream discharge data. Instead, STIC rSC values remain relatively stable and slightly increase with rising limb runoff. The STIC logger stopped logging on June 12, 2018.

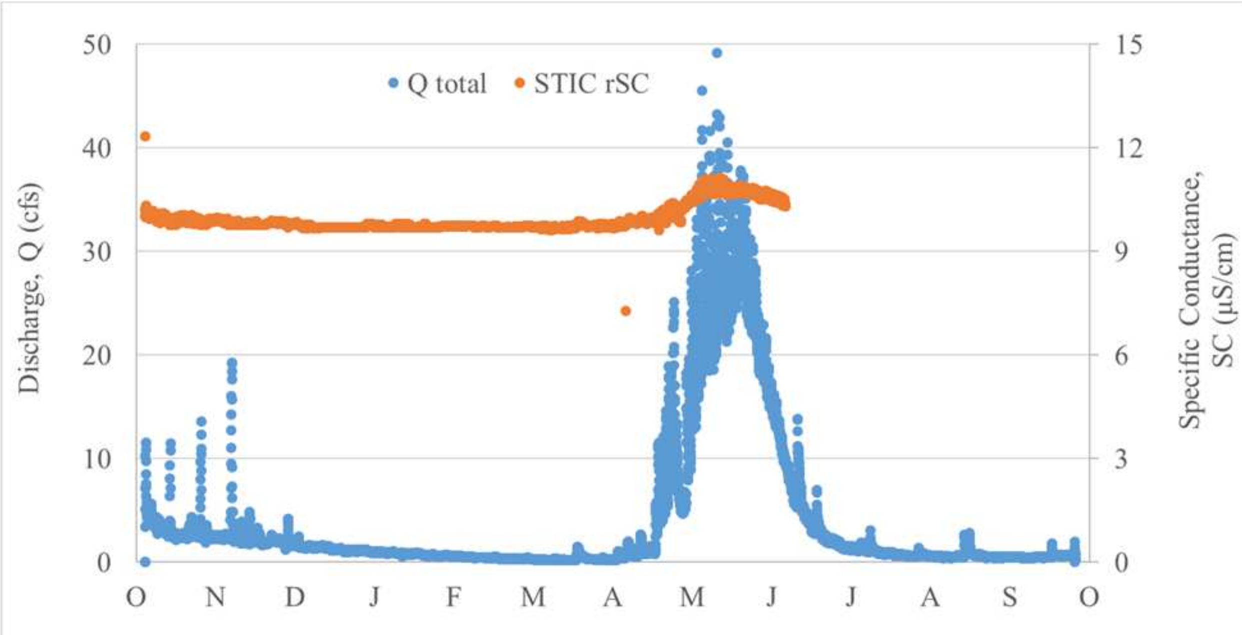

Figure 3.22. Hourly stream discharge (blue) and hourly STIC logger rSC (orange) data for October 2017 – October 2018 at Site 3, English Creek.

Figure 3.23 shows Encampment River (Site 4) hourly stream discharge (10/12/17 – 8/19/18), and hourly STIC rSC data (10/12/17 – 10/03/18.) STIC rSC values are inversely related to stream discharge. These values drop quickly with increasing discharge. STIC rSC values arrive at a minimum during peak discharge. STIC rSC values rise slowly with decreasing discharge. STIC rSC values reach a maximum during baseflow once runoff ends, and so this site is suited for the CMB method.

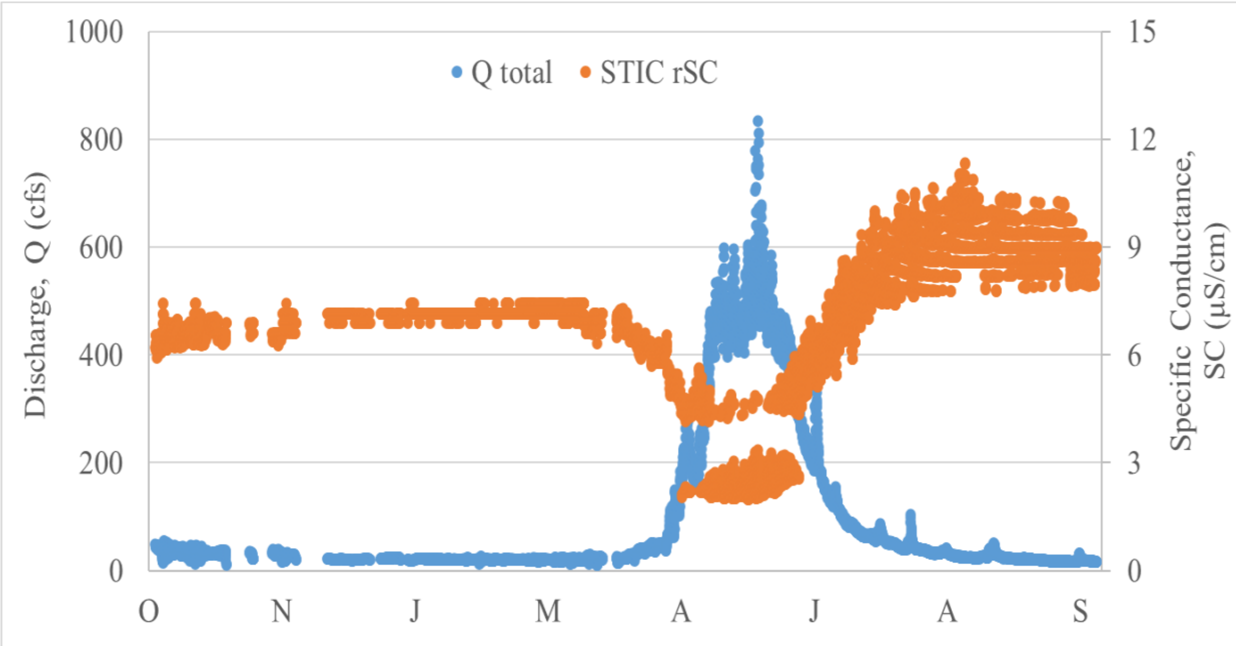

Figure 3.23. Hourly stream discharge (blue) and hourly STIC logger rSC (orange) data for October 2017 – October 2018 at Site 4, Encampment River.

Figure 3.24 presents the Elkhead Creek (Site 5) hourly stream discharge and hourly U24 SC data for February 9, 2018 – September 23, 2018. As is the case for Site 3, SC values are not inversely related to stream discharge. SC data do not drop quickly with increasing discharge nor do they arrive at a minimum during peak discharge; they begin to decrease after peak flows and reach a minimum during the falling limb of the hydrograph. SC values do not rise slowly with decreasing discharge; instead, they rise during the second half of the falling limb of the hydrograph. Site 5 is not suited for the CMB method.

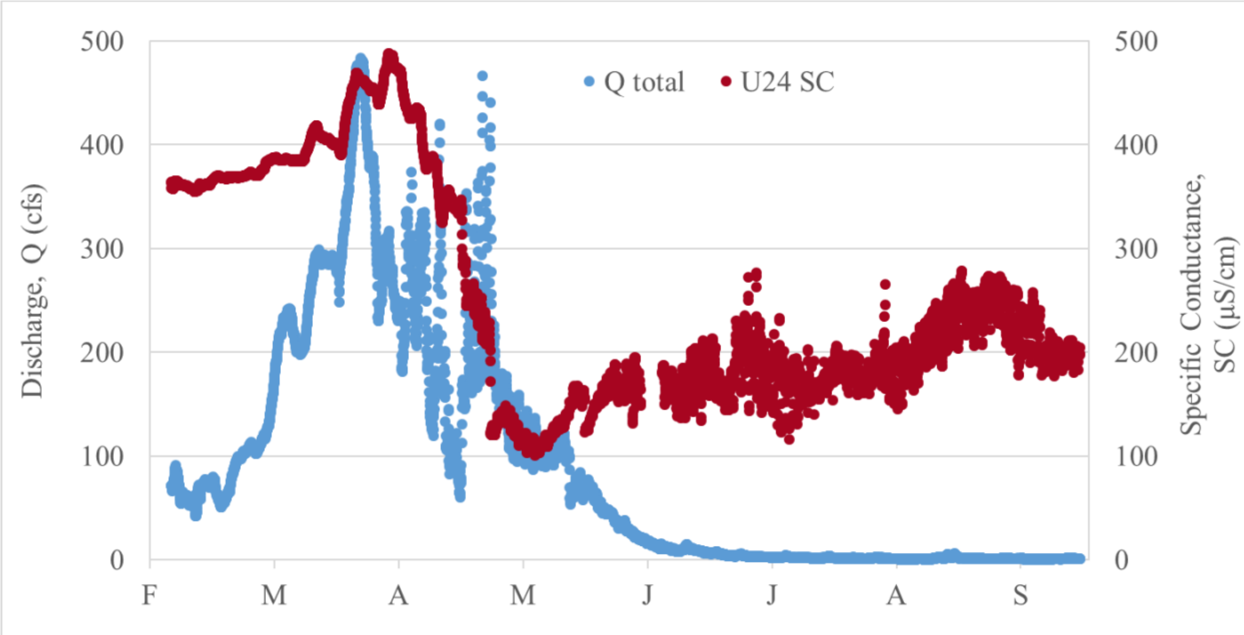

Figure 3.24 Hourly stream discharge (blue) and hourly U24 SC (maroon) data for February 2018 – September 2018 at Site 5, Elkhead Creek.

Figure 3.25 displays the First Creek (Site 6) inverse relationship between hourly stream discharge (Q) and hourly STIC rSC data for April 19, 2018 - October 1, 2018.

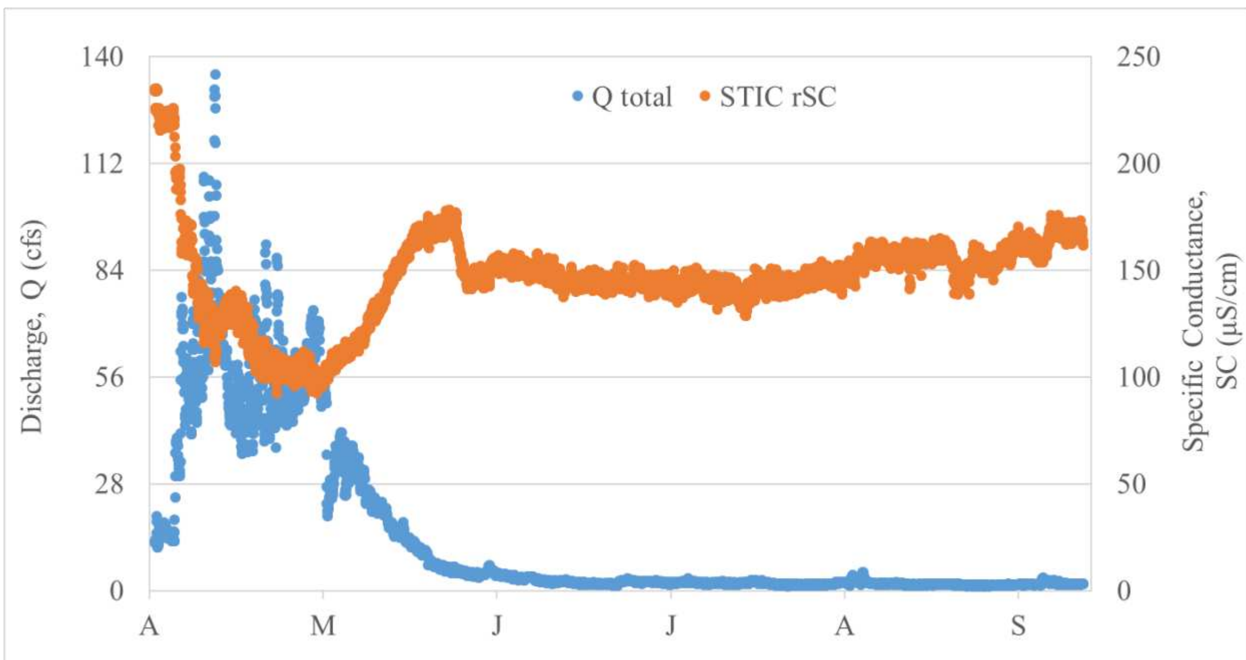

Figure 3.25. Stream discharge (blue), STIC rSC (orange) for 4 – 10/2018 at Site 6, First Creek.

Figure 3.26 shows the Roaring Fork of Slater Creek (Site 7) stream discharge and STIC 7a rSC inverse relation for May 6, 2018 – August 13, 2018.

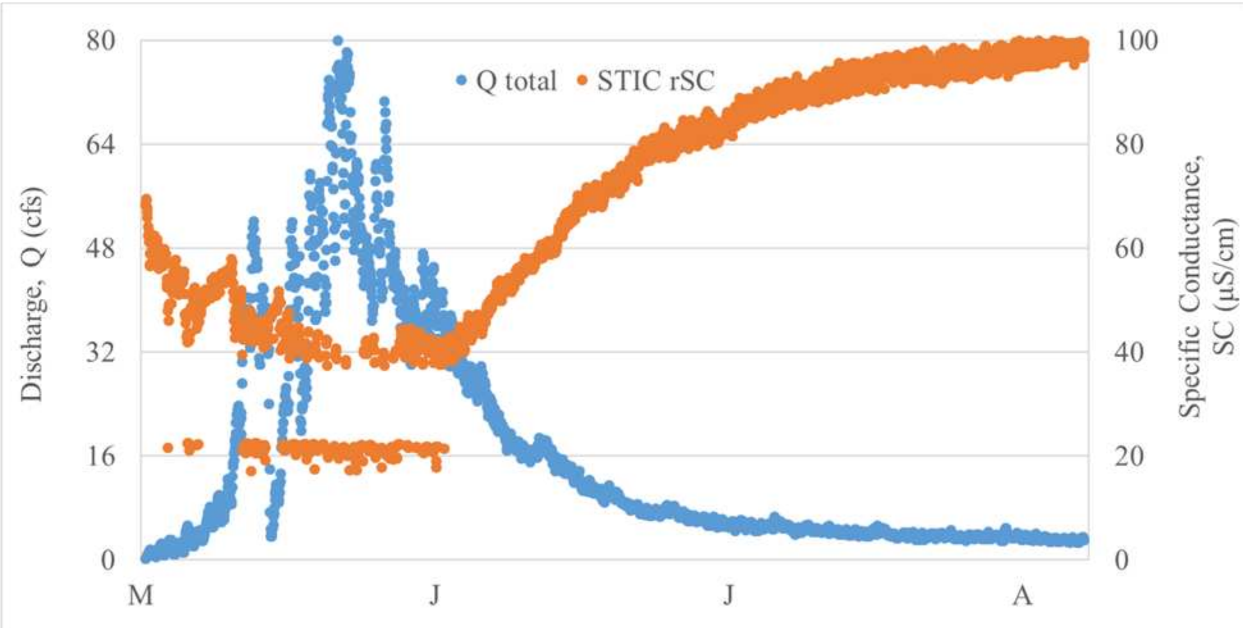

Figure 3.26. Stream discharge (blue), STIC rSC (orange) for May – August 2018 at Site 7, Roaring Fork of Slater Creek.

Figure 3.27 displays the Silver Creek (Site 8) stream discharge and U24 SC inverse relation for February 11, 2018 – September 30, 2018.

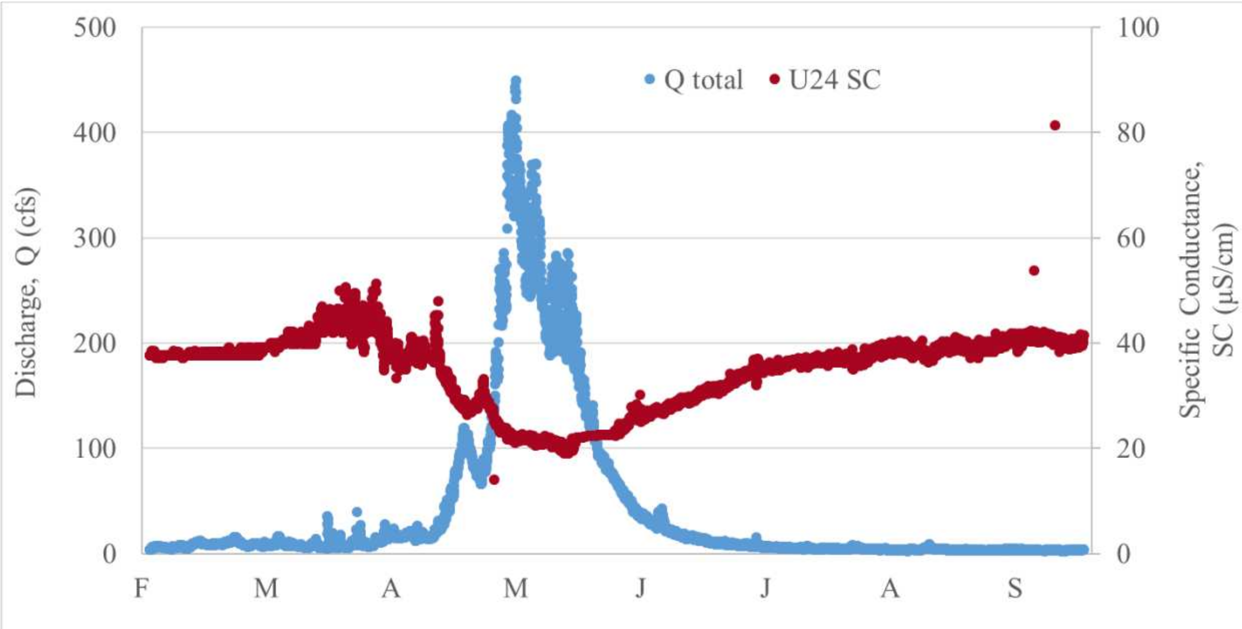

Figure 3.27. Stream discharge (blue) and U24 SC (maroon) for February – September 2018 at Site 8, Silver Creek.

Figure 3.28 shows the East Fork of the Williams Fork (Site 9) stream discharge and STIC rSC inverse relation for December 26, 2017 – October 4, 2018.

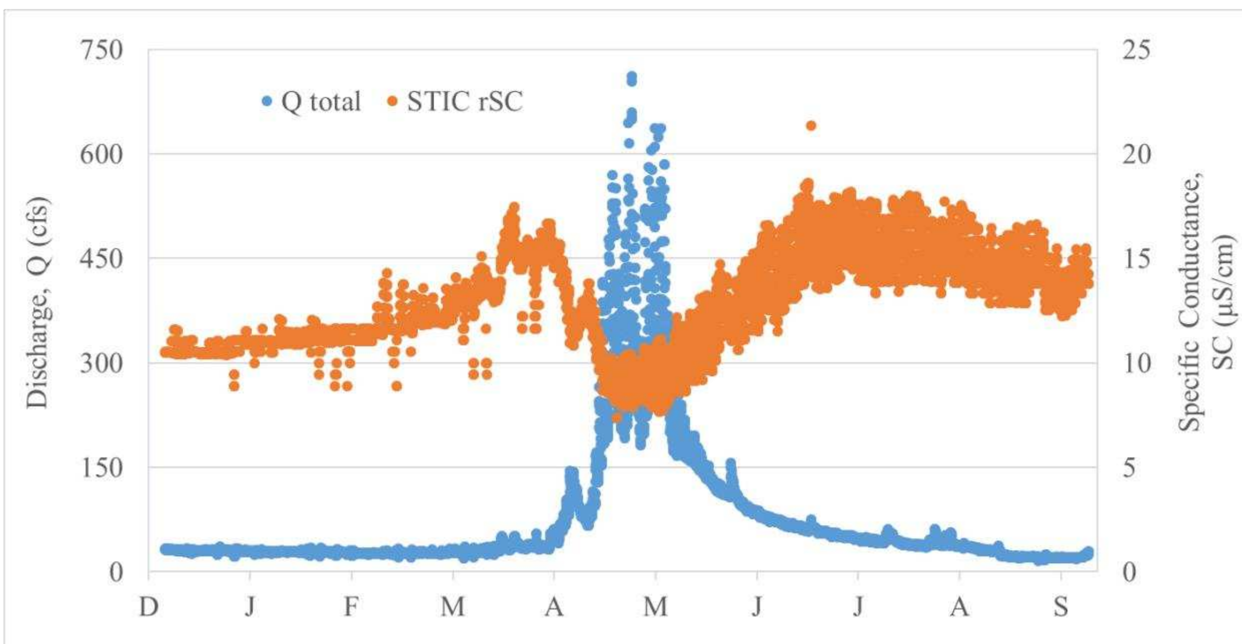

Figure 3.28. Stream discharge (blue) and STIC rSC (orange) for December 2017– September 2018 at Site 9, East Fork of the Williams Fork.

Figure 3.29 displays the Poose Creek (Site 10) stream discharge and STIC rSC inverse relation for March 25, 2017 – October 1, 2017.

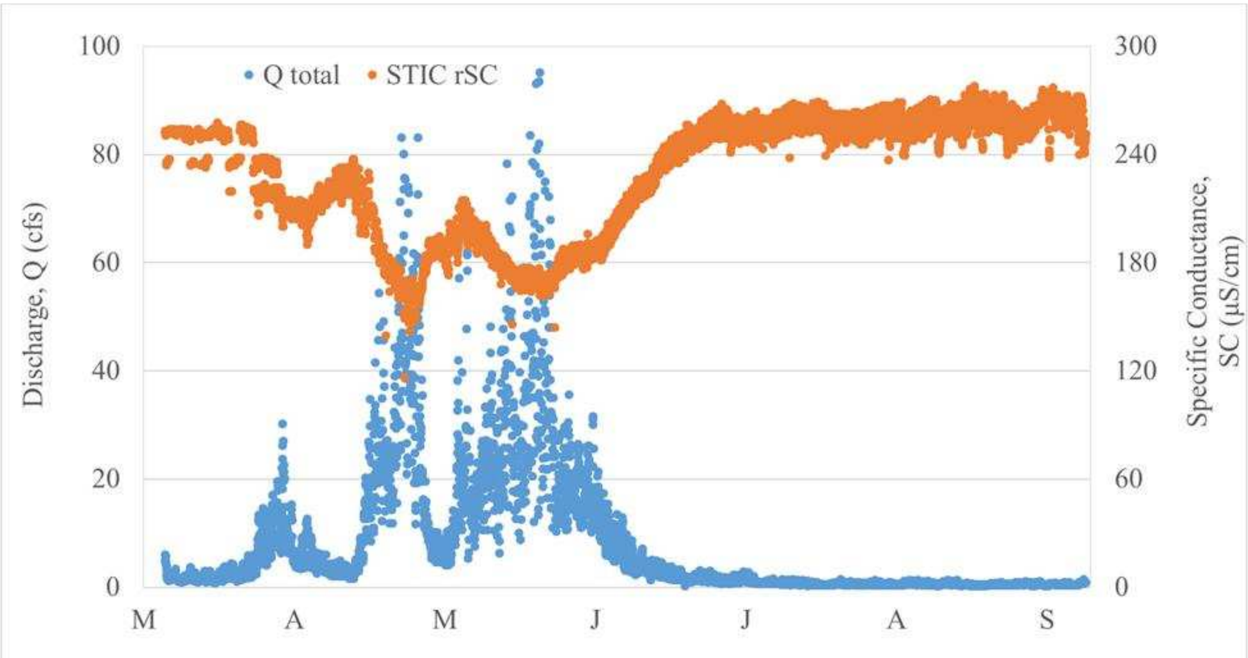

Figure 3.29. Hourly stream discharge (blue) and hourly STIC rSC (orange) data for March – October 2017 at Site 10, Poose Creek.

Table 3.5 summarizes the findings of this section, showing which eight sites are suitable for the CMB method to estimate baseflow. The details of the baseflow estimations for these sites are outlined in sections 3.6 and 3.7.

Table 3.5. Sites Suitable for the CMB Method Equation to Estimate Baseflow

Site Number	Site Name
1	South Fork of the Elk River
2	North Fork of the Elk River
4	Encampment River
6	First Creek
7	Roaring Fork of Slater Creek
8	Silver Creek
9	East Fork Williams Fork
10	Poose Creek

3.6 Baseflow Estimation: Sites with Both U24 and STIC Loggers

North Fork of the Elk River (Site 2) and Silver Creek (Site 8) are suitable for the CMB method of baseflow estimation and both had U24 and STIC data loggers deployed. Annual and post snowmelt-dominated baseflow indexes (BFIs) were calculated with daily data from both data logger types, where possible. At Site 2, the post snowmelt-dominated period was determined to start on June 23, 2018, when daily data from both U24 and STIC loggers could be used to calculate a daily BFI consistently greater than 18 percent. The daily data from the U24 logger were used to calculate an annual BFI of 26 percent and the daily STIC logger data were used to calculate a BFI of 13 percent. Annual BFI calculations for Site 2 were made for the period of April 5, 2018 to October 3, 2018. Post snowmelt-dominated BFI calculated with daily STIC data was 56 percent and when calculated with daily U24 data, was 60 percent.

A hydrograph that was separated using the CMB method with hourly discharge and U24 SC data is shown for Site 2 (gold), followed by a hydrograph separated using the CMB method with hourly discharge and STIC rSC data (fuchsia) in Figure 3.30. The hourly baseflow (Q_{bf}) graphs have slightly different shapes during peak flow, with very similar shapes during low flow. The baseflow discharges calculated with hourly data from the two different data loggers have similar low values, but the high values differ by about 95 cfs (a range of 0 – 214 cfs for the U24 and 0 – 119 cfs for the STIC). As can be seen in Figure 3.17 (section 3.4.1), both U24 SC and STIC rSC data recorded values close to zero for the 13-day period between July 26 – August 7, 2018. Data during this timeframe were omitted.

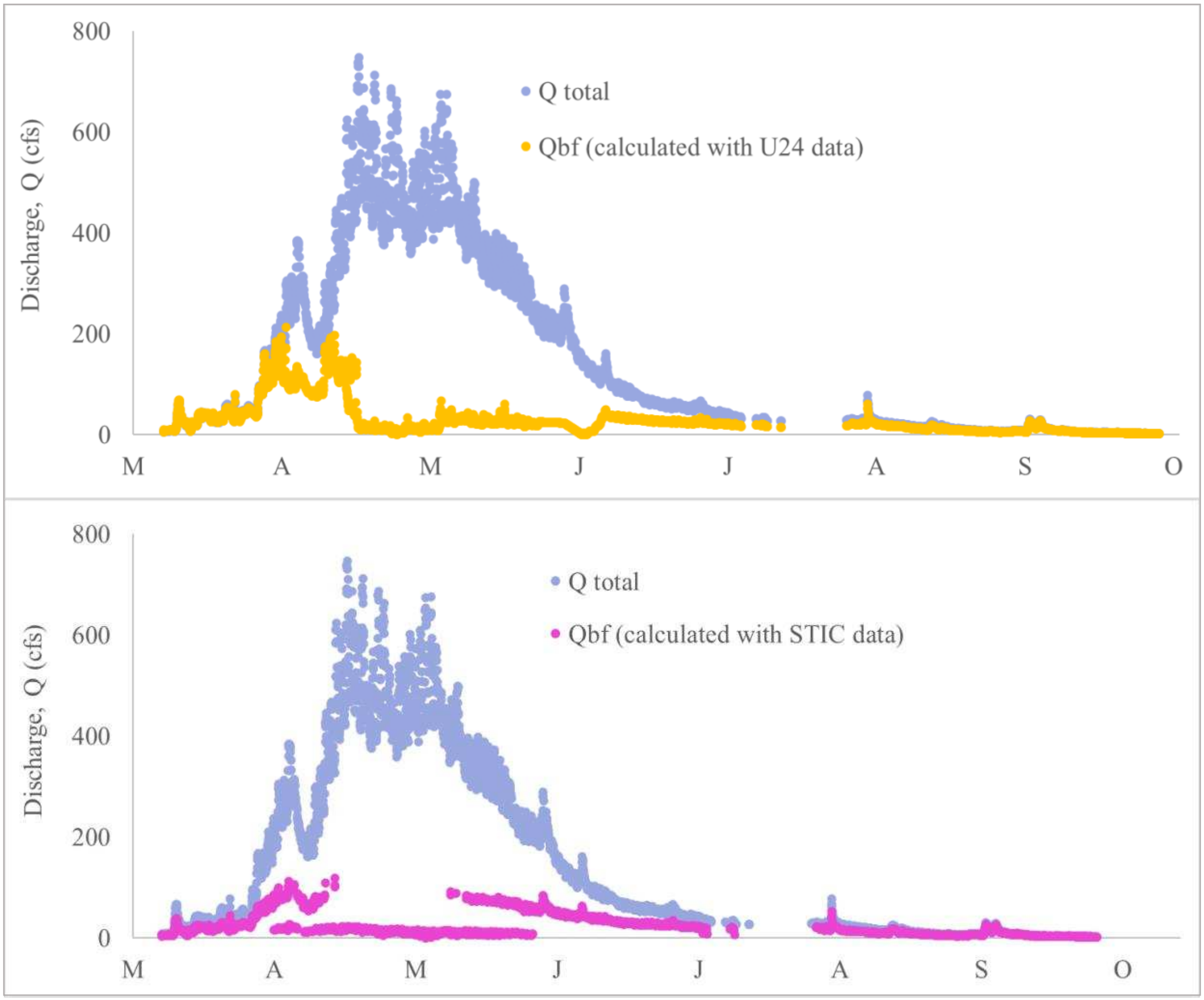

Figure 3.30. Site 2 CMB method separated hydrographs calculated with hourly discharge and U24 logger data (gold, top), and with hourly discharge and STIC logger data (fuchsia, bottom) for the period of April 5 to October 3, 2018.

At Site 8, Silver Creek, STIC logger 8 stopped logging its hourly rSC data on March 30, 2018 while the U24 logger continued to log a full year of hourly SC data. STIC logger 8 was not able to log a rSC runoff end-member value nor a rSC baseflow end-member value, making baseflow estimation impossible with data from this STIC logger. Because BFI requires a baseflow discharge estimate, an accurate BFI could not be calculated using data collected by STIC logger 8. Therefore, the only means for data logger comparisons at Site 8 are in section 3.4.1, U24 and STIC logger field Data (Figure 3.19).

Annual and post snowmelt-dominated BFIs calculated with daily discharge and daily U24 logger SC data are displayed in Table 3.6. Annual BFI calculations were for February 11 – September 30, 2018. The post snowmelt-dominated period began on June 8, 2018, when the BFI for that day was 26.3 percent when the change in slope of the hydrograph dropped consistently below 114 cfs. Because STIC logger 8 stopped logging at the end of March while the U24 logger continued, Site 8 used hourly U24 SC data to separate its hydrograph (Figure 3.31). Hourly baseflow increases slightly during the first peak flows and returns to lower baseflow discharges by June 2018.

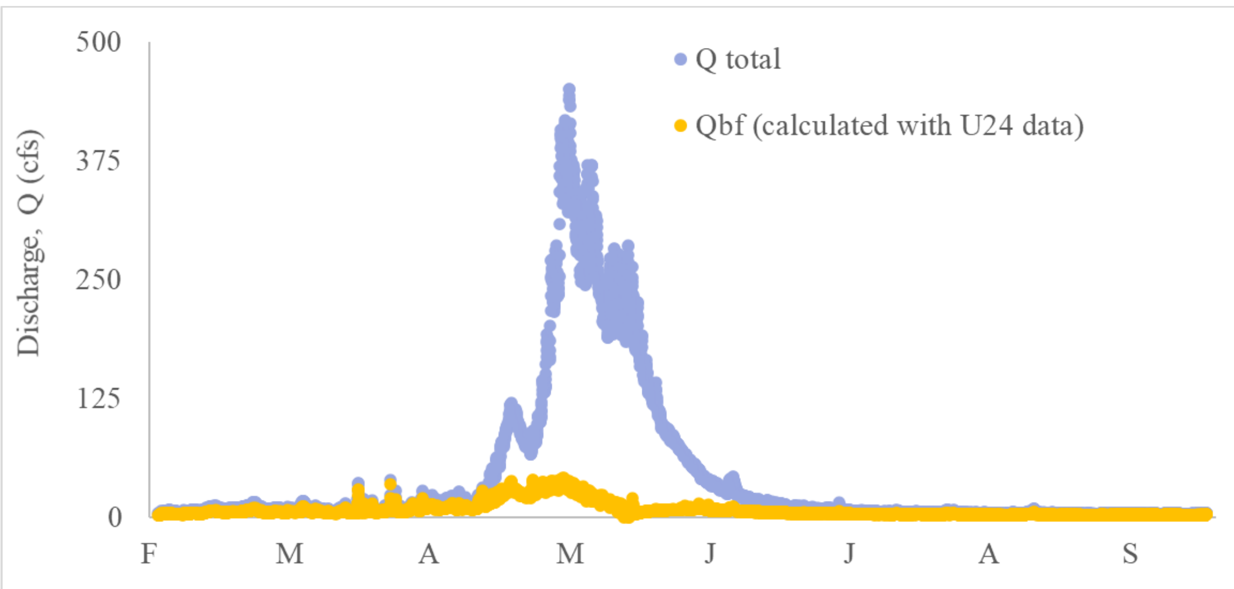

Figure 3.31. Silver Creek (Site 8). CMB method separated hydrograph. Calculated with hourly discharge and U24 logger SC data for the period of February 11 to September 30, 2018.

Table 3.6 summarizes the BFI percentages calculated with daily data (the final value at the end of each day) including daily data from both U24 and STIC loggers at North Fork of the Elk River and Silver Creek. Post snowmelt dominated BFI is 0.3 percent higher when calculated with SC data from the U24 logger. Please note that annual BFI began in April 2018 at Site 2 and in February 2018 at Site 8.

Table 3.6. North Fork of the Elk River annual and post snowmelt-dominated baseflow index summary based on calculations made with daily discharge and daily data from a U24 and STIC logger. Silver Creek annual and post snowmelt-dominated baseflow index summary based on calculations made with daily discharge data and daily data from a U24 logger. N/D* signifies not enough data to calculate.

Site Number: Stream Name	STIC Annual BFI	U24 Annual BFI	STIC Post Snowmelt Dominated BFI	U24 Post Snowmelt Dominated BFI
2: North Fork of the Elk River	12.8%	26.0%	55.9%	59.6%
8: Silver Creek	N/D*	25.2%	N/D*	53.9%

3.7. Hydrograph Separation, All Other CMB Suitable Sites with STIC Logger Data

This section examines the hydrograph separations for all additional CMB suitable sites, where only STIC loggers were deployed. Baseflow estimations computed with hourly data from STIC loggers launched at Sites 1, 4, 6 – 7, and 9 – 10 are displayed in this section, BFI estimates calculated with daily data are presented, and the different flows and time periods for each site are reviewed.

3.7.1. Site 1: South Fork of the Elk River

STIC logger 1a was launched at South Fork of the Elk River (Site 1) June 26, 2017 until September 10, 2018. Based on daily STIC 1a data and daily discharge data, groundwater contribution to streamflow starts to become more significant on July 4, 2017 (when that day’s BFI is 27.5 percent) and on June 20, 2018 (BFI for that day of 28.0 percent), which mark the start dates of the post snowmelt-dominated periods. Annual BFI for 2017 was 33 percent and for 2018 was 32 percent (October 1, 2017 to September 10, 2018, calculated with daily data). This is summarized in Table 3.7. Post snowmelt-dominated BFI was 50 percent in 2017 and 53

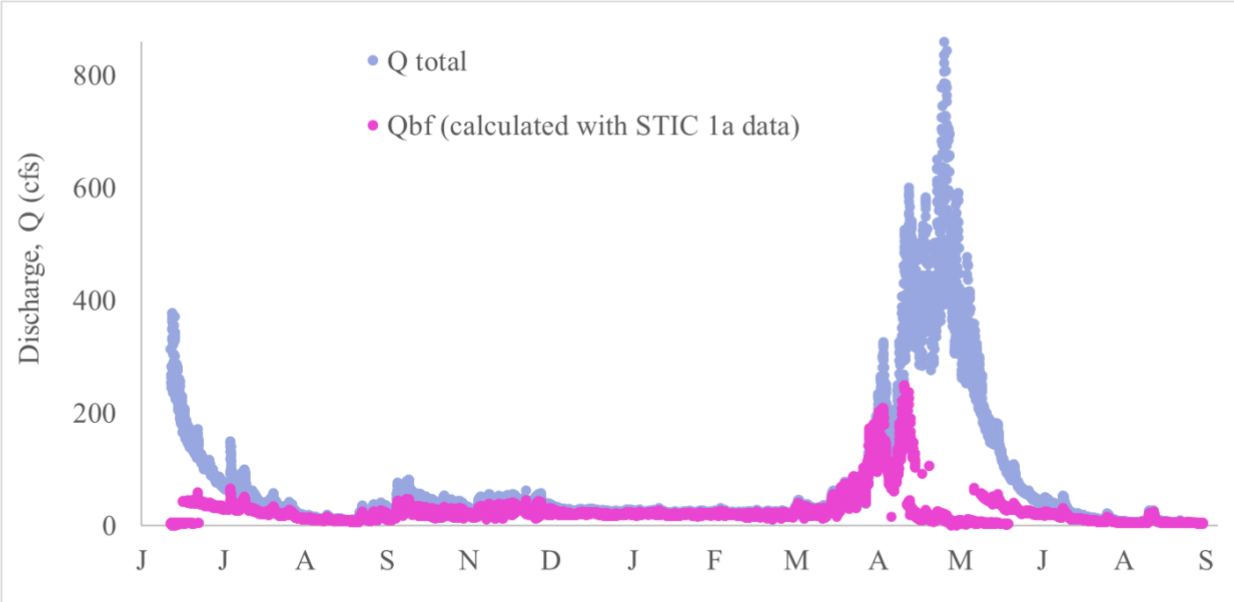

Figure 3.32. Site 1 South Fork of the Elk River CMB method separated hydrograph calculated with STIC 1a hourly data and hourly Q data for the period of June 26, 2017 – September 10, 2018.

percent in 2018 (calculated with daily data). Figure 3.32 displays hourly baseflow discharge (fuchsia) with hourly total stream discharge (blue) for June 26, 2017 to September 10, 2018.

3.7.2. Site 4: Encampment River

STIC logger 4a was deployed at Encampment River October 12, 2017 to September 30, 2018. Based on daily STIC 4a data and daily discharge data, groundwater contribution to streamflow starts to become more significant on June 8, 2018 (when that day's BFI is 31.4 percent). 2018 annual BFI was 29 percent (October 12, 2017 to September 30, 2018, calculated with daily data). Post snowmelt-dominated BFI was 63 percent, with an annual BFI of 28 percent (calculated with daily data). This is summarized in Table 3.7. Figure 3.33 displays hourly baseflow discharge (fuchsia) with hourly total stream discharge (blue) for 2018.

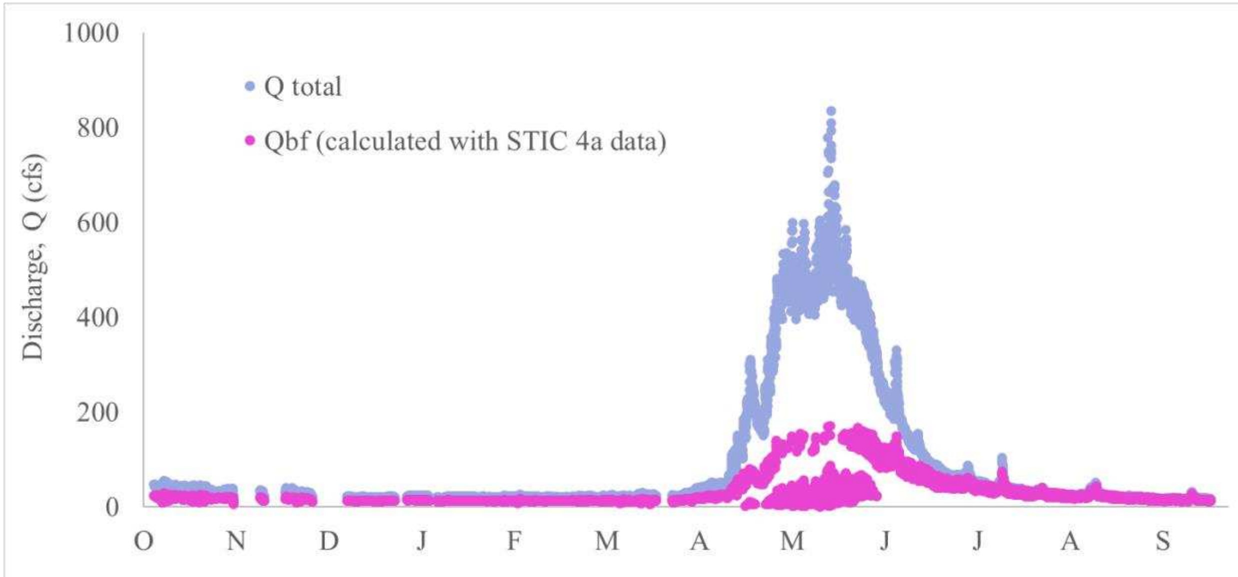

Figure 3.33. Site 4 Encampment River CMB method separated hydrograph calculated with STIC 4a hourly data and hourly Q data for the period of October 12, 2017 – September 30, 2018.

3.7.3. Site 6: First Creek

STIC logger 6a was launched at First Creek November 9, 2016 to October 1, 2018. The April 19 – October 1, 2018 separated hydrograph (baseflow calculated with hourly STIC 6a rSC data and hourly discharge data) is displayed in Figure 3.34. Corrections were made by eliminating unreasonably high flows and unreasonably high rSC values in winter. Groundwater contribution to streamflow begins to become more significant on May 27, 2018 (daily BFI of 23.1 percent), which marks the start of the post snowmelt-dominated period. Annual BFI for 2018 was 67 percent and the 2018 post snowmelt-dominated BFI was 78 percent (calculated with daily data).

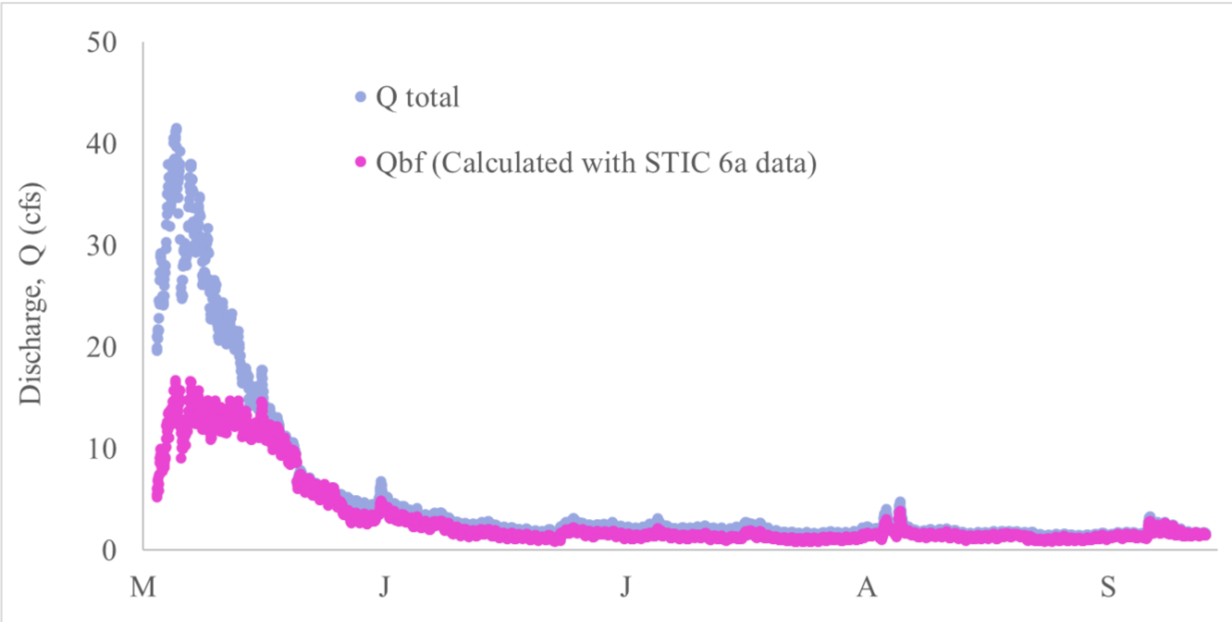

Figure 3.34. Site 6 First Creek falling limb of the CMB method separated hydrograph calculated with hourly Q and hourly STIC 6a data for the period of May 19 – October 1, 2018.

3.7.4. Site 7: Roaring Fork of Slater Creek

STIC logger 7a and 7b were launched at an hourly frequency at Roaring Fork of Slater Creek November 9, 2016 – August 13, 2018. The data for these STIC loggers overlaps during water year 2017, so the hourly baseflow estimates calculated with hourly discharge data and hourly rSC data from both STIC loggers are compared in the top portion of Figure 3.35. Daily data from STIC 7a and 7b were used to calculate BFI estimates within 0.2 percent of one another for the 2017 post snowmelt-dominated period. Daily data from STIC logger 7a was used to calculate a post snowmelt-dominated BFI of 61.0 percent and daily data from STIC 7b was used to calculate a BFI of 61.2 percent for the same period.

The 2017 post snowmelt-dominated period began on June 21 (STIC 7a daily BFI of 21.9 percent and STIC 7b daily BFI of 27.2 percent). In 2018 this period began on June 7 (STIC 7a BFI for this day was 22.2 percent). 2018 post snowmelt-dominated BFI calculated with daily data from STIC logger 7a was 59 percent. Annual BFI calculations were made for April 7, 2017

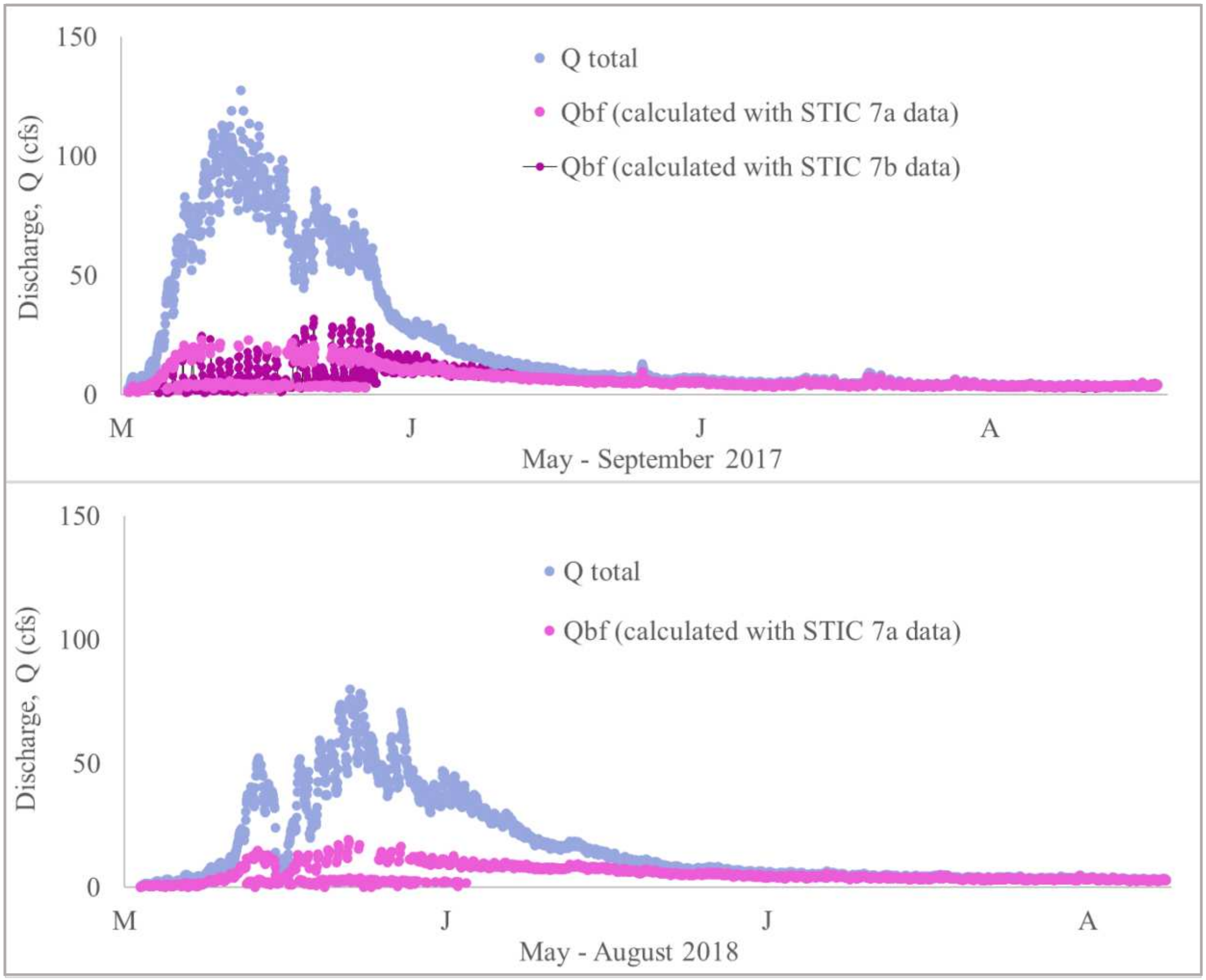

Figure 3.35. Roaring Fork of Slater Creek (Site 7) CMB method separated hydrograph. STIC 7a and 7b hourly data were used for baseflow calculations plotted in the top graph (May 27 – September 14, 2017) and STIC 7a hourly data were used for baseflow calculations plotted in the lower graph (May 6 - August 13, 2018).

to September 30, 2017 and April 7, 2018 to August 13, 2018. Figure 3.35 shows the separated hourly hydrographs for 2017 and then 2018. 2017 peak flows are higher than those in 2018 (127 cfs vs, 80 cfs), and the hourly baseflow estimates also drop in 2018.

3.7.5. Site 9: East Fork of the Williams Fork

STIC 9 was launched at East Fork of the Williams Fork from December 15, 2017 until October 4, 2018. The post snowmelt-dominated period began on June 6, 2018 when the BFI for that day was 29 percent. BFI was calculated with daily data for the post snowmelt-dominated and annual time periods (Table 3.7). Annual 2018 BFI was 33 percent and post snowmelt-dominated BFI was 60 percent. Figure 3.36 shows the CMB method separated hydrograph calculated with hourly discharge and rSC data from STIC 9. Baseflows are generally stable throughout the year and increase slightly during higher flows.

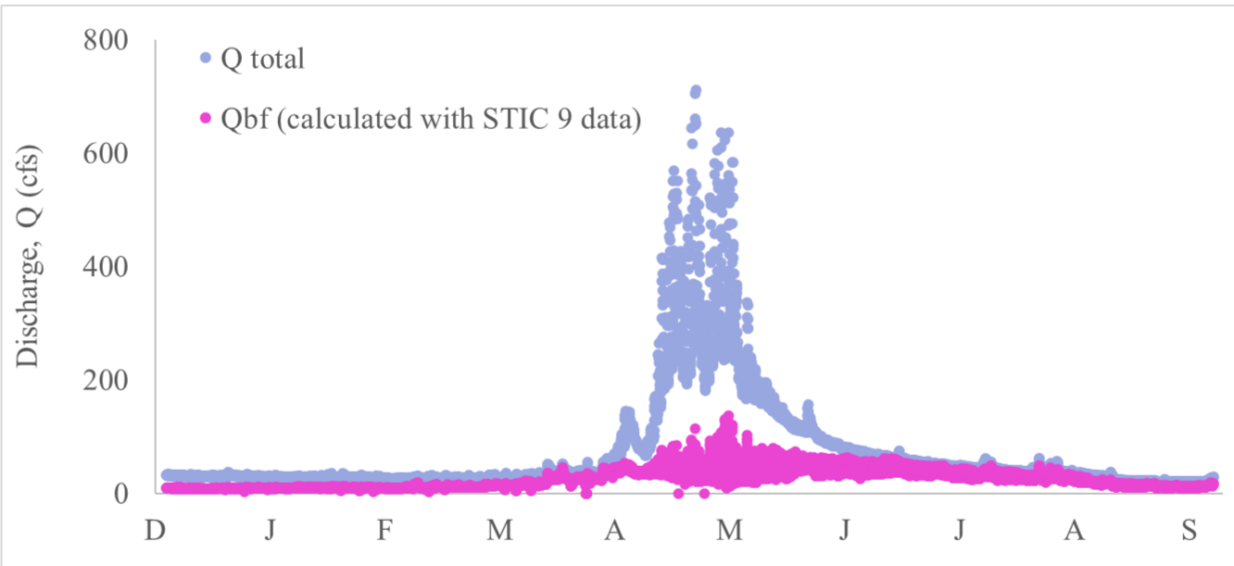

Figure 3.36. East Fork of the Williams Fork (Site 9) CMB method separated hydrograph. Baseflows were calculated with hourly STIC 9 rSC data and hourly discharge data for the period of December 26, 2017 – October 04, 2018.

3.7.6. Site 10: Poose Creek

STIC 10a was launched at Poose Creek November 7, 2016 – October 1, 2017, when discharge was also computed. STIC 10b was launched at Poose Creek from November 16, 2017 until October 4, 2018, but hourly discharge data has not been computed for this period. Because STIC logger 10a and 10b were deployed during different water years, even with hourly discharge data for 2018, the baseflows computed with STIC 10a and 10b hourly data cannot be compared to determine duplicate STIC logger data consistency. Hourly data from STIC 10a was used with hourly discharge data for baseflow calculations. The 2017 CMB method separated hydrograph using hourly STIC 10a data can be viewed in Figure 3.37. Hourly baseflows appear to increase with each set of higher stream discharges and decrease when the total flows fall. The post snowmelt-dominated period began on June 23, 2017 when the daily BFI was 29.7 percent. Daily BFI was calculated for 2017 – 2018 (annual, 37 percent) and for the post snowmelt-dominated period (68 percent), using daily discharge and rSC data. These results are presented in Table 3.7.

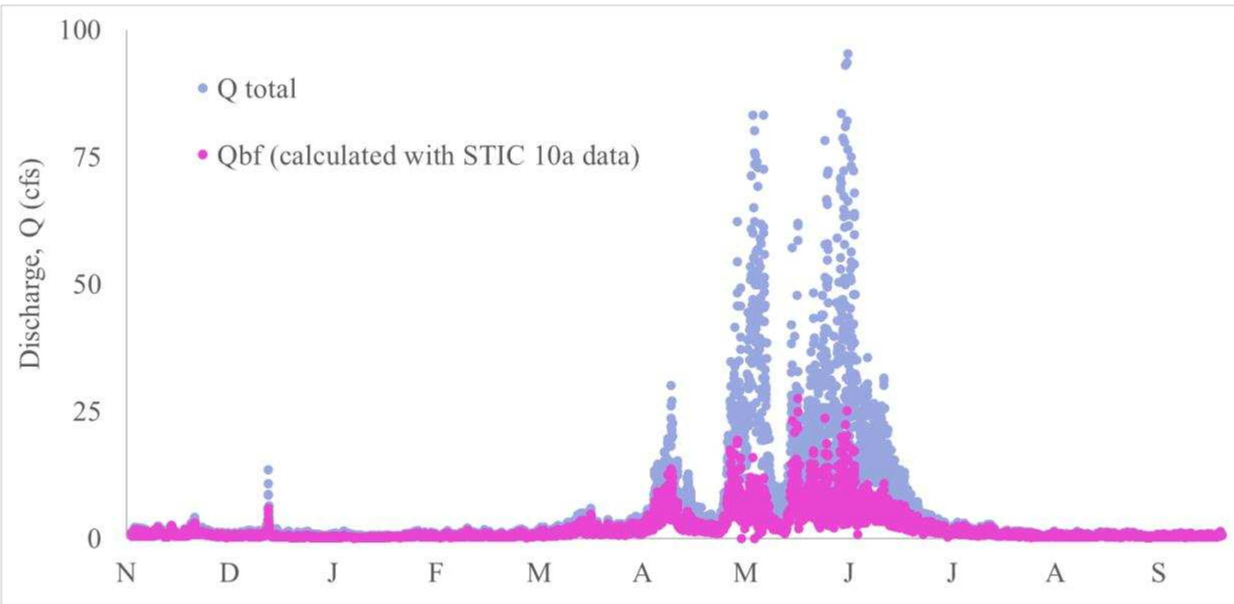

Figure 3.37. Poose Creek (Site 10) CMB method separated hydrograph calculated with hourly STIC 10a data and hourly discharge data for November 7, 2016 – October 01, 2017.

3.8. Summary

Table 3.7 provides a summary of annual and post snowmelt-dominated BFI estimates for all sites suitable for the CMB method of baseflow estimation (using daily data). Based on these estimates, First Creek and Poose Creek had the highest 2017 post snowmelt-dominated baseflow indexes. South Fork of the Elk River had the lowest BFI during this timeframe. The effect of end-member selection on BFI results, detailed daily BFI estimates specifically during the post snowmelt-dominated period, and potential causes for lower or higher BFI estimates will be

Table 3.7. Summary of 2017–2018 BFI estimates calculated with daily discharge and daily STIC data (and with daily U24 data at Site 8*) for all CMB method suitable sites. Note that different timespan lengths are used for annual BFIs at different sites. N/A indicates data were not collected. N/S indicates data collection was attempted but was unsuccessful due to unreasonable flow data (Site 6), unreasonable rSC data (Site 7), or the STIC logger stopping logging early (Site 8).

STIC Number: Stream Name (Site Number*: Stream Name)	Annual 2017 BFI	Annual 2018 BFI	Post Snowmelt Dominated 2017 BFI	Post Snowmelt Dominated 2018 BFI
1: South Fork of the Elk River	33.4%	31.7%	49.5%	52.9%
2: North Fork of the Elk River	N/A	12.8%	N/A	55.9%
4: Encampment River	N/A	28.5%	N/A	63.0%
6: First Creek	N/S	66.9%	N/S	78.3%
7a: Roaring Fork of Slater Creek	31.9%	28.5%	61.0%	59.3%
7b: Roaring Fork of Slater Creek	25.6%	N/S	61.2%	N/S
8*: Silver Creek	N/A	25.2%*	N/A	53.9%*
9: East Fork of the Williams Fork	N/A	33.0%	N/A	59.5%
10: Poose Creek	37.0%	N/A	67.7%	N/A

discussed in Chapter 4. Also in Chapter 4 will be a discussion of rating curves and hourly discharge, STIC loggers long term in extreme field conditions with comparisons to U24 loggers, STIC logger calibrations, and specific conductance temporal variations.

4. DISCUSSION

This study was designed to (1) gauge previously ungauged headwater streams; (2) compare the data produced by higher cost U24 data loggers and lower cost STIC loggers after both were subjected to extreme field conditions for extended periods of time; (3) quantify groundwater contributions to streamflow in headwater streams with snowmelt-dominated hydrographs and diverse SC ranges (both wide and narrow differences between end-members); (4) inform managers about watershed water budget and stream resilience to change; and (5) support management, baseline data collection, and monitoring activities. This study accomplished the following objectives:

(O1) Instrument nine ungauged snowmelt-dominated headwater streams in northwestern Colorado with staff gauges and pressure transducers to generate continuous discharge data (a tenth stream was already gauged);

(O2) Deploy low-cost STIC loggers in ten snowmelt-dominated headwater streams for at least one year under extreme field conditions;

(O3) Calibrate 17 STIC loggers in a lab using logger readings at different temperatures and known SC standards, and apply this to each STIC logger's continuous in-stream field data;

(O4a) Deploy both U24 and STIC loggers at 3 sites;

(O4b) Quantitatively and qualitatively compare STIC and U24 logger temporal data trends, limitations, and advantages;

(O5) Deploy STIC loggers at watersheds that, based on geology, are likely to have different SC ranges (both wide and narrow differences between runoff and baseflow end-member values);

(O6) Plot SC data with stream discharge data to determine which sites have data that are suited for the CMB method, then estimate baseflow at these sites; and,

(O7) Compare BFI estimates calculated with STIC and U24 logger data.

4.1. Rating Curve and Final Hourly Discharge Discussion and Interpretation

After instrumenting and collecting discharge data at nine ungauged snowmelt - dominated headwater streams in northwestern Colorado for one to two years, stage-discharge rating curves were established. The rating curves fit measured points very well when using data from a one-to-two-year period. Sites 9 and 10, East Fork of the Williams Fork and Poose Creek had rating curves that fit measured points well, although there was limited data to create these curves. The fits for these sites can be improved by acquiring more discrete measured discharge data points and updating the curves. These rating curves can be improved over time, and the existing rating curves are appropriate for the goals of this study.

The final goal of this study is to determine if baseflow index (BFI) estimates calculated with STIC and U24 logger data are similar. BFI should not be greatly affected by updates to rating curves because it is a relative percentage of baseflow and total flow. When the total flow changes, so does the baseflow, and therefore the BFI percentage should not be greatly altered by minor total discharge changes. The rating curve depends on the hydraulic characteristics of the stream channel and floodplain and will vary over time at almost every location. There might be slight changes to a stream channel, like seasonal vegetation changes or frequent shifting of a sand-bed stream bottom, or extreme changes like floods. Some channel changes have a negligible effect, some require minor or temporary adjustments, and others require a total reassessment of the rating curve (USGS, 2021).

As specified in Chapter three, hourly discharge data were calculated using the equations shown in Table 3.1. As chapter two stated, pressure transducer data were used to determine stage, also known as water level (x). Hourly discharges at some sites (First Creek Figure 3.7 and Roaring Fork of Slater Creek Figure 3.8) included some unreasonably high (above peak summer flow) stream discharges in wintertime. This was likely due to less accurate wintertime pressure data caused by freezing of water or temperatures outside of the loggers' calibrated and operation range. Any suspected errors in water level data are likely due to temperatures below or near 0°C, as Onset U20-001-01 HOBO Freshwater Water Level Data Loggers (non-vented pressure transducers) have a factory calibrated range of 0° to 40°C (32 to 104°F) and an operation range of –20° to 50°C (–4 to 122°F). The unreasonable discharge data values occur in the wintertime or early spring only, and not for the entirety of any dataset.

4.2. STIC Loggers Long Term in Extreme Field Conditions

Seventeen STIC loggers were modified and deployed at ten field site locations (some sites had one STIC logger, others had two) for one to two years. These data loggers were subjected to the extreme field conditions of high and low temperatures, frozen water, high and low flows, and sudden sediment influxes. Overall, the STIC loggers demonstrated success in long-term field deployment. One STIC logger logged unreasonable data during freezing temperatures, another recorded inconsistent data when buried under sediment, and most other STIC loggers did not experience data logging issues during extreme field conditions.

4.2.1 STIC Loggers Compared to U24 Loggers

At North Fork of the Elk River, STIC 2 logged some unreasonable rSC values during winter months (Figure 3.2). The U24 logger that was launched at the same site did not have the same inconsistencies during winter. STIC 2 began logging unreasonably low rSC values on December 22, 2021. On this date, the U24 logger recorded temperature was –0.36°C and the STIC 2 recorded temperature was 0.784°C. It should also be noted that the U20 pressure transducer that was also deployed at Site 2 may be a better measure of more minute changes in temperature. The Site 2 U20 logger was recording temperatures of 0.01°C until December 22, when temperatures briefly dropped to –0.102°C. On December 23, temperatures remained at -0.102°C for 33 consecutive hours, when the water near the riverbank edge where STIC 2 was deployed likely froze, causing unreasonable rSC values to be recorded until thawing temperatures in March 2018.

By March 22, 2018, when STIC 2 temperatures reached 1.44°C that day with 12 consecutive hours above 0.784°C, the bank edge water had likely thawed and STIC 2 began recording reasonable rSC values again. Although the U24 logger did not log unreasonable values in winter at North Fork of the Elk River, it did record some lower than expected SC values after peak flow, at the beginning of the falling limb of the hydrograph (in mid-June 2018) when SC data were expected to begin rising. STIC logger 2, on the other hand, maintained consistent and reasonable rSC values during this time.

At Elkhead Creek, the U24 logger recorded some unreasonably high SC values during winter months, while STIC 5a continued recording consistent rSC values (Figure 3.18). The unreasonable U24 SC values occurred between December 12, 2017 and January 05, 2018, when temperatures ranged from –0.15 to –1.16°C. After spring peak flows, STIC 5a began logging unreasonable rSC values on April 21 until June 5, 2018 (Figure 3.18). Field notes indicate that during the first field visit of 2018 (on May 23) that the STIC loggers could not be located. On June 5, 2018, field notes state that the STIC loggers were located, unburied, and cleared of sediment. STIC 5a was not able to continue recorded reliable rSC data while buried under sediment, but it resumed proper recording once cleared of sediment, and was able to record reasonable rSC data during winter freezing temperatures at this site.

At Silver Creek, STIC 8 stopped logging on April 4, 2018, prior to the start of rising flows (Figure 3.19). Field notes from May 2018 indicate that STIC 8 was in good condition after winter, though its electrodes were slightly bent. When removed from the creek in October, there was 63 percent battery remaining and 100 percent of the memory had been used. The most likely cause for STIC 8 stopping logging in early April is due to lack of available memory. The U24 logger that was deployed at Silver Creek did not experience any data collection issues. Section 3.4.1 gives some additional examples of how STIC loggers performed in the field compared to U24 loggers.

To summarize comparisons between STIC and U24 logger data recorded in extreme field conditions: (1) STIC loggers fared just as well as U24 loggers subjected to freezing temperatures, as each type of data logger had an issue during cold winter months and neither data logger is designed to operate in freezing temperatures. (2) Both data logger types did not experience any issues with warmer water temperatures or with low flows. (3) At the start and end of peak flows at North Fork of the Elk River, STIC 2 rSC values suddenly dropped about 20-30 relative µS/cm. (4) As a STIC logger is smaller than a U24 logger, it may be more easily buried by sediment, which also proved to affect its rSC data at Elkhead Creek. (5) Although a U24 logger is capable of 18,500 temperature and conductivity measurements and a STIC logger can retain 28,000 temperature and relative conductivity measurements, the STIC logger memory was more limited than the U24 at one creek, perhaps due to having a partially full memory before being deployed. Battery comparisons did not come into play when comparing the two types of data loggers.

4.3. STIC Logger Calibrations

All STIC loggers were collected in the fall of 2018 and then underwent at least one of three lab calibrations in 2019. STIC loggers were not calibrated prior to 2019 nor prior to being deployed in the field. After the first February 2019 calibration, every regression equation calculated with subsequent calibration data (the ranges of which are presented in Tables 4.1 to 4.3) was retained if predicted values fit the known values better than previous regressions. Later regressions were discarded if they did not predict SC as well as previous results. Fifteen STIC loggers were calibrated in 2019, thirteen of which fit known SC values well, and two of which (STIC 1b and 6b) did not fit reasonably enough to use with the CMB equation to predict baseflow.

In February, ten STIC loggers were calibrated at same time. Table 4.1 displays the conditions during each point of this calibration as well as the preliminary data that was used to for regression analysis. Four of the ten STIC loggers recorded all five calibration points successfully (40 percent initial success). All four of these STIC loggers used the data from this calibration for their final regressions (40 percent final success), producing data that if the stream was suited for the CMB method, could be used for baseflow estimation. Four STIC loggers did not log all five calibration points as they stopped logging before the end of the calibration, and two had batteries die during calibration.

In April, all seventeen STIC loggers were simultaneously calibrated. Table 4.2 displays the conditions during each point of this calibration as well as the preliminary data that was used

Table 4.1. February 2019 calibration conditions and preliminary data for calibration curves.

Calibration Point	Start SC (µS/cm)	End SC (µS/cm)	Start Temperature (°C)	End Temperature (°C)	Start Time	End Time
1	16.1	15.6	1.1	19.0	2/4 18:00	2/6 16:25
2	61	56	1.8	19.4	2/6 16:40	2/8 17:35
3	139	125	1.4	20.0	2/8 17:45	2/10 17:45
4	324	294	2.3	19.5	2/10 18:00	2/12 17:35
5	505	473	1.4	20.1	2/12 17:45	2/14 12:30

to for regression analysis. Eleven of seventeen STIC loggers completed all five calibration points (65 percent initial success). Four loggers experienced battery failure before all five calibration points were complete. One logger displayed a force offload error making data inaccessible, and another couldn't be read with the coupler or by HOBOware after repeated attempts. STIC 6b retained its regression that was based on the April calibration, but it also did not produce reasonable data that could be used for baseflow calculations (predicted rSC increased during peak flows and decreased post-snowmelt). Two STIC loggers used data from the April calibration to predict rSC well with known values, and their regressions were used in final baseflow calculations if the stream was suited for the CMB method.

In summary, twelve percent of STIC loggers that underwent the April calibration used this data for regressions that were used for baseflow calculations. This lower success rate may have been related to the two higher starting temperature above 2°C, the two lower ending temperatures below 20°C, one point in the calibration when a longer time elapsed during warming than for other calibration points (41 hours vs. 24 to 27 hours), or the larger number of STIC loggers (17) being calibrated at the same time in the same 100mL beaker with little remaining space. The lack of consistencies of time and temperature between calibration points create more curves of varying shapes, which require a greater number of iterations to regress, and may not regress as well. More STIC loggers in the same sized beaker allowed for more

Table 4.2. April 2019 calibration conditions and preliminary data for calibration curves.

Calibration Point	Start SC (µS/cm)	End SC (µS/cm)	Start Temperature (°C)	End Temperature (°C)	Start Time	End Time
1	11.4	11.2	1.3	19.9	4/16 10:00	4/17 13:30
2	51	47	3.2	20.3	4/17 14:17	4/18 17:05
3	105	94	0.9	19.8	4/18 17:14	4/19 17:33
4	195	171	1.9	21.7	4/19 17:44	4/21 11:06
5	442	413	2.1	20.4	4/21 11:30	4/22 13:48

possibility of (1) electrodes interfering with one another, and (2) STIC loggers recording less averaged, more stratified SC values.

In August, nine STIC loggers were simultaneously calibrated. Table 4.3 displays the conditions during each point of this calibration as well as the preliminary data that was used to for regression analysis. Eight of the nine loggers continued logging through all five calibration points, and one logger's battery failed, making calibration completion impossible (89 percent initial success). Of the eight loggers that completed all five points of the August calibration, all had data that could be used for their regressions, and all but STIC 1b used these equations to predict baseflow with the CMB method if the stream was suited for this method (78 percent success for use in the CMB method equation). STIC 1b logged inconsistent, overlapping data during the third point of August's five-point calibration (largely differing data recorded for the same standard), leading to predicted rSC results that did not fit known SC standards very well. One flaw in the August calibration was waiting to calibrate the conductivity meter until after the fourth calibration point instead of after the third. The conductivity meter measured a known SC standard within four to five percent accuracy by the fourth calibration point, rather than within 1 to 2 percent as it did for previous calibrations.

The most STIC loggers calibrated at the same time with fewest issues occurred during the

Table 4.3. August calibration conditions and preliminary data for calibration curves.

Calibration Point	Start SC (µS/cm)	End SC (µS/cm)	Start Temperature (°C)	End Temperature (°C)	Start Time	End Time
1	15.2	15.2	0.89	21.4	8/24 24:10	8/25 10:30
2	64.8	61.3	1.1	21.44	8/25 11:00	8/26 20:20
3	157	140	1.6	21.6	8/26 20:35	8/28 08:05
4	320	273	0.92	20.1	8/28 08:55	8/29 19:05
5	441	451	0.88	21.4	8/29 20:23	8/31 09:15

August 2019 lab calibration. The most success occurred when nine STIC loggers were calibrated in the same beaker at the same time, rather than a larger number of loggers at the same time. The most success occurred when there were shorter logging periods between each calibration point, allowing the STIC loggers to log more extreme temperature changes and not logging the minor warming towards the end of the February and April calibrations. The ending temperatures were higher than the previous calibrations, and the warmer lab room in August may have contributed to this. It should be noted that when possible, SC standards were put into the refrigerator after equilibrating with the atmosphere, prior to being put onto an ice bath.

When switching between calibration points during the August calibration, STIC loggers were submerged in the beaker of the new known SC standard, which was in the ice bath in the freezer prior to initial point measurements (prior to the first SC and temperature measurements for that calibration point). Measurements to start each new calibration point did not begin until temperatures dropped below 1 degree Celsius, which was colder than how most previous calibrations began. Switching between calibration points was therefore slower than previous calibrations, and data between calibration points was simply deleted after the calibration process was complete. The physical calibration process takes about one hour every other day, with some set up and clean up time, totaling about four hours. Organization of calibration data and regression processing is about one to two hours per STIC logger. This makes it most efficient to calibrate many STIC loggers at once, although the best calibration results will come from nine or fewer in the same beaker at the same time. Calibrating multiple beakers of STIC loggers at once is a viable option.

Two STIC loggers (3b and 5b) could not be calibrated. One STIC logger (3b) consistently displayed a header/offload error and the other STIC logger (5b) had repeated battery failures during all three lab calibration attempts. Deploying in the field prior to lab calibration runs the risk of such technical problems, and of bending or polarization of electrodes. Technical problems could be avoided by calibrating STIC loggers first and only deploying those that successfully calibrated with good fits. This also leaves the option of re-calibrating after field deployment. SPSS Statistics v26 proved to be an efficient means of regressing calibration data with known conductivity standards. The software is especially helpful for constraining temperature coefficients to positive values only.

4.4. STIC Logger Data Trends and Duplicate STIC Logger Data

To now focus on the STIC logger data specifically, results section 3.5 describes all other STIC logger field rSC data. The figures for Sites 1, 2, 4, and 7 (North Fork of the Elk River, South Fork of the Elk River, Encampment River, and Roaring Fork of Slater Creek) all display similar rSC trends during peak flows: some lower rSC values that overlap with higher rSC values, and that drop from the higher rSC values, then jump up again without a smooth connected transition (see dotted black lines in Figure 4.1).

In Figure 3.12, the uncalibrated STIC logger 2 data collected at North Fork of the Elk

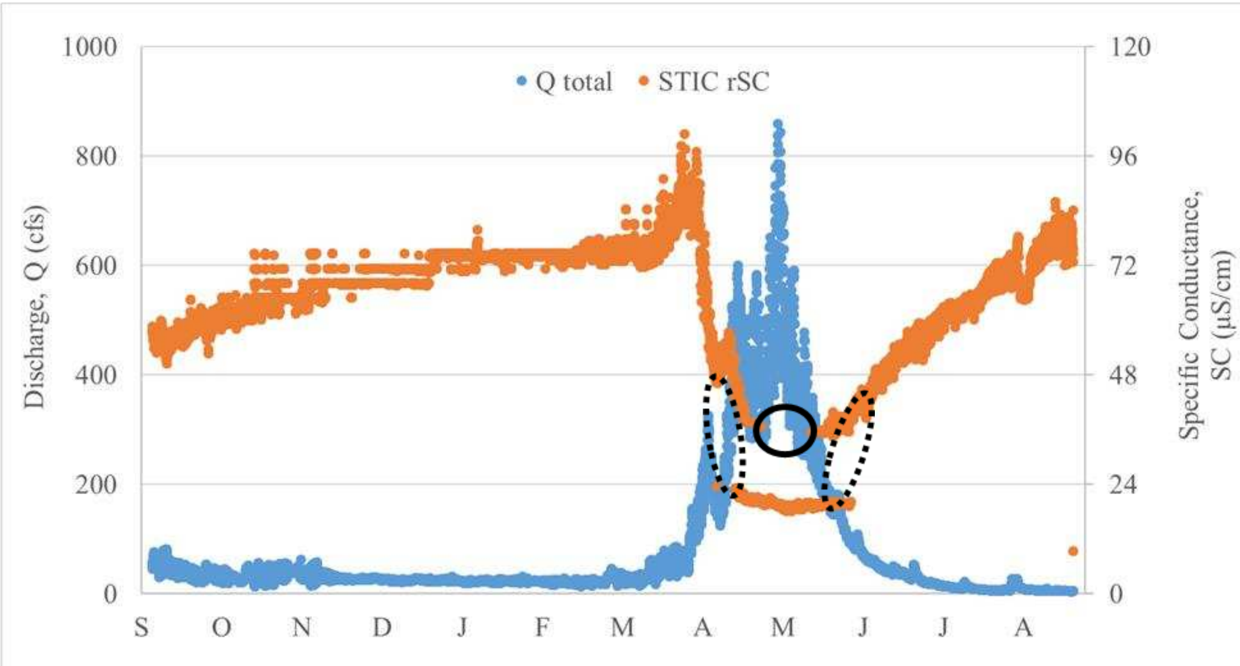

Figure 4.1. South Fork of the Elk River STIC 1a hourly rSC data in orange. Trends during peak flows (blue) are similar to Sites 2, 4 and 7.

River shows the same drop that can also be seen in STIC logger 2's rSC data post-calibration. This is also true of Sites 4 and 7. Based on this evidence, the STIC logger calibration is not likely the cause of this drop in rSC data during peak flows. There are three other strong possibilities for the cause of the sudden drop in rSC values: (1) the modified, uncalibrated data logger itself recording these inconsistent drops; (2) a characteristic of the watershed; or (3) in-stream conditions or compositions.

To investigate the possibility that the modified data logger may be triggering the recorded drop in rSC during high flows, daily duplicate STIC logger data from Encampment River and Roaring Fork of Slater Creek are examined for inconsistencies and/or trends (Figure 4.2 is the first of these). The duplicate STIC loggers at Encampment River and at Roaring Fork of Slater Creek show consistent temporal rSC data trends. At Encampment River, the daily rSC data for

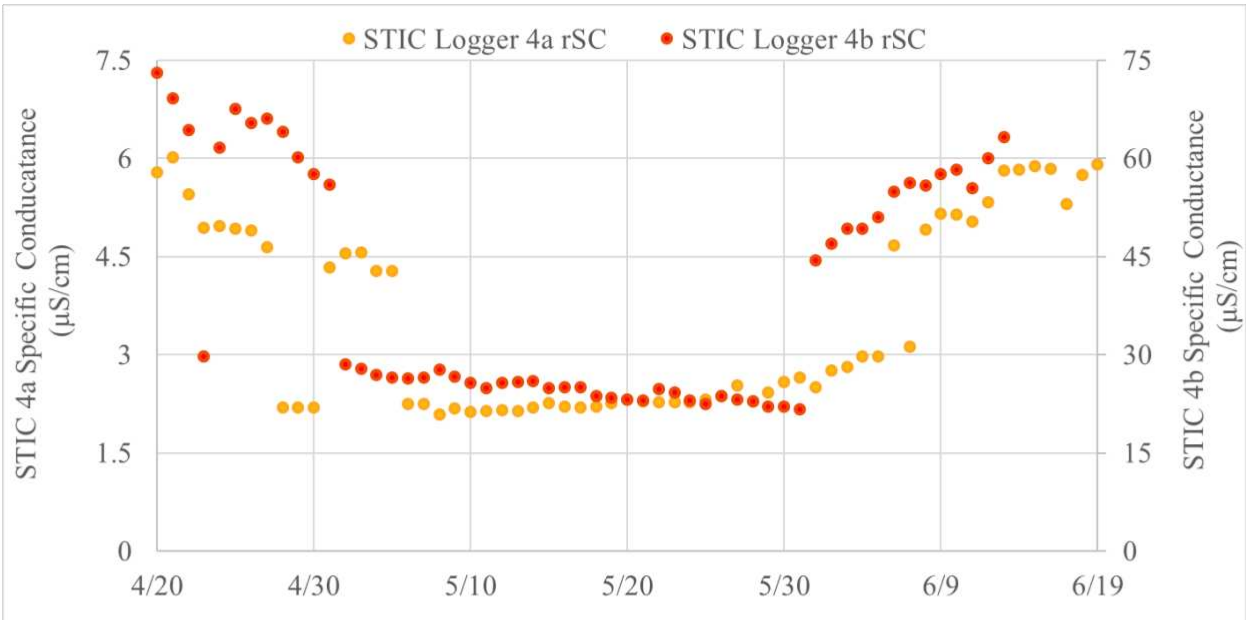

Figure 4.2. Encampment River daily rSC data recorded by STIC loggers 4a (light orange) and 4b (dark orange).

STIC logger 4a drops between April 28 and May 5, 2018 (it fluctuates down and back up, essentially dropping twice during this period). The daily rSC data for STIC logger 4b drops after May 1, 2018. STIC logger 4a then jumps again between June 5 and June 8, 2018 and logger 4b jumps on June 1, 2018, just prior to STIC logger 4a. Between May 1 and June 1, both duplicate STIC loggers record relatively flat, stable data.

One STIC logger at Site 7 recorded a drop and then a jump in rSC during high flows, and the duplicate at this site recorded the same trends (Figure 4.3). STIC logger 7a recorded its drop in rSC between May 29 and May 30, 2018, while STIC logger 7b recorded its drop between May 30 and May 31. STIC logger 7b jumps from June 20 to 21, 2018 and STIC logger 7a jumps from June 22 to 23, 2018. These data also remain relatively consistent and level between the drops and jumps (May 31 to June 20, 2018).

The duplicate STIC loggers at both previously mentioned sites are displaying

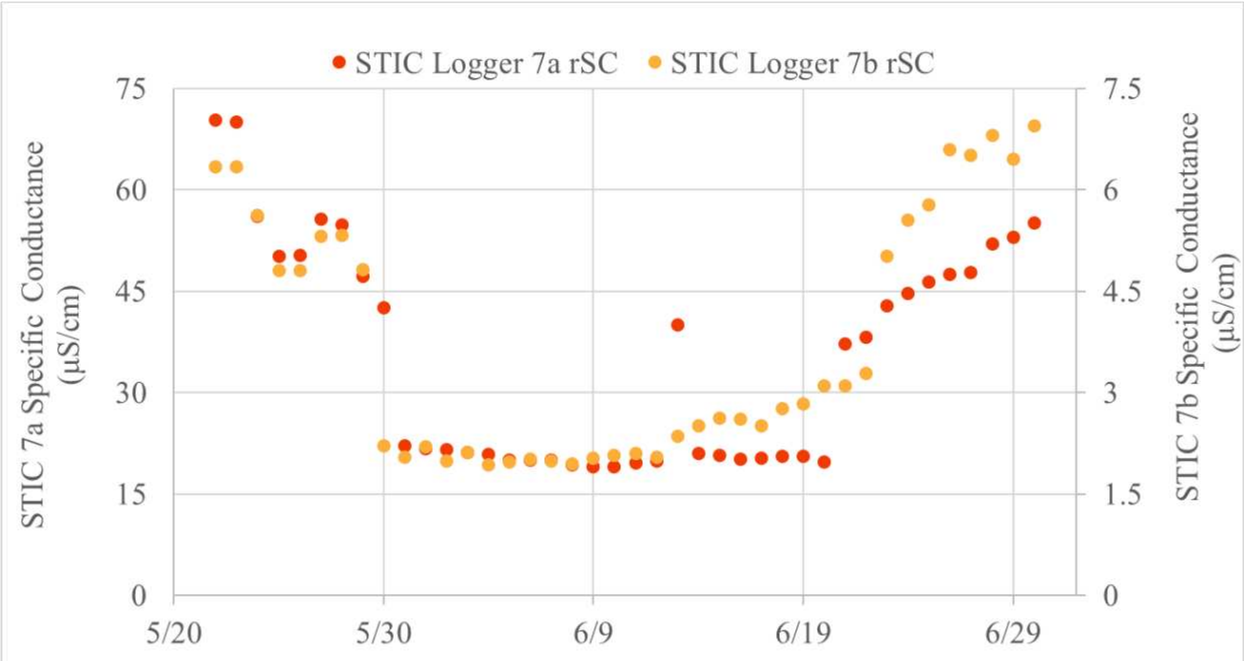

Figure 4.3. Roaring Fork of Slater Creek duplicate STIC logger daily rSC trends during 2018 peak flows.

similar rSC trends, which makes it less likely that the modified loggers themselves are signaling for this drop to occur during high flows. From this it can be deduced that the most likely cause is either a watershed characteristic, or in-stream conditions or compositions.

Four watersheds had STIC loggers deployed that recorded this rSC drop during peak flows, while the other six watersheds recorded smoothly connected rSC data through peak flows. None of the geology types categorized by this study, generalized watershed size (large or small), elevation (high or low), stream order, gradient, or precipitation amount have clear commonalities between the four watersheds that experience this drop in rSC during high flows. Three of the four sites have headwaters in the Mt. Zirkle Wilderness. Although it is still possible that the cause of these drops in rSC are related to one or many watershed characteristics, there was not a watershed characteristic investigated in this study that was able to link all four of the watersheds for the South and North Fork of the Elk River, Encampment River, and the Roaring Fork of

Slater Creek. Therefore, based on this study's investigation, the most likely causes for the sudden drops in rSC during high flows are in-stream conditions or compositions.

A sudden increase in turbidity or flushing of sediment during higher flows in a sand-bed or soft channel would more likely make the STIC logger rSC data steadily increase over time rather than suddenly drop (Swanson and Baldwin, 1965). As can be seen in Figure 3.18, the rSC data steadily increase when this STIC logger was buried in sediment at Elkhead Creek during the beginning of May high flows. However, in streams with imbricated sediments, coarse or cobbled beds, and in-stream boulders, a surge in cold, high velocity water due to quickly melting snow may not create as much suspended sediment as in sand-bedded channels. This lowers the risk of STIC loggers being buried or disturbed by sediment in streams like North and South Fork of the Elk River, Encampment River, and Roaring Fork of Slater Creek during high flows.

What is expected to come with low-conductivity snowmelt and higher water velocities are increases in mixing and air circulation in the water, especially in the large cobble and boulder-filled channels being discussed here. Because both snowmelt and air are poor conductors of electricity (especially air), it is possible that the turbulence caused by high-velocity water at North and South Fork of the Elk River, Encampment River, and Roaring Fork of Slater Creek reduced the ability of the water to conduct an electrical current. This effect may have been extreme-enough during high flows that the U24 and STIC loggers had difficulty reading the low electrical conductivities, or had data collection interference. (Figure 4.4). It is possible that with more high velocity inflows came reduced SC and more turbulent rapids. With the turbulence came more air and more inconsistent, low, or unreadable electrical conductivities. It

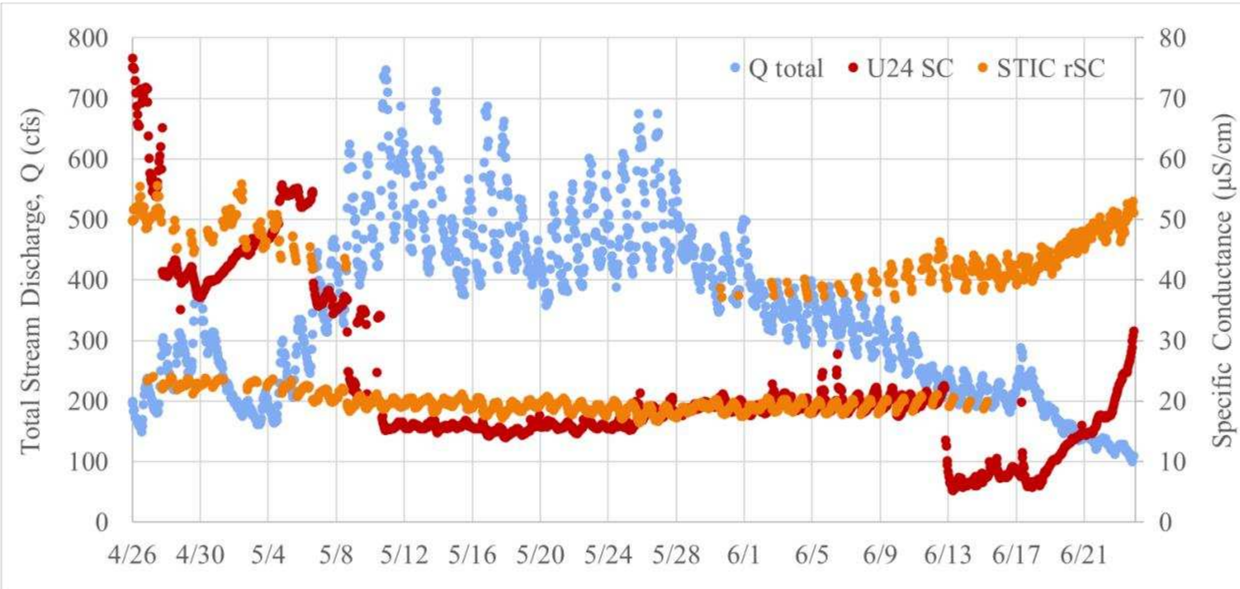

Figure 4.4. North Fork of the Elk River total hourly stream discharge (blue), hourly SC as recorded by the U24 logger (maroon), and hourly rSC as recorded by the STIC logger for April 26 – June 21, 2018.

is also possible that certain boulders came into play once a particular stream discharge was reached, were covered with water during peak flows, and came back into play again once stream discharge had declined again.

There are 3 to 4 drops in SC recorded by the U24 logger that was deployed at the North Fork of the Elk River, and one drop in rSC recorded by the STIC logger deployed there (Figure 4.4). The drops occurred when stream discharge was greater than 250 to 300 cfs and likely very turbulent. The rSC recorded by the STIC logger jumps up again when discharge falls below 380 cfs, while the U24 logger steadily records its increasing SC with more continuously. Discharge (Q) data fluctuates during the day, with the higher Q generally occurring in the late afternoon and evening (2:00 pm – 12:00 am) and the lower Q generally in the morning and early afternoon (8:00 am – 2:00 pm). Relative SC and SC are generally the opposite of this. The stream discharge data is more variable during spring runoff than during the falling limb of the hydrograph, which may partially explain why the U24 logger was able to log higher SC values during the falling limb without jumping, or dropping as it did earlier in the year.

The South Fork of the Elk River has similar bed forms and in-stream conditions as the North Fork of the Elk River, but rSC drops in early May rather than April (Figure 4.5). The sudden drop in rSC occurred when stream discharge was greater than 450 cfs and likely quite turbulent. The rSC recorded by the STIC logger jumped up again when discharge fell below 250 cfs. Discharge (Q) data fluctuates during the day, with the higher Q generally occurring in the afternoon (1:00 pm – 5:00 pm) and the lower Q generally in the night (12:00 am – 4:00am). Relative SC is generally the opposite of this.

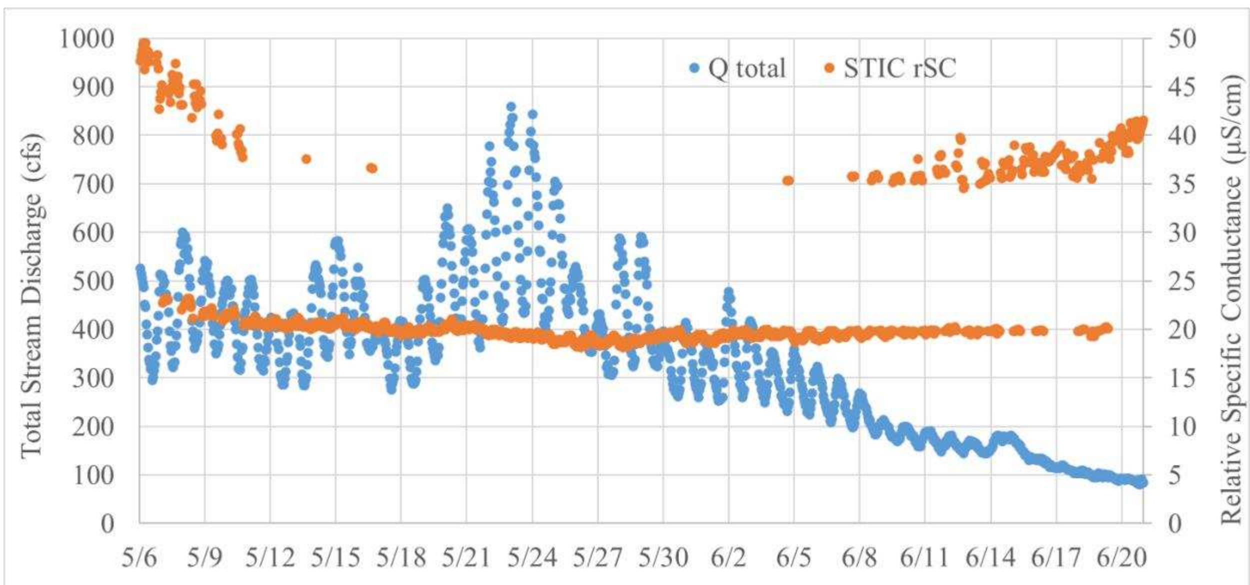

Figure 4.5. South Fork of the Elk River total hourly stream discharge (blue) and hourly rSC (orange) for May 6 – June 20, 2018.

Encampment River has a coarse cobble bed with imbricated clasts that were deposited in relatively high energy. More variation can be seen in this site's rSC data after they drop than what can be seen at North or South Fork of the Elk River, due to its SC range being wider than these other sites (Figure 4.6). An in-stream condition like a surge in snowmelt, increased water

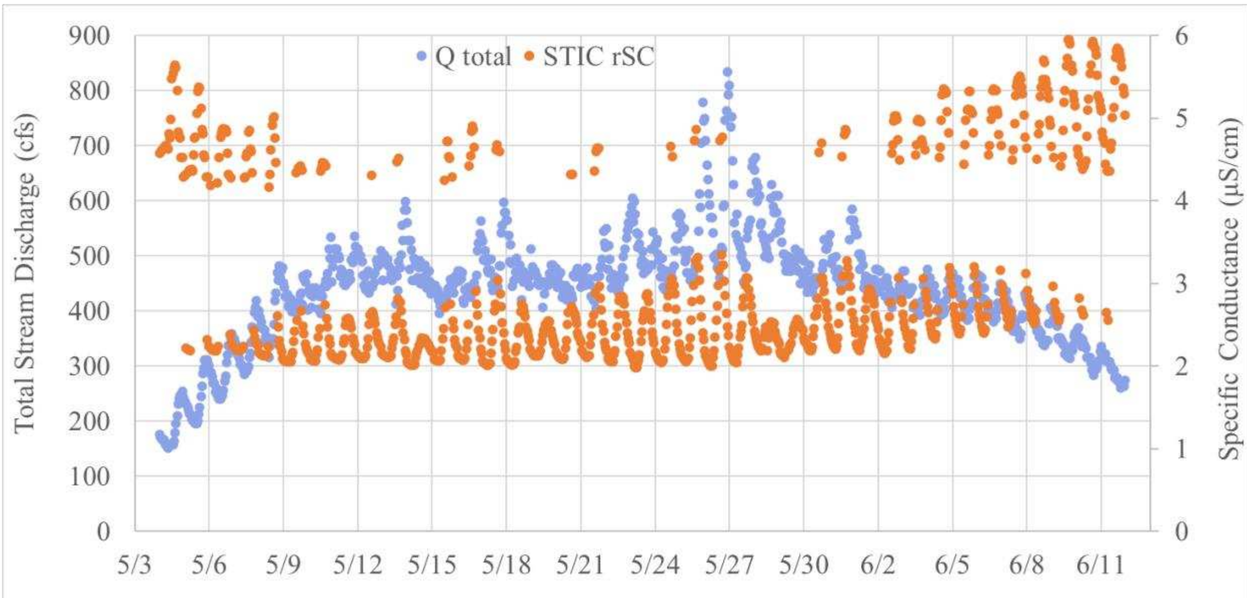

Figure 4.6. Encampment River total hourly stream discharge (blue) and hourly rSC (orange) for May 3 – June 11, 2018.

velocities, more mixing and therefore more air, potentially with some suspended solids or turbidity specifically at Encampment River, all could be affecting the data recorded by this STIC logger. Discharge (Q) data fluctuates during the day, with the higher Q generally occurring in the late afternoon and evening (3:00 pm – 11:00 pm) and the lower Q generally in the early morning (4:00 am – 7:00am). Relative SC is generally the opposite of this.

Figure 4.7 shows hourly Roaring Fork of Slater Creek total stream discharge plotted with hourly STIC rSC data. The rSC trends at this site fall between those of Figure 4.6 and those of Figures 4.4 and 4.5. The stream discharge at this site generally is higher in the early morning (between 6:00 am and 9:00 am) as well as in the late afternoon and evening (4:00 pm – 12:00 am) and is generally lower in the afternoon (between 11:00 am and 5:00 pm).

Because duplicate STIC loggers were attached to their own individual bags of rocks, it is not possible to be sure if the STIC loggers were in slightly different locations experiencing different field conditions within each stream. Further research is recommended on this topic, by

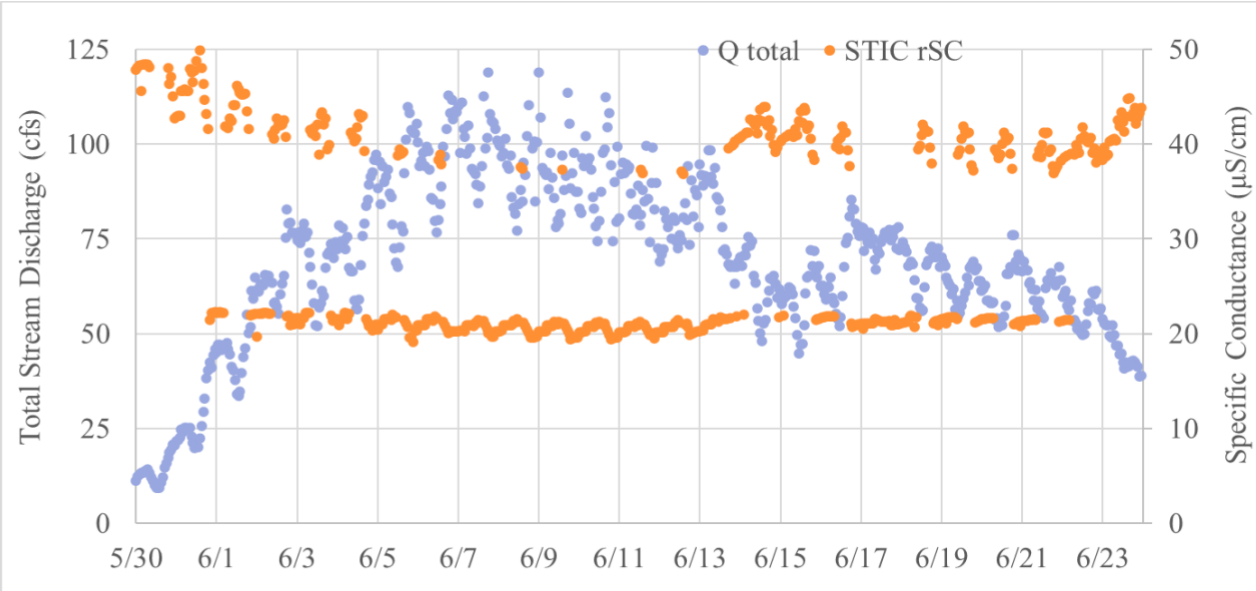

Figure 4.7. Roaring Fork of Slater Creek total hourly stream discharge (blue) and hourly rSC (orange) for May 30 – June 23, 2018.

deploying two or more STIC loggers at each site location, attached to the same T-post, PVC pipe, or bag of rocks. The data acquired from these methods would confirm or eliminate the question of a watershed caused vs data logger caused drop and then jump in rSC during high flows. The baseflow and BFI results are considered valid for all sites eligible to use the CMB method, whether calculated at sites that recorded a sudden rSC drop trend or at the sites that did not.

The U24 data at North Fork of the Elk River had a clear choice for the SC_{RO} end-member value, while the STIC logger data had two different possibilities (the top and bottom of the rSC drop). Both of these SC_{RO} end-member possibilities were experimented with in the CMB equation, and baseflow results compared. Using the lowest recorded rSC value as the SC_{RO} end-member produced the most reasonable baseflow results that were also most comparable to the baseflow results attained using U24 logger SC data. Therefore, the lowest consistent rSC values recorded should be used as recorded by the STIC logger during peak flow. The drops in rSC or

SC do not pose a problem when using these data in the CMB method equation to calculate baseflow.

Also in section 3.5 is data from STIC logger 3a, which stopped logging on June 12, 2018. (Figure 3.22). When STIC logger 3a was removed from English Creek in October 2018, all its memory had been used. It is likely that STIC 3a stopped logging due to lack of memory over time. STIC loggers that did not experience any long term or extreme field condition issues and had nothing unique to mention about their final rSC data appearance include STIC 6a deployed at First Creek, STIC 9 deployed at the East Fork of the Williams Fork, and STIC 10a and 10b deployed at Poose Creek.

4.5. Specific Conductance Temporal Variations and End-Member Selection

Temporal variations in rSC and SC were recorded as expected at some sites in this study, and not as expected at others. Previous studies were able to use the 99th percentile SC value for each year as their SC_{BF} end-member at each site (Lyu et al., 2020; Miller et al., 2014). This is likely because the SC data recorded at each of their sites generally exhibited expected temporal variations for snowmelt-dominated streams, where the highest SC values were logged during low flow, later in summer or early in fall.

There were five CMB suited sites that had their highest rSC or SC values recorded during Spring, just before snowmelt (North Fork of the Elk River and Silver Creek's U24 data as well as South Fork of the Elk River and First Creek's STIC data). The STIC deployed at East Fork of the Williams Fork recorded this as well, but logged rSC values nearly as high in July as in April, and rSC values began to slowly decline after July 23, 2018 rather than increasing. It is unknown what is happening at these sites during these time periods, so the 99th percentile method (Miller et al., 2014) for selecting a baseflow end-member was modified at these sites by using the low-flow stable average rSC or SC maximum as the baseflow end-member instead. This modification had the largest impact on the baseflow results at First Creek (Figure 4.8).

As previously stated, despite its 99th percentile rSC occurring in April, we used the low-flow rSC maximum as the final baseflow end-member of choice. Figure 4.8 shows a series of two different daily baseflow indexes that could be calculated if the baseflow end-member selected was the highest rSC value in April (~253 µS/cm), used to calculate the teal BFI series, or the low-flow stable maximum rSC value in June (~173 µS/cm) used to calculated the pink BFI series). Total discharge holds constant for these calculations, while baseflow discharge changes based on the rSC_{BF} end-member selected.

All other sites (Encampment River, Roaring Fork of Slater Creek, and Poose Creek) with expected rSC temporal variations used the 99th percentile rSC value for the year of interest as

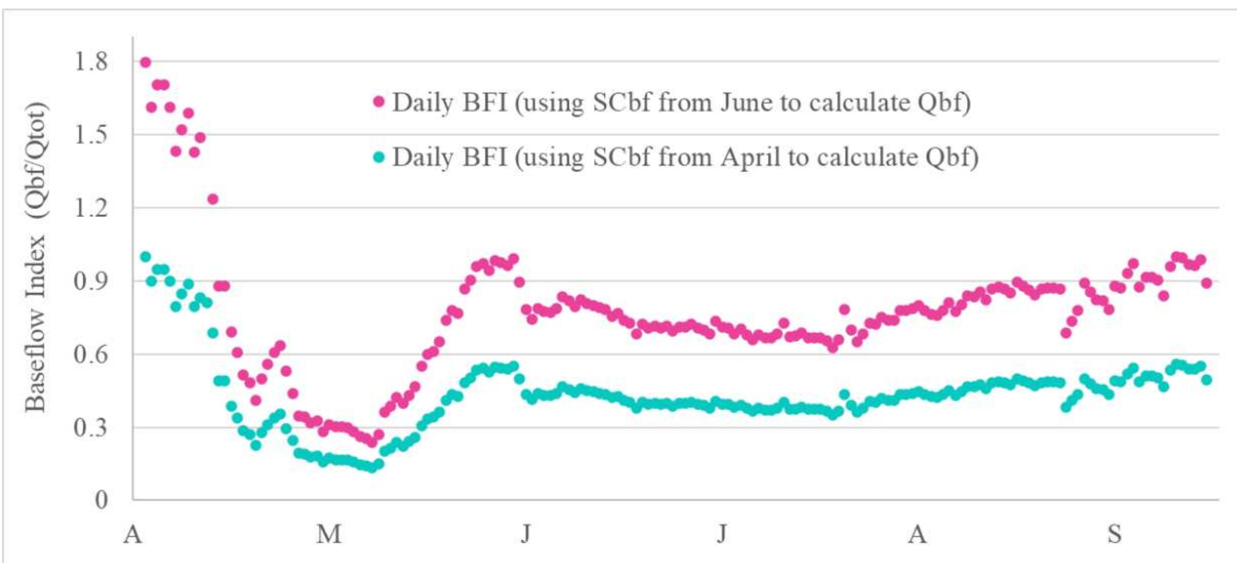

Figure 4.8. Two different series of daily baseflow indexes at First Creek based on different rSC_{BF} values. Using the highest rSC value in April (~253 µS/cm) as the baseflow end-member (teal) calculates the lower daily baseflow indexes (BFI) and using the low-flow stable maximum rSC in June (~173 µS/cm) as the baseflow end-member (pink) results in higher daily BFI.

the SC_{BF} end-member (Miller et al., 2014).

4.6. Baseflow Estimation and where the CMB Method is Appropriate

At Site 1, South Fork of the Elk River, STIC logger 1a and 1b were deployed to record continuous rSC in 2017 and 2018. rSC data from STIC 1a were used to predict baseflow with the CMB method at Site 1, but STIC logger 1b could not be calibrated with a good-enough fit to use its rSC data in this method. The SC range for this site, based on discrete conductivity measurements, is 19 to 60 µS/cm, which is a relatively narrow range. Although continuous data will widen this range some, the difference between end member values at this site is likely less than what other studies (Rumsey et al., 2015) have used (at least 100 µS/cm). However, there were no apparent issues calculating baseflow with this narrower range between end members.

The selection of a date to mark the start of the post snowmelt-dominated period was done for the purpose of objectivity and to compare BFI for this period across multiple sites.

Site 1 had the lowest post snowmelt-dominated BFI in 2017 (50 percent) and 2018 (53 percent). Although lower than the other study sites, South Fork of the Elk River still has groundwater-supported wetlands just upstream as well as large floodplains. It should be noted that the post snowmelt-dominated BFI incorporates daily baseflow indexes spanning from 21 to over 99 percent, and its purpose is as an objective means for comparison between site locations. Site 1's post snowmelt-dominated baseflow indexes in the lower 50 percent range should not be considered the low-flow BFIs. Figure 4.9 displays daily BFI (pink) at Site 1 alongside baseflow discharge (purple) and total discharge (blue) to provide an example of what most daily baseflow

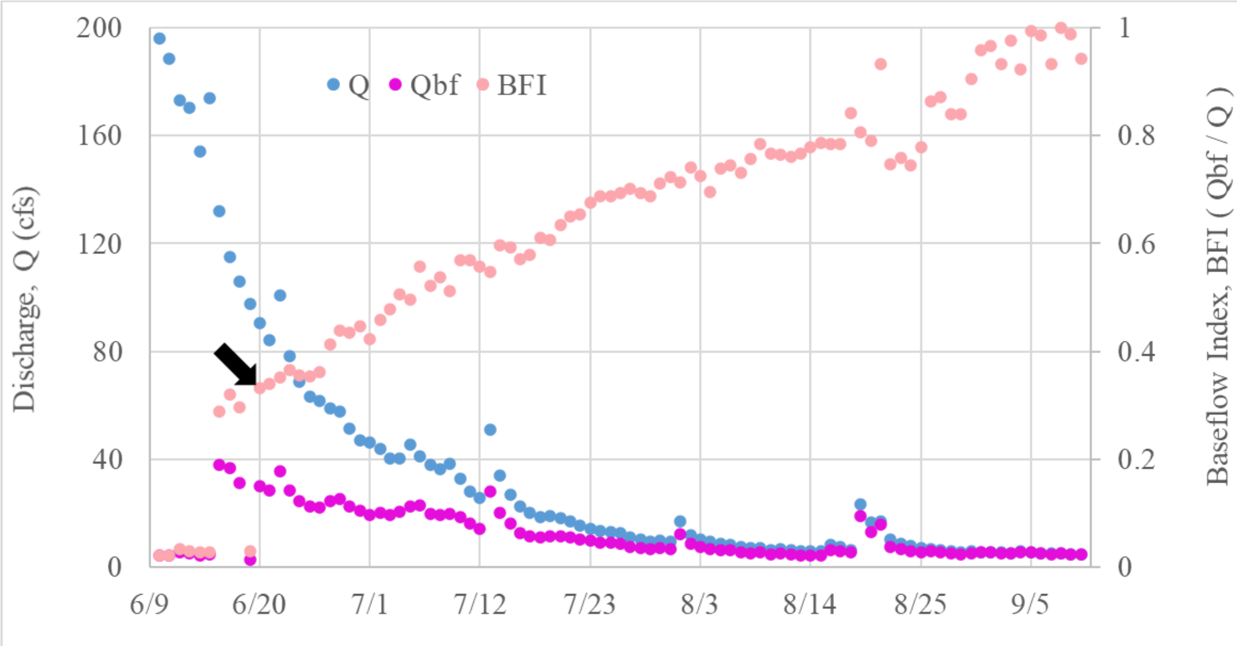

Figure 4.9. Daily total discharge (Q, blue), baseflow discharge (Qbf, purple) and baseflow index (BFI, pink) at South Fork of the Elk River. The post snowmelt-dominated start date is indicated with a black arrow.

indexes look like at this study's sites. The daily BFI starts low (33 percent on the post snowmelt-dominated start date of June 20 (black arrow on Figure 4.9)) and increases later into the season (90 to 100 percent during the month of September).

The stream discharge at South Fork of the Elk River falls steadily and slowly through the summer. Some groundwater contributions are likely from seepage of the Burn Ridge pond upslope of Site 1. South Fork of the Elk River has one of the larger watersheds (fourth largest) of the CMB method suitable sites, with the steepest slope (31 percent) and the most annual precipitation. The steep slopes at this site come most into play in the uplands, and the floodplains at South Fork of the Elk River remain wide and the slopes gentle. These characteristics support this study's low-flow BFI findings, as it can receive more precipitation that replenishes a high alpine pond as well as the water table.

At Site 2, North Fork of the Elk River, both U24 and STIC loggers were deployed to measure continuous SC and rSC, respectively. The SC range at this site, acquired with continuous U24 data, is about 5 to 92 μS/cm. This is an average range compared to other site locations in this study, and the end-member values are less than 100 μS/cm apart from one another. Overall, this is considered narrow or perhaps not significantly different according to some, but there were no apparent issues calculating baseflow discharge with these end-member values (Rumsey et al., 2015).

Despite the STIC and U24 logger rSC and SC data following the same relative trends, STIC logger 2 fails to maintain the consistency of being relatively lower than the U24 logger SC values after early summer peak flows that may have some direct or indirect effects on some STIC loggers (Figure 3.17 displays this). Though no other STIC loggers appeared to have the same relativity issue as STIC logger 2, this is part of the rationale for recommending 2 STIC loggers at each site location desiring a continuous baseflow estimate.

North Fork of the Elk River had a lower annual BFI for 2018 than any other CMB method suitable site that estimated BFI with STIC logger rSC data (13 percent). The periods when baseflow estimates are of most interest are during the post snowmelt-dominated or low-flow periods, as this is when streamflow is more scarce and fluvial ecosystems are most at risk to changes in flow. For this reason as well as high velocity surface water inflow (during high flow) potentially affecting some STIC logger data (Figure 4.1), unavoidable data gaps during winter months, and the different time frames used when calculating each site's annual BFI, the post snowmelt-dominated BFI will be the results that are focused on for the discussion. The 2018 post snowmelt-dominated BFI at Site 2 is average compared to other sites using STIC logger rSC data (55 percent) and was slightly higher than the 2018 post snowmelt-dominated BFI calculated for Silver Creek. The spring upstream of this site and other subsurface water sources are contributing more groundwater than surface water is during lower flows.

North Fork of the Elk River has the second largest drainage area of the CMB suitable sites (106 square kilometers). Runoff in the form of snowmelt and rain is contributing to stream flow annually from a large area. Site 2 has the highest peak elevation out of all sites, making it likely that much of its runoff contributions are coming from snowmelt. This site has the second highest slope (28 percent) and third highest annual precipitation of the other CMB method suitable sites. Site 2's steeper slopes and more dead trees encourage precipitation to travel more quickly on the watershed's land surface, allowing less time for this water to percolate into the ground. Additional comparisons of North Fork of the Elk River and Silver Creek post snowmelt-dominated BFIs are discussed later in this chapter with Site 8.

At Site 4, Encampment River, STIC logger 4a and 4b were deployed October 2017 to 2018. The SC range is about 17-140 µS/cm (Clark et al., 2000), and most would consider the end-members of this range to be significantly different. Encampment has the second highest post snowmelt-dominated BFI (63 percent), and a larger drainage area than any other site (189 square kilometers). However, it gets less annual precipitation than them. This as well as the BFI results indicate a strong groundwater presence at this site location above Hog Park Creek, likely sourced from upstream in the Mount Zirkle Wilderness headwaters.

At Site 6, First Creek, STIC logger 6a and 6b were deployed to record continuous rSC in 2017 and 2018. The rSC data from STIC logger 6a were used to estimate baseflow with the CMB method. The rSC data logged by STIC logger 6b was not reasonable because it increased during high flows and decreased during low flows. STIC logger 6b has an R-squared, or coefficient of multiple determination, of 0.982. If its regression is corrected by a factor of negative one, temporal variations in rSC recorded by STIC 6b become reasonable. The regression for STIC 6b represents the threshold for STIC logger calibration data that did not fit well enough to use in the CMB method to estimate baseflow. Therefore, the coefficient of multiple determination should be greater than that of STIC 6b (greater than 0.982) to generate rSC data that can reliably be used to estimate baseflow with this method.

Based on 2017 to 2018 discrete field data, SC ranges from 65 to 194 μS/cm here. This wider SC range (significantly different end-members) makes this site an excellent candidate for the CMB method (Rumsey et al., 2015). Post snowmelt-dominated BFI was 78 percent (the highest for this timeframe in 2018 compared to the other CMB suitable site locations). At First Creek the snow melts early and quickly due to the open high-meadow having high sun exposure, and not as much vegetation to slow down surface runoff. This site receives less annual precipitation than any other CMB suited site (33.6 inches). Therefore, later in the summer into winter, streamflow sources are primarily groundwater (baseflow).

At Site 7, Roaring Fork of Slater Creek, STIC logger 7a and 7b were deployed to record continuous rSC in 2017 and 2018. Both STIC loggers were calibrated with a good enough fit to use their rSC data with the CMB method to estimate baseflow, though STIC logger 7a had a slightly higher coefficient of multiple determination than STIC logger 7b. Based on discrete 2017 to 2018 data, the SC ranges from 28.5 to 83.7 μS/cm. Although continuous data would widen this range, the end-members that would come from this SC range may not be considered significantly different to some (Rumsey et al., 2015). However, there were no issues calculating baseflow discharge here.

Despite the rSC range of STIC logger 7a being slightly wider than that of 7b, they follow the same relative temporal trends, shown in Figure 4.10. This supports the hypothesis that

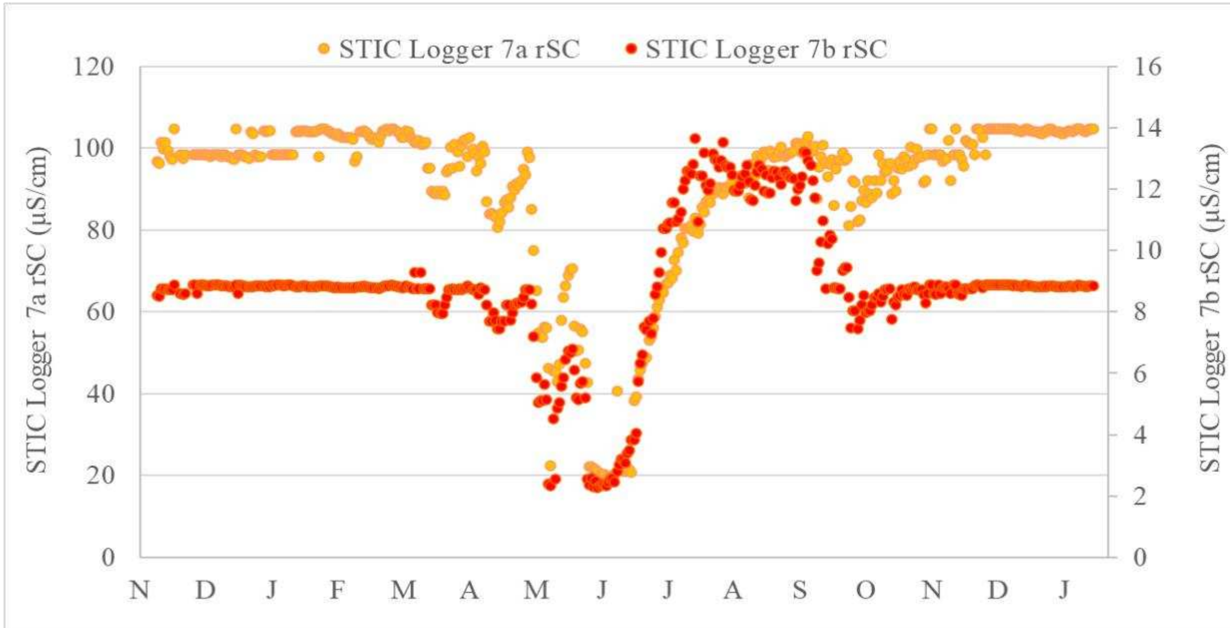

Figure 4.10. STIC 7a (light orange, primary axis) and 7b (dark orange, secondary axis) 2017 daily rSC data. Despite different scales, STIC 7a and 7b log similar relative end-member SC values.

temporal STIC logger rSC data trends are comparable to temporal rSC data trends measured using a duplicate STIC logger.

The post snowmelt-dominated BFI estimates calculated with data from STIC logger 7a and from 7b differ by 0.2 percent, which are quite similar and support this study's final hypothesis that BFI estimates are similar at the same site location (within 5%) when calculated with (duplicate) STIC logger data.

Post snowmelt-dominated BFIs at Roaring Fork of Slater Creek are high compared to other CMB method suitable sites. Although Site 7 has one of the smallest drainage areas, it receives more annual precipitation than any other site, which is likely able to seep into the ground easily with the area's low to average slopes and the large amount of surrounding mossy vegetation. Post snowmelt-dominated BFI is high at this site because of a lower proportion of surface runoff and a large groundwater component in the form of a rock glacier or other source of groundwater. Based on the low discrete SC values measured at this site, it is likely that a large component of the groundwater source is from a rock glacier or new groundwater like a fen where the water table is at or near the ground surface.

Because post snowmelt-dominated BFI is higher, this stream appears to be less vulnerable to reductions in snowpack. On the other hand, this site is more vulnerable if reductions in baseflow occur. This includes a reduction in the rock glacier melt output, another reduction in the groundwater supply from pumping nearby, or preventing surface water runoff from infiltrating the water table.

At Site 8, Silver Creek, STIC logger 8 and a U24 logger were deployed to record continuous rSC and SC data, respectively, in the fall of 2017. STIC logger 8 stopped logging on April 4, 2018, and as its memory was at 100 percent capacity, this was likely the cause of STIC 8 stopping logging early. The SC data recorded by the U24 logger was used to estimate baseflow with the CMB method at Silver Creek. Based on continuous U24 data, the end-member values at this site are 19 µS/cm and 43 µS/cm, which is a relatively narrow but expected SC range. There were no issues estimating baseflow with the CMB method at this site.

U24 loggers were deployed at both Silver Creek and the North Fork of the Elk River. These watersheds have essentially identical slopes, but Silver Creek has a smaller drainage basin area (about 25 square miles). Site 8 has the lowest elevation of all the study sites and the third lowest annual precipitation. North Fork of the Elk River has a slightly higher U24 post snowmelt-dominated BFI (56 percent) than Silver Creek (54 percent). Overall, these sites have similar BFI results.

Site 8 post snowmelt-dominated BFI for 2018 was the second lowest (54 percent) as compared to the other CMB method suitable sites. Silver Creek has a wetland upstream and a tributary (the South Fork of Silver Creek) that may have a strong groundwater component. The upstream wetland, tributary, or other groundwater sources contribute to the further downstream streamflow at Site 8. The site location at Silver Creek is about seven miles downstream of the South Fork and wetland on the east side of this system. The daily baseflow indexes in the month of September range from 88 to nearly 99 percent. Site 8 would be slightly at risk at any time of year if there were reductions in upstream surface water runoff supply. The biggest impact to this site during low flow would be groundwater pumping or impacts to the upstream tributaries or wetland.

Site 9, the East Fork of the Williams Fork River, had one STIC logger deployed in fall 2017 for one year. Data from STIC logger 9 was used in the CMB method to estimate baseflow. One discrete SC measurement was collected in July 2017 that measured 110 μS/cm. This slightly higher SC value is reasonable here where the geology consists mainly of the Cretaceous Mancos Shale Formation (CSU CNHP, 2019). 2018 BFI for the post snowmelt-dominated period was among the highest (nearly 60 percent) of the CMB suited sites. The East Fork of the Williams Fork may not be dominated by groundwater during snowmelt runoff, but it is during low flows.

Site 9 sits at one of the highest elevations, with average to high precipitation (over 43 inches annually), in the third largest drainage basin of the CMB suitable sites (35 square miles). The mean slope of the watershed is the second lowest (23 percent) after Poose Creek. The larger drainage area and gentler slopes at this site with its many deciduous riparian trees, conifers, and other vegetation encourage a greater quantity of water to percolate into the ground. Information about the components of the source waters in the Flat Tops Wilderness is not widely known, but there is likely to be a strong groundwater component coming from the headwaters, or the water table may be at or above stream level at Site 9. Because the post snowmelt-dominated BFI is higher at Site 9, this stream is less vulnerable to changes that could affect surface runoff water sources during this timeframe. It also means that any changes to groundwater (like pumping or lowering of the water table) would be much more detrimental to this site following snowmelt.

STIC loggers 10a and 10b were deployed at Site 10, Poose Creek- one during water year 2017 (STIC 10a) and the other (STIC 10b) during water year 2018. Both STIC loggers recorded rSC data that could be used in the CMB method equation to estimate baseflow, but because continuous stream discharge was computed for 2017–2018, only data from STIC logger 10a was used to estimate 2017 BFIs, and comparisons were not made between these duplicate STIC loggers. Based on June and July 2017 discrete measurements, SC falls between 131 and 194 µS/cm, and with continuous data this range is expected to widen. These higher rSC values are expected here where the geology consists mainly of the Cretaceous Mancos Shale Formation with inter-tongues of Frontier sandstone and Mowry Shale (CSU CNHP, 2019).

Poose Creek had the highest 2017 post snowmelt-dominated BFI of all CMB suited sites (68 percent). This isn't surprising considering that it is downstream of Vaughn Lake and dam, which help with groundwater retention. This site also has a low slope, average elevation, low to average precipitation, and one of the smallest drainage area sizes (tied with Roaring Fork of Slater Creek) as compared to the other CMB suitable sites. These characteristics support this site's high post snowmelt-dominated BFI. Because of this, this site is resilient to surface water runoff changes during low flows, but it is vulnerable to any changes in the water table or to groundwater pumping during this timeframe. If water levels at Vaughn Lake decline dramatically, this could reduce groundwater inflow, which is about 68 percent of Poose Creek's water supply following snowmelt and 82 to nearly 99 percent of total flow during the month of

September. This stream does rely on snowmelt for much of its annual hydrograph and would be affected annually by reductions in snowpack or other surface water runoff reductions during spring and early summer.

Overall, 2018 BFI results were lower than those in 2017 at Roaring Fork of Slater Creek (Site 7) and the opposite at South Fork of the Elk River (Site 1). Total stream discharge peak flows decreased at all sites between 2017 and 2018 (where both years of data were available). The lower BFI results in 2018 may suggest that there was less groundwater contribution or a scaled down contribution to total streamflow that year. The decreases in surface water runoff in 2018 meant less water percolating into the ground. Ground water tables may have dropped in many locations in 2018 due to less recharging of aquifers. Based on this discussion and interpretation of the results of this study, chapter 5 will summarize the final findings of each hypothesis and give recommendations for future work with STIC loggers for baseflow estimation.

5. CONCLUSION

5.1. Hypothesis 1: Calibrated STIC loggers can be used to measure continuous relative SC in snowmelt-dominated headwater streams for at least one year in freezing temperatures, in both high and low stream flows, and while buried under sediment.

This hypothesis is partially confirmed. Calibrated STIC loggers can be used to measure relative SC for extended periods of time in most extreme field conditions, but not while buried under sediment, not consistently while submerged in frozen water, and not consistently after extremely high peak flows. It is recommended to:

(1) Place future STIC loggers in a location in the stream where they are protected from being buried by sediment, but also protected from being washed downstream by high flows. In other words, a pool or riffle may not be ideal placement locations. A glide or run would be more appropriate, potentially on the upstream side of a boulder or dead wood, if it is also possible to place where the highest water velocities are not occurring. Another potential location could be just before a cut bank and just after the deposition area, or right after a cut bank and just before the deposition area (not the thalweg of the stream segment, but deep enough to keep the STIC loggers submerged year round with minimal freezing). Making sure to not place STIC loggers in eddy's or point bars where the slowest stream flows exist will also help to prevent placement in an area that is likely to be frozen much of the year. Each ideal STIC logger location will be different and site-specific.

(2) Placing the STIC loggers in a stilling well may be a great solution to avoid being buried in as much sediment as they have the potential to be when connected to a mesh bag filled with cobbles from the stream, as was done in this study. Stilling wells often stay frozen once freezing conditions arise, which should be considered depending on the site.

Additional work is required to be sure if calibrated STIC loggers can be used to measure relative SC for extended periods of time in the field. It is recommended to:

(1) Calibrate STIC loggers using the August 2019 calibration methods prior to launching in the field to evaluate if the recorded rSC values were reasonable field deployment. Polarization or physical bending of electrodes didn't seem to be a problem for this study, but the physical bending has the potential to cause unreasonable data if not calibrated prior to field deployment. Also, one STIC logger could not be calibrated due to a header/offload error. If any STIC loggers experience technical issues during calibration, these should not be deployed in the field. The coefficient of multiple determination should be greater than that of STIC logger 6b (R-squared greater than 0.982 to generate rSC data that can be used to estimate baseflow with the CMB method).

(2) Launch two successfully calibrated STIC loggers at each site location in case one stops logging, or in case one washes downstream. Comparing the baseflow estimates of the duplicate STIC loggers to confirm these is recommended.

(3) Further test the memory and battery capabilities of each STIC logger by recording memory and battery status during each data download at least twice per year, in the fall and in the spring. It is recommended for data to be downloaded, and loggers re-launched if memory is becoming full.

5.2. Hypothesis 2: Temporal STIC logger data trends are comparable to temporal SC data trends measured using a duplicate STIC logger or a higher-cost HOBO U24 logger.

This hypothesis is confirmed. Temporal STIC logger data trends are comparable to temporal data trends measured with a U24 logger. The STIC loggers follow the same relative SC trends as the U24 logger, although there were some minor discrepancies found at North Fork of the Elk River (described in chapter 4.1.5). Because of the relativity of the STIC logger SC data, end-member values must be measured with the STIC logger when possible. It is recommended to:

(1) Log end-member values with STIC loggers from a spring or groundwater source within the watershed before and/or after stream data collection as a test of the rSC_{BF} end-member value. It would also be beneficial to log pure snowmelt from the watershed with the STIC logger to be deployed in the watershed's stream to test that watershed's runoff end-member value (Stewart et al, 2007).

5.3. Hypothesis 3: STIC logger data are more suitable for estimating baseflow with the CMB method at snowmelt-dominated headwater streams with a wide range of relative SC values (min and max end-member SC values differ by greater than 100 µS/cm) than those with a narrow range (Rumsey, 2015).

This hypothesis was disproved. SC ranges and differences between end-member values should be significantly different from one another (Rumsey et al., 2015), but may be less than 100 µS/cm without having apparent problems calculating baseflow discharge. Chapter 4.1.5 describes the sites that had narrower rSC and SC ranges and less difference between end-members (such as Silver Creek), where there were no problems estimating baseflow with the CMB method. End-member values must be measured with the STIC logger. It is recommended to:

(1) Log end-member values with STIC loggers from a spring or groundwater source within the watershed before and/or after stream data collection as a test of the SC_{BF} end member value. It would also be beneficial to log pure snowmelt from the watershed with the STIC logger to be deployed in the watershed's stream to test that watershed's runoff end-member value (Stewart et al, 2007).

5.4. Hypothesis 4: BFI estimates are similar (within 5%) at the same site location when calculated with STIC or U24 logger data or with duplicate STIC loggers.

This hypothesis was confirmed at the two sites where data were available, although more research is necessary to compare data from both U24 and STIC loggers and from duplicate STIC loggers at additional sites. North Fork of the Elk River (Site 2) is the only site where post snowmelt-dominated BFI estimates were calculated with both a STIC logger and a U24 logger. The STIC logger data were used to calculate a 55.9 percent BFI for this period and the U24 logger data were used to calculate a 59.6 percent BFI for the same period. These BFI estimates are within 3.7 percent of one another, which are very similar to one another. Therefore, STIC logger data can be used to compute very similar post snowmelt-dominated BFI estimates as what U24 logger data can be used to compute. Annually, STIC loggers do not log data that can be used to calculate similar BFI estimates as U24 loggers due to high velocity surface water inflow (during high flow) potentially affecting some STIC logger data and unavoidable data gaps during winter months. However, annual baseflow is not the period of interest for this study. As the post snowmelt-dominated period is the most important period of interest for BFI estimates, the above BFI results confirm this hypothesis, but it is recommended to:

(1) Further study comparisons between post snowmelt-dominated BFI calculated with STIC logger data and with higher-cost EC logger data during the same year at the same sites.

In addition, duplicate STIC loggers were deployed at the Roaring Fork of Slater Creek in 2017. The post snowmelt-dominated BFI estimates calculated with data from STIC logger 7a and from 7b differed by 0.2 percent, which are quite similar and support this hypothesis. It is recommended to:

(1) Further study duplicate STIC loggers by deploying two at each future site location and compare the post snowmelt-dominated baseflow estimates calculated with their data.

5.5. Hypothesis 5: Contribution of groundwater input to post snowmelt-dominated stream discharge in headwater streams can be estimated using the CMB method with STIC logger data.

This hypothesis was confirmed. Contribution of groundwater input to post snowmelt-dominated stream discharge in seven headwater streams was estimated using the CMB method with STIC logger data (Silver Creek used U24 logger data). Four sites had estimates for 2017 and seven sites had estimates for 2018 (including Silver Creek). Baseflow estimates for the post snowmelt-dominated period have high confidence, although the SC_{BF} end-member selection has a large effect on daily baseflow and BFI results. STIC logger rSC data can be used to estimate baseflow with the CMB method at any site location where continuous flow data can also be acquired, ideally at an hourly frequency, where STIC loggers will not be subjected to frozen water long-term, or enough sediment to bury the loggers. For example, in a run or near a pool-tail crest of a stream. High velocity surface water inflow (during high flow) may be affecting some STIC logger rSC data, but this does not affect post snowmelt-dominated groundwater contribution estimations.

5.6. STIC Logger Cost and Efficiency

With a few hours of data processing time needed per STIC logger, this approximately doubles the cost of each STIC logger. The four total hours of calibration time should also be accounted for, for any number of STIC loggers. If one were to calibrate 36 STIC loggers at once, this would require about four hours calibration time, plus 36 to 72 additional hours for data processing. On average this is about 58 hours for 36 STIC loggers (about 1000 to 2000 dollars in wages), plus the cost of each logger (about 2300 dollars for 36), bringing the grand total to 3300 to 4300 US dollars for 36 rSC data loggers. For 36 U24 data loggers, this would cost about

27,000 US dollars. In other words, about seven low-cost STIC loggers can be deployed for the same price as every higher priced U24 data logger.

5.7. Conclusion

These findings open the possibility of collecting more data at more snowmelt-dominated headwater streams with both wide and more narrow SC ranges, due to the low cost of these rSC data loggers. The low cost of these rSC loggers in turn increases potential for more baseflow data to be acquired at these streams, to inform and support public land and water management decisions and add to the active area of research surrounding baseflow estimation.

REFERENCES

Bauch, N.J., Moore, J.L., Schaffrath, K.R., and J.A. Dupree. 2012. Water-quality assessment and macroinvertebrate data for the Upper Yampa River watershed, Colorado, 1975 through 2009: U.S. Geological Survey Scientific Investigations Report 2012–5214. Available at https://pubs.usgs.gov/sir/2012/5214/

Bloomfield, J. P., Allen, D.J., and K. J. Griffiths. 2009. Examining geological controls on baseflow index (BFI) using regression analysis: An illustration from the Thames Basin, UK, J. Hydrol., 373, 164–176, doi:10.1016/j.hydrol.2009.04.025.

Boussinesq, J. 1877. Essai sur la theorie des eaux courantes. Mem. Acad. Sci. Inst. France 23, 252–260.

Carelton, T. 2020. Baseflow Study Area Watershed Map. ESRI.

Carleton, T. 2021. Personal Communication.

Chapin, T. P., Todd, A.S., and M. P. Zeigler. 2014. Robust, low-cost data loggers for stream temperature, flow intermittency, and relative conductivity monitoring, Water Resources Research, 50, doi:10.1002/2013WR015158.

Clark, M.L., Eddy-Miller, C.A., and M.A. Mast. 2000. Environmental characteristics and water-quality of Hydrologic Benchmark Network stations in the West-Central United States, U.S. Geological Survey Circular 1173-C, chapter 14. Available at https://pubs.usgs.gov/circ/circ1173/circ1173c/chapter14.htm

Colorado State University Colorado Natural Heritage Program (CSU CNHP). 2019. Level 4 Potential Conservation Area (PCA) Report. East Fork of the Williams Fork. Available at https://cnhp.colostate.edu/ourdata/pca-reports/

CSU CNHP. 2019. Level 4 Potential Conservation Area (PCA) Report. Middle Fork of the Elk River. Available at https://cnhp.colostate.edu/download/ documents/pca /L4_PCA-Middle%20Fork%20Elk%20River_11-27-2019.pdf

CSU CNHP. 2019. Level 4 Potential Conservation Area (PCA) Report. Poose Creek. Available a: https://cnhp.colostate.edu/download/documents/pca/L4_PCA -Poose%20Creek_11-27-2019.pdf

CSU CNHP. 2019. Level 4 Potential Conservation Area (PCA) Report. Wolverive Lake. Available at https://cnhp.colostate.edu/download/documents/pca/L4_ PCA-Wolverine%20Lake_11-27-2019.pdf

Colorado Water Conservation Board. 2009. Yampa River Basin Information. Available at https://dnrweblink.state.co.us/cwcb/ElectronicFile.aspx?docid=146636&dbid=0
Covino, T.P., and B.L. McGlynn. 2007. Stream gains and losses across a mountain-to valley transition: impacts on watershed hydrology and stream water chemistry. Water Resources Research 43, W10431.

Dinçer, T., Payne, B.R., Florkowski, T., Martinec, J., and E. Tongiorgi. 1970. Snowmelt runoff from measurements of tritium and oxygen-18. Water Resources Research, 6, 110–124, doi:10.1029/WR006i001p00110.

Dorn, T. and K. Costigan. 2018. Channel Morphology, Streamflow Patterns, and Sediment Transport of Two Intermittent Rivers along the Balcones Escarpment. ProQuest Dissertations Publishing. University of Louisiana at Lafayette.

Gillman, M. A., Lamoureux, S.F., and M. J. Lafrenière. 2017. Calibration of a modified temperature-light intensity logger for quantifying water electrical conductivity, Water Resources Research, 53, 8120–8126, doi:10.1002/ 2017WR020634

Halford, K.J., and G.S. Mayer. 2000. Problems associated with estimating ground water discharge and recharge from stream-discharge records. Groundwater 38, 331– 342.

Hodge, B.W., Henderson, R., Rogers, K.B. and K.D. Battige. 2015. Efficacy of Portable PIT Detectors for Tracking Long-Term Movement of Colorado River Cutthroat Trout in a Small Montane Stream, North American Journal of Fisheries Management, 35:3, 605-610, DOI: 10.1080/02755947.2015.1012280. Available at https://www.tandfonline.com/doi/full/10.1080/02755947.2015.1012280?scroll=top&needAccess =true

Kendall, S., and E. A. Caldwell. 1998. Fundamentals of isotope geochemistry, in Isotope Tracers In Catchment Hydrology, edited by C. Kendall and J. J. McDonnell, pp. 51–86, Elsevier, Amsterdam.

Lott, D.A. and M.A. Stewart. 2013. A Power Function Method for Estimating Base Flow. Groundwater 51, no. 3, 442-451.

Lui, H.W. and Chow, K. 2018. A Novel Calibration Procedure of Pulse Transit Time based Blood Pressure measurement with Heart Rate and Respiratory Rate. Conference proceedings: ... Annual International Conference of the IEEE Engineering in Medicine and Biology Society. IEEE Engineering in Medicine and Biology Society. Available at: https://www.researchgate.net/publication/326835368_A_Novel_Calibration_Procedure_of_Pulse_Transit_Time_based_Blood_Pressure_measurement_with_Heart_Rate_and_Respiratory_Rate

Lyu, H., Xia, C., Zhang, J., and Bo Li. 2020. Key challenges facing the application of the conductivity mass balance method: a case study of the Mississippi River basin. Hydrology and Earth System Sciences 24, 6075–6090. Available at https://doi.org/10.5194/hess-24-6075-2020

Miller, M.P. 2021. Personal Communication.

Miller, M. P., Susong, D.D., Shope, C.L., Heilweil, V.M., and B. J. Stolp. 2014. Continuous estimation of baseflow in snowmelt-dominated streams and rivers in the Upper Colorado River Basin: A chemical hydrograph separation approach, Water Resources Research, 50, 6986–6999. Available at doi:10.1002/ 2013WR014939

Miller, M. P., Johnson, H.M., Susong, D.D., and D.M. Wolock. 2015. A new approach for continuous estimation of baseflow using discrete water quality data: Method description and comparison with baseflow estimates from two existing approaches. Journal of Hydrology 522, 203–210. Available at http://dx.doi.org/10.1016/j.jhydrol.2014.12.039

Nadeau, T. L., and M. C. Rains. 2007. Hydrological connectivity between headwater streams and downstream waters: How science can inform policy, J. Am. Water Resour. Assoc., 43(1), 118–133. doi:10.1111/j.1752-1688.2007.00010.x.

Onset. 2021. HOBO Fresh Water Conductivity Data Logger. Available at: https://www.onsetcomp.com/products/data-loggers/u24-001

Onset. 2020. HOBO 30-Foot Depth Water Level Data Logger. Available at: https://www.onsetcomp.com/products/data-loggers/u20-001-01

Pinder G. F., and J. F. Jones. 1969. Determination of the ground-water component of peak discharge from the chemistry of total runoff, Water Resources Research, 5, 438–44, doi:10.1029/WR005i002p00438.

Routt National Forest. 1998. Final Environmental Impact Statement and Revised Land and Resource Management Plan. Appendix F – Research Natural Areas. Available at: https://www.fs.usda.gov/detail/mbr/landmanagement/planning/?cid=fsbdev3_025110

Rumsey, C.A. 2020. Personal Communication.

Rumsey, C.A., Miller, M.P., and G.A. Sexstone. 2020. Relating hydroclimatic change to streamflow, baseflow, and hydrologic partitioning in the Upper Rio Grande Basin, 1980 to 2015. Journal of Hydrology 584, 124715.

Rumsey, C.A., Miller, M.P., Susonga, D.D., Tillmanb, F.D., and D.W. Anningc. 2015. Regional scale estimates of baseflow and factors influencing baseflow in the Upper Colorado River Basin. Journal of Hydrology: Regional Studies 4, 91–107. Available at http://dx.doi.org/10.1016/j.ejrh.2015.04.008

Sanders, L.L. 1998. Surface Water: Current-Velocity Meter. Pub by Prentice Hall, Inc. A Manual of Field Hydrogeology, Chapter 3, 62-75.

Sklash and Farvolden. 1979. The Role of Groundwater in Storm Runoff. Journal of Hydrology 43, 45-65

Sklash, M.G., Stewart, M.K., and A.J. Pearce. 1986. Storm Runoff Generation in Humid Headwater Catchments: A Case Study of Hillslope and Low-Order Stream Response. Water Resources Research, Vol. 22, No. 8, pages 1273-1282.

Sanford, W.E. and T.A. Hack. 2013. Comparison of baseflow estimates from hydrograph separation using end-member mixing analysis and analytical techniques: American Geophysical Union, Fall Meeting 2013, abstract id. H23N-02.

Schnackenberg, L. 2017. USDA Forest Service Watershed Condition Framework. Watershed Restoration Action Plan: Headwaters Elkhead Creek. Available at https://apps.fs.usda.gov/wcatt/

Schnackenberg, L. 2021. Personal Communication.

Sloto, R.A., and M.Y. Crouse. 1996. HYSEP: A computer program for streamflow hydrograph separation and analysis. U.S. Geological Survey Water-Resources Investigation Report 96-4040.

Stewart, M., Cimino, J., and M. Ross. 2007. Calibration of baseflow separation methods with streamflow conductivity. Groundwater 45, no. 1: 17-27.

Strahler, A. N. 1952. Hypsometric (area-altitude) analysis of erosional topology. Geological Society of America Bulletin 63 (11): 1117–1142.

Swanson, H.A., and Baldwin, H.L. 1965. A Primer on Water Quality. U.S. Geological Survey. Available at: https://www.usgs.gov/special-topic/water-science-school/science/turbidity-and-water?qt-science_center_objects=0#qt-science_center_objects

Turnipseed, D.P. and V.B. Sauer. 2010. Discharge Measurements at Gaging Stations. USGS Chapter 8 of Book 3, Section A, page 2. Available at: https://pubs.usgs.gov/tm/tm3-a8/tm3a8.pdf

University of Nebraska – Lincoln. 2020. The Platte River Basin. NATIONAL SCIENCE FOUNDATION NATIONAL RESEARCH TRAINEESHIP PROGRAM. Available at https://nrt.unl.edu/platte-river-basin

U.S. Bureau of Reclamation. 2012. Colorado River Basin water supply and demand study, study report, 95 pp., U.S. Department of the Interior, Washington, D. C. Available at http://www.usbr.gov/lc/region/programs/crbstudy/finalreport/studyrpt.html

U.S. Bureau of Reclamation. 2019. North Platte River Basin Water Supply and Utilization Report, Wyoming Area Office. Available at https://www.usbr.gov/gp/lakes_reservoirs/wareprts/wsnpmar.pdf

U.S. Geological Survey. 2019. Encampment River Above Hog Park Creek Hourly Discharge data.

U.S. Geological Survey. 2020. StreamStats: Streamflow Statistics and Spatial Analysis Tools for Water-Resources Applications. Available at: https://www.usgs.gov/mission-areas/water-resources/science/streamstats-streamflow-statistics-and-spatial-analysis-tools?qt-science_center_objects=0#qt-science_center_objects

U.S. Geological Survey. 2021. What is a rating curve? Why does it change over time? Available at: https://www.usgs.gov/faqs/what-a-rating-curve-why-does-it-change-over-time?qt-news_science_products=0#qt-news_science_products

U.S. Forest Service: Routt National Forest (USFS RNF). ND. EIS Appendix F – Research Natural Areas. Available at https://www.fs.usda.gov/Internet/FSE_DOCUMENTS/stelprdb5166048.pdf

USDA Forest Service. 2003. Integrated Management Plan for the California Park Special Interest Area. Available at https://www.fs.usda.gov/nfs/11558/www/nepa/105600_FSPLT3_4052542.pdf

USDA Forest Service. 2009. Routt National Forest Map.

Wahl, K.L., and T.L. Wahl. 1995. Determining the flow of Comal Springs at New Braunfels, Texas. Available at http://www.usbr.gov/pmts/hydraulics_lab/twahl/bfi/texaswater95/comalsprings.html

Wallin, T.J. 2019. Recovery of a native southwestern trout under threat of wildfire and warming temperatures: An assessment of survival and thermal limits of gila trout. New Mexico State UniversityProQuest Dissertations & Theses Global. 2334771882. Available at https://search-proquest-com.ezproxy2.library.colostate.edu/docview/2334771882?account id =10223

Wyoming Water Data Support Team. 2020. USGS 06623800 ENCAMPMENT RIVER AB HOG PARK CR, NR ENCAMPMENT, WY. Available at: https://waterdata.usgs.gov/nwis/uv?06623800

Zhang, R., Li, Q., Chow, T.L., Li, S., and S. Danielescu. 2013. Baseflow separation in a small watershed in New Brunswick, Canada, using a recursive digital filter calibrated with the conductivity mass balance method. Hydrol. Process. 27, 259–2665